Max L. Porter Bradley W. Hughes
Bruce A. Barnes Kasi P. Viswanath

Non-Corrosive Tie Reinforcing and Dowel Bars for Highway Pavement Slabs

November 1993

Submitted to:

Highway Division of the
Iowa Department of Transportation
and
Iowa Highway Research Board

Project Number: HR-343

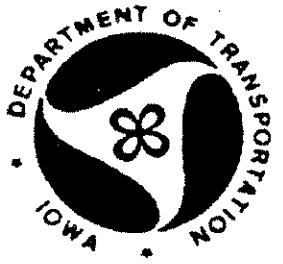

final

report

Max L. Porter Bradley W. Hughes
Bruce A. Barnes Kasi P. Viswanath

Non-Corrosive Tie Reinforcing and Dowel Bars for Highway Pavement Slabs

November 1993

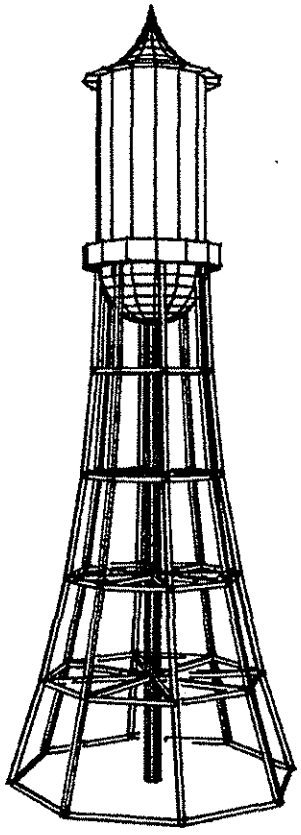

engineering research institute

iowa state university

Disclaimer

The contents of this report do not represent a warranty of the products used on behalf of the State of Iowa, Iowa State University, Iowa Department of Transportation, Highway Research Board, or the authors. The opinions, findings, and conclusions expressed in this publication are those of the authors and not necessarily those of the Highway Division of the Iowa Department of Transportation. Engineering data, design, details, with recognized professional principals and practices are for general information only. The data, designs, and suggested conclusions should not be used without first securing competent advice with respect to the suitability for any given application. The responsibility for the use of information in this report remains with the user. This report is for information purposes and is made available with the understanding that it will not be cited without the permission of the authors.

TABLE OF CONTENTS

LIST OF FIGURES

LIST OF TABLES

LIST OF SYMBOLS

a = distance from a support to the nearest load point in four-point bending (in.)

A, B, C, D = constants in the solution for deflection of a dowel in concrete

A_d = cross sectional area of a FC dowel (in^2)

b = distance from load points to center of span in four-point loading (in.)

c = distance from the neutral axis to a point of interest for stress (in.)

d = dowel diameter (in.)

E = modulus of elasticity (psi)

E_b = flexural modulus of elasticity (psi)

E_c = modulus of elasticity of concrete (psi)

E_f = modulus of elasticity of E-glass fibers (psi)

E_m = modulus of elasticity of resin matrix (psi)

E_x = longitudinal modulus of elasticity of FC material (psi)

E_y = transverse modulus of elasticity of FC material (psi)

EI = flexural rigidity of a pavement dowel ($lbs\text{-}in^2$)

EI_z = flexural rigidity of a finite beam ($lbs\text{-}in^2$)

f'_c = concrete compressive strength (psi)

f_r = modulus of rupture of concrete (psi)

F = form factor, equal to 10/9 for a solid circular section

G = shear modulus (psi)

G_m = shear modulus of the resin matrix (psi)

G_f = shear modulus of E-glass fibers (psi)

G_{xy} = transverse shear modulus of the FC material (psi)

I = moment of inertia of a flexural specimen ($in.^4$)

I_d = moment of inertia of a FC dowel specimen ($in.^4$)

k_o = modulus of dowel support (pci)

K = modulus of subgrade reaction (pci)

l = dowel length (in.)

L = length between supports for a simple span (in.)

L_D = length of a dowel (in.)

M = bending moment at a section (in.-lbs)

P = load applied in Iosipescu shear test in Figure 4.6 (lbs)

P_s = dowel shear (lbs)

P_1 = load applied in three-point bending (lbs)

P_2 = load applied in four-point bending (lbs)

P/Δ = slope of the applied load versus deflection curve for a flexural test, where P is equal to P_1 or P_2 (lbs/in.)

R = resultant of distributed load applied to supporting beams by the test slab (lbs)

$S_{1.5}$ = measured dowel strain at 1.5 inches from the joint (μin./in.)

SG_d = specific gravity of the FC dowel material

SG_f = specific gravity of E-glass fibers

t = thickness of a highway pavement (in.)

v_f = volume fraction of glass fibers

v_m = volume fraction of resin matrix

v_v = volume fraction of voids within the FC material

V_f = volume of glass fibers in one dowel (ft^3)

V_D = volume of one FC dowel (ft^3)

W_e = external work (ft-lbs)

w_i = internal work (ft-lbs)

W_D = weight of one FC dowel (lbs)

W_f = weight of glass fibers in one FC dowel (lbs)

x = distance along the length of a beam (in.)

y_o = deflection of a dowel within concrete (in.)

δ = shear deformation (in.)

Δ = deflection at the middle of a simple span flexural test (in.)

Δ_r = relative displacement at the joint (in.)

γ_d = unit weight of FC dowel material (lbs/ft^3)

γ_f = unit weight of glass fibers (lbs/ft^3)

γ_{water} = unit weight of water (lbs/ft^3)

ϵ = strain (in./in.)

σ = normal stress (psi)

ν_f = Poisson's ratio of E-glass fibers

ν_m = Poisson's ratio of resin matrix

ν_{xy} = Poisson's ratio of a FC material for transverse (y-direction) strain when loaded in the direction of fibers (x-direction).

ABSTRACT
for the final report on HR343:
Non-Corrosive Tie Reinforcing and Dowel Bars for Highway Pavement Slabs

Bradley W. Hughes
Bruce A. Barnes
Max L. Porter
Kasi P. Viswanath

The use of non-metallic load transfer and reinforcement devices for concrete highway pavements is a possible alternative to avoid corrosion problems related to the current practice of steel materials. Laboratory and field testing of highway pavement dowel bars, made of both steel and fiber composite materials, and fiber composite tie rods were carried out in this research investigation.

Fatigue, static, and dynamic testing was performed on full-scale concrete pavement slabs which were supported by a simulated subgrade and which included a single transverse joint. The behavior of the full-scale specimens with both steel and fiber composite dowels placed in the test joints was monitored during several million load cycles which simulated truck traffic at a transverse joint.

Static bond tests were conducted on fiber composite tie rods to determine the required embedment length. These tests took the form of bending tests which included curvature and shear in the embedment zone and pullout tests which subjected the test specimen to axial tension only.

Fiber composite dowel bars were placed at two transverse joints during construction of a new concrete highway pavement in order to evaluate their performance under actual field conditions. Fiber composite tie rods were also placed in the longitudinal joint between the two fiber composite doweled transverse joints.

CHAPTER 1 INTRODUCTION

1.1 General

Deterioration of the infrastructure of the United States has resulted in the engineering profession examining alternatives to the current practices and materials used in all types of construction. One of the causes of the large amount of deterioration is the corrosion of metallic materials used for reinforcement of concrete. Many materials are now available that can reduce or eliminate reinforcement corrosion because of their resistance to the corrosive agents that attack reinforcement. One such material with applications in the construction of transportation structures is fiber composites (FC).

Specifically, this research dealt with the study of the use of fiber composite materials as load transfer devices in concrete highway pavements. Load transfer devices are structural members which are placed at the locations of transverse joints in a highway pavement, and which act to transfer shear across the joints. The devices studied in this research were in the form of dowels, or dowel bars, which are a standard type of load transfer device in the State of Iowa. Dowels are placed along the length of joints because the concrete pavement is assumed to crack at that location due to shrinkage and thermal contraction of the concrete, thus

eliminating shear transfer across the joint by the concrete. When the pavement is cracked at the joint, the transfer of shear is then provided by the dowels.

Because the dowels are placed at the location of a crack in a highway pavement, corrosion of the dowel due to de-icing salts leaching through the crack is a concern. Corrosion of a dowel within the concrete is undesirable because a problem could be created that is referred to as a "binding" or "locking" of the joint. Binding of a dowel occurs when the dowel is unable to move longitudinally within the pavement. The function of a dowel is only to transfer shear forces at a joint, so no axial force is desired in the dowel even though temperature variations cause the concrete to shrink and expand in the axial direction. Therefore, the dowel must be able to move freely within the concrete in the direction of the pavement. If corrosion occurs on the surface of the dowel, free movement may be restricted.

The most common material used for dowel bars is steel, but, according to Heinrichs (1989) corrosion of steel dowels is a problem, as uncoated steel dowels often become severely corroded in as little as five years, leading to joint performance problems. Permanent coatings of dowels has been used to prevent these corrosion problems, the most common of which is epoxy, but epoxy has not been proven to be effective for long-term use. The only alternatives to steel which have been proven in long-term usage are stainless steel or plastic-

coated steel dowels. These have been used successfully in New Jersey, New York, and Michigan (Bryden 1975).

The corrosion resistance of FC materials has been observed in research by Lorenz (1993) through accelerated aging studies of FC dowel bars and reinforcing rods in concrete. In the study by Lorenz, which was shown to be indicative of actual aging effects, little or no effect on the performance of the FC dowels and rods was observed. Results of the aging study indicated that the FC materials provide corrosion resistance at least as well as currently used steel products. Consideration must now be given to the performance of FC dowels when subjected to actual field conditions or simulated field conditions, including cyclic loading.

1.2 Fiber Composite Materials

Great advances in materials technology has resulted in many new materials found to have valuable applications in engineering. Fiber composite materials have been found, through research and actual application, to have advantages over previously used materials in some applications. According to Talreja (1987),

> Indeed, the applications for which composite materials are being found to be most advantageous are precisely those situations in which the degradation of strength and life by fatigue processes are most likely.

Fiber composite materials are made of a combination of

glass fibers and resin. The glass fibers are extremely high in tensile strength while being lightweight relative to steel. Resins are also lightweight and provide an adhesive to hold the fibers in place, while also protecting them against corrosive agents.

The FC materials studied in this research consist of E-glass fibers and a thermoset vinyl ester resin molded into the shape of a rod. The rod was produced by the pultrusion process, which involves pulling a bundle of glass fibers through a bath of liquid resin and then through a heated die. When heat is added at the die, the resin becomes "set", keeping its shape and bonding to the fibers (EXTREN 1989). The rod material then consisted of unidirectional fibers with either a smooth exterior for dowel applications, or a textured exterior for reinforcing bar applications.

1.3 Experimental and Analytical Investigation

The concept of this research was to compare the performance, while under approximately the same conditions, of FC dowels to that of steel dowels for use as pavement load transfer devices. To perform a comparison, a means of evaluating the performance of pavement dowels in a laboratory must be developed while modeling as close as possible the actual conditions experienced by a dowel in the field. These conditions include the type of support and loading applied to

a pavement slab. In the laboratory, a support system was to be provided which simulated a soil subgrade underneath a pavement, and loads were to be applied which approximate a standard truck loading.

While the greatest interest from the research standpoint was with the performance of the fiber composite materials, a baseline for comparison was necessary, which required testing of steel materials as well. Previous laboratory testing had been performed to evaluate the performance of pavement dowels under repeated loading (Teller 1958). However, only steel dowels were investigated during the previous study. In this research, a procedure for testing and evaluating the fatigue behavior of steel and FC dowels in a full-scale pavement slab was developed and applied. From the testing in this research, a comparison of the performance of the two materials under similar conditions was made.

1.3.1 Objective

The objectives of this study were:

1. to develop a laboratory test method for the evaluation of highway pavement dowels which approximates actual field conditions,
2. to compare static, fatigue, and dynamic behavior of FC dowels to those for steel dowels when used as load transfer devices in transverse joints of highway pavements, and
3. to study the bond characteristics of the FC tie rod.

1.3.2 Scope

The scope of this study included:

1. an evaluation of previous testing performed on pavement dowels and an extensive review of literature dealing with pavement dowels and fiber composite materials,
2. placement of FC dowels and FC tie rods in an actual highway pavement during new construction,
3. development of a program for monitoring and evaluating the performance of FC dowels placed in an actual pavement,
4. monitoring and evaluation of the performance of FC dowels placed in an actual pavement,
5. computer modeling and analysis of an actual highway pavement joint system and a laboratory full-scale pavement joint system in order to design a laboratory testing setup,
6. design and construction of experimental test setups and specimens for static, fatigue, and dynamic testing of FC and steel dowels, and static bond tests on FC tie rods,
7. testing of elemental dowel specimens under static loading,
8. testing of full-scale slab specimens which use FC and steel dowels, and full-scale beams with FC tie rods, and
9. analyzing results of tests on full-scale pavement slabs, elemental dowel specimens, and on FC tie rod beams.

1.4 Literature Review

1.4.1 Theoretical modeling of dowel behavior

An extensive search of literature related to the topics in this report included a review of previous work on modeling

of dowels within concrete. A model for the behavior of pavement dowels embedded in concrete is discussed in Section 4.2.6 and was developed and verified in experimentation through work by Lorenz (1993). The model was based on work covered in Timoshenko (1925) and Timoshenko (1976), in which a finite beam on an elastic foundation was analyzed for determination of deflections along the length of the beam. The general solution presented by Timoshenko is an expression for deflection, y, which is a function of the stiffness of the foundation and the location along the beam. The solution is expressed as:

$$y=e^{\beta x}(A\cos\beta x+B\sin\beta x)+e^{-\beta x}(C\cos\beta x+D\sin\beta x) \qquad \text{Eqn. 1.1}$$

where,

$$\beta=\sqrt[4]{\frac{k_o d}{4EI_z}}\,(in.^{-1})$$

A, B, C, D	= constants in the solution for deflection of a dowel in concrete
k_o	= modulus of foundation (psi)
d	= dowel diameter (in.)
EI_z	= flexural rigidity of the beam (lbs-in^2)

Successive differentials of the general solution results in relationships for moment and shear along the beam length. The expressions for deflection, moment and shear were then applied by Lorenz for use in the analysis of dowels embedded in concrete. The moment and shear relationships will be included in Section 4.2.6, which contains further discussion

regarding their application to this research.

Additional background information from several sources was considered throughout the development of the model, but were not used specifically in the analysis included in this report. These included Bradbury (1933), Friberg (1938), Westergaard (1928) and Westergaard (1926).

1.4.2 Rigid highway pavements and dowels

A thorough search was conducted on literature dealing with the design, analysis, performance and evaluation of rigid highway pavements and doweled joints. Rigid pavement design and analysis considerations are covered in AASHTO (1986), Heinrichs (1989), and Pavement Design, dealing with recommended design practices as well as discussions of previous research conducted by the American Association of State Highway Officials (AASHO, which is now called the American Association of State Highway and Transportation Officials, or AASHTO) on actual highway pavements. An extensive research program was carried out by the AASHO on the performance of actual pavements under known loading conditions and with many combinations of the variables that influence pavement performance, such as subgrade type, pavement type, joint spacing, etc. (Heinrichs 1989).

A non-destructive method of evaluation of highway pavements and joints used by the Iowa Department of

Transportation (IDOT), called the Road Rater™, is covered in Potter (1989). The Road Rater™ is a means of dynamic evaluation of the performance of pavements and joints, and is discussed in greater detail in Section 2.3.

1.4.3 Full-scale pavement dowel fatigue testing

The test method used in the experimental evaluation of dowels under fatigue in full-scale pavement slabs was based on work performed by Teller and Cashell, and is covered in Teller (1958). Included in the previous work was a testing system using steel beams to support a concrete slab with a doweled test joint. Testing by Teller and Cashell was performed on joints to evaluate the performance of steel dowels under repeated loading.

The work by Teller and Cashell studied the efficiency of dowels as load transfer devices in highway pavements and the change in the efficiency as repetitive loading was applied. The effect of dowel design variables on the efficiency of load transfer was also evaluated in the previous study, though results of that portion of the study were not directly pertinent to this research.

1.4.4 Fiber composite materials

Properties of the components of FC materials were

determined from several sources, including the references Auborg (1986), DERAKANE (1990), EXTREN (1989), Fiber (1991). Component properties were applied to methods discussed in Tsai (1980) in order to determine theoretical composite properties of the materials studied in this research. Experimental test methods for determining structural properties of FC materials are discussed in Adams (1987), Annual (1991), Munjal (1989), Walrath (1983).

The methods discussed in the above references include testing for flexural and shear properties of unidirectional fiber composites. Because of the anisotropic nature of these composites, great consideration must be given to the type of testing methods that are applied to determine composite properties. Munjal evaluated several test methods for determination of design allowables, and discusses those methods which are most accurate and reasonable. Walrath and Adams discuss extensive research that has been performed regarding the Iosipescu shear test for determining shear properties of FC materials.

Fatigue characteristics of unidirectional fiber composite materials are largely a function of the type and orientation of loading with respect to the direction of the fibers. Talreja (1987) discusses fatigue characteristics of FC materials, including the variation of properties with fatigue cycling. The fatigue performance of fiber composites is largely a function of the matrix properties when loaded

transversely to the fiber direction, as was the case in the testing included in this study. Monitoring of fatigue damage is best accomplished through observing material stiffness change during cyclic loading instead of material strength degradation. Material stiffness components to be considered, include: longitudinal and transverse elastic modulus, Poisson's ratios, and shear modulus.

CHAPTER 2 FIELD PLACEMENT AND MONITORING OF FC DOWELS AND TIE RODS

2.1 Introduction

Included in this research project was the field testing of the performance of FC dowels as load transfer devices in a highway pavement. From the field testing, a comparison of performance can be made between FC and steel materials under the same, or very similar, field conditions, such as subgrade, concrete, weather, traffic, and placement. Field placement of the FC dowels was performed in conjunction with the Iowa Department of Transportation (IDOT) during the construction of a new section of concrete pavement on U.S. Highway 30 east of Ames, Iowa. Two lanes of pavement were constructed during the project, and two transverse joint locations were selected as test joints. The test joints are located on the westbound lanes of Highway 30 at stations 1527+00 and 1527+20, which are approximately three miles east of Interstate Highway 35.

Placed in the two test joints were 1.75-inch FC dowels, replacing 1.5-inch steel dowels. All other transverse joints in the new pavement used steel dowels, which are common for such construction, and will be referred to in this discussion as control joints. The FC dowels were 18 inches in length and were placed at a spacing of eight inches. Steel dowels placed at all other locations were the same length, but were spaced at 12 inches.

The field test portion of the research must be considered as a long term and ongoing program. A comparison of the performance of FC dowels to steel dowels in a highway pavement is best done over the design life of the pavement, which may be in excess of 20 years (Heinrichs 1989). Continuing observation of the performance of the test joints and adjacent joints is necessary in order to fully evaluate the advantages or disadvantages of either material when compared to the other.

Included in the discussion of the field study will be a description of the procedures used for preparation and placement of the test dowels, including construction techniques. A program for evaluating the performance of the test joints relative to adjacent control joints will also be described. Several methods for monitoring the performance of both types of joints will be included, along with preliminary results of the test program will be discussed.

2.2 Preparation and Placement

The standard practice in the construction of new concrete highway pavements in the State of Iowa closely follows the guidelines recommended by AASHTO, including the use of steel dowels placed at the transverse joint locations. In the design of rigid pavements, the dowel diameter is selected to be approximately one-eighth of the thickness of the pavement,

and the length is set at 18 inches. After paving is completed, a saw cut is made over the top of the dowels to a depth of one-third of the pavement thickness (AASHTO 1986). Shrinkage of the concrete is assumed to cause the pavement to crack at these locations, which is shown in the diagram of Figure 2.1. When using a slip-form type of paving system, the dowels are held in place by steel "baskets" constructed of steel rod stock. The baskets hold the dowels at the correct height and restrain the dowels from movement as the concrete is placed over the top of them. Steel loops on the baskets

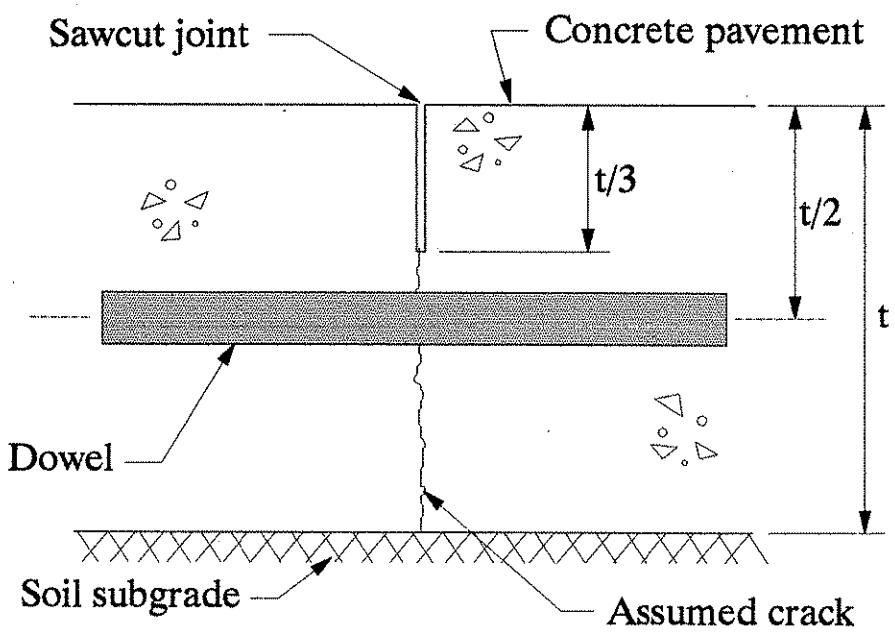

Figure 2.1 **Typical rigid highway pavement contraction joint with a dowel**

hold the dowels at the correct locations. One end of the dowel is spot-welded to the basket, with adjacent dowels having opposite ends welded. Welding serves two purposes: first, the weld provides a means of holding the dowels in place as the baskets are handled, and second, one end of each dowel is tied into the concrete on one side of the joint. The latter purpose allows the pavement slabs on either side of the joint to move independently in the longitudinal direction due to shrinkage or temperature variation.

In the State of Iowa, transverse joints used in concrete pavements are often placed skewed to the center line of the roadway. This skew is at a magnitude of one foot in the longitudinal direction to six feet in the transverse direction. Each dowel, though, is placed so that its longitudinal direction is parallel to the roadway to prevent "binding" of the pavement, while the mid-length of the dowel is located at the joint. Therefore, a line drawn through the mid-point of each dowel coincides with the joint location, and is skewed to the center line of the roadway. The spacing of the dowels is measured in the transverse direction (AASHTO 1986). Figure 2.2 shows a typical highway pavement with dowels placed across joints.

Use of the FC dowels in place of steel dowels was to be completed without a supporting "basket" made specifically for them, therefore, baskets manufactured for 1.5-inch diameter steel dowels were used to hold the dowels in place during

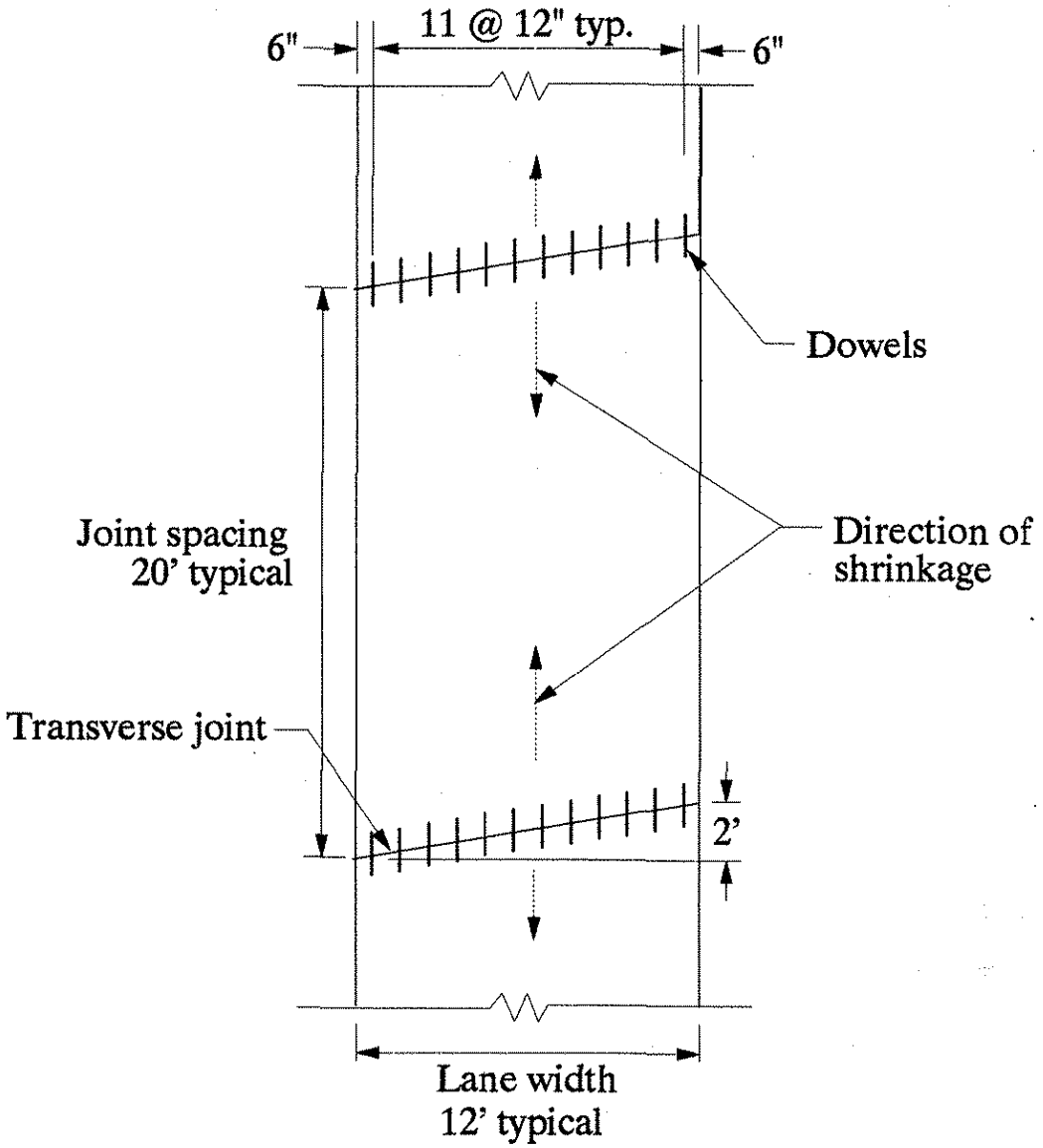

Figure 2.2 Typical jointed concrete highway pavement using dowels at transverse joints

construction. Because the FC dowels to be placed in the pavement at the two test contraction joints had a larger diameter and would be placed at a smaller spacing than their steel counterparts, there was a problem in supporting the dowels properly. The FC dowels were 1.75-inch in diameter and were placed in the pavement at a spacing of eight inches, while the steel dowels that they replaced were 1.5-inch in diameter and spaced at 12 inches. To allow for the placement of the FC dowels, the steel loops holding the dowels in place had to be removed. Then, so to maintain the dowels in their proper positions, heavy steel wire was used to tie the dowels to the baskets.

Using wire to hold the dowels did not provide as rigid of a support of the dowels as steel loops would have, and slight problems did occur when the concrete was placed over the test dowels. As the concrete flowed over the FC dowels, its weight pushed several of the dowels from their original position so that they no longer lied parallel to the center line of the pavement. Where possible, though, construction personnel and observers straightened the dowels before they were completely covered by concrete. Dowels moved during the concrete placement could result in problems if they lie at an angle to the direction of the pavement. When the concrete shrinks or when contraction due to cold weather occurs, the transverse joint will open, and the separate slabs at the joint will move away from one another. Since one side of each dowel is free

from the slab, the pavement slides over the dowels. If, though, a dowel is not parallel to the direction that the pavement moves, there is a binding of the pavement. In the extreme case, binding of the joint causes the concrete to crack at a point just behind the dowels.

As mentioned earlier, only one end of each dowel is actually tied into the concrete, while the other end is meant to move freely within the concrete. In order for this movement to take place, the dowels must not bond with the concrete. Therefore, besides the epoxy coating that is placed on steel dowels, a bond-breaking material, which is a tar-like substance, is applied to the steel dowels and baskets. In the case of the FC dowels to be placed in the concrete, another means of freeing one end was used. When the dowels and the baskets were in place on the subgrade, form oil was applied to one half of each dowel. Adjacent dowels had opposite ends oiled to provide a similar condition as for steel dowels with one end tied to the slab.

2.3 Evaluation and Monitoring

In order to make the study of the field performance of FC dowels and tie rods complete, a comprehensive program of evaluation and monitoring was developed. Since the main objective of the field study was to compare the performance of the test dowels to that of the current standard, the FC

materials were evaluated and monitored relative to steel materials.

The initial and most basic means of comparison was visual inspection of the test joints. During visual inspection, any cracking of the pavement was noted, either at the joint or away from the joint. Also, the joint opening was checked, which would indicate whether the dowels were allowing movement of the slab in the longitudinal direction. Visual inspection was most effective during cold temperatures when the pavement experienced the most thermal contraction. Another location for inspection was at the pavement edges, where an inspection was made of whether the pavement was cracked through the full depth of the slab by digging away the soil at the edge of the pavement.

A more experimental method of evaluation of the test joint performance was the Road Rater™. The Road Rater™ is a tool used by the IDOT to evaluate pavements, subgrades and joints. To evaluate a pavement, a mass was applied to the pavement and oscillated over a range of from approximately 2,500 to 4,500 pounds at 30 Hertz. Velocity sensors measure the amplitude of the pavement movement, which was referred to as displacement. A total of four sensors monitored displacements, one located at the load point, and three others spaced at one-foot intervals. To evaluate transverse pavement joints, the load was applied to one side of the joint and the displacements were measured on the opposite side of the joint

(Potter 1989).

Testing with the Road Rater™, though, did not only consider dowel performance because the performance was also a function of the soil subgrade, pavement, and any aggregate interlock at the joint. By testing the joints with FC dowels and the nearby joints with steel dowels at the same time, a comparison of performance was made. Any comparison, though, was made while assuming that the other variables mentioned above were approximately equivalent for all joints tested.

Another non-destructive means of evaluating the pavement joint performance was a load test of the joint. Such a test included placing displacement measuring devices at the joint and using a loaded truck to apply loads to one side of the joint at a time as displacements were measured. While this was a static test of the pavement, an indication was given of the load transfer abilities of the test joints relative to others nearby. Like the Road Rater™ testing, the performance of the joint during a load test evaluation was a function of many other variables other than the dowels. Again, though, the assumption that these variable were approximately equivalent for adjacent joints were made to allow for a comparison of the performance of FC to steel dowels.

A final means of evaluation of the dowels is the coring of the pavement exactly at the joint and through a dowel. Coring, of course, is a less desirable method because the dowel is destroyed for future performance. A core at a dowel

location would, though, provide a means of observing whether any fatiguing of the concrete has taken place around the dowel. Fatigue of the concrete might be indicated by the hole around the dowel becoming oval-shaped due to repeated loading of the joint by traffic.

2.4 Discussion of Results

The two test joints where the 1.75-inch diameter FC dowels were placed were visually inspected in the summer and fall following their placement in the roadway. During these inspections, no deviations from the performance of adjacent joints with steel dowels were observed at the test joint locations.

Further inspection was carried out along with IDOT personnel in January of 1993. The day of this inspection was quite cold, with temperatures at approximately 10 degrees F. Such cold temperatures caused significant contraction of the concrete, and, therefore, rather substantial joint openings were observed for the two test joints as well as the adjacent joints with steel dowels. At that time, some slight spalling of the surface concrete was noticed at several locations along the joints. Surface damage was also noticed at adjacent joints and was most likely due to vehicles impacting at the joints, not due to the joint or dowel performance. Because damage was noted at adjacent joints with steel dowels, the

damage was not specific to the FC dowels.

IDOT personnel conducted Road Rater™ testing at a total of six joints in the outside traffic lane of the Westbound portion of U.S. Highway 30 during the field test. The joints included the two with FC dowels, along with the two adjacent joints on either side of the test joints which had steel dowels in place. At each of the joints, a test was performed at the locations of the two wheel tracks observed at the joints. The wheel tracks were the locations where a majority of the traffic appeared to pass over the joint. The tracks were located approximately two to three feet inside of each edge of the traffic lane.

During the Road Rater™ testing, the applied dynamic load ranged approximately from 2,500 to 4,500 pounds, and cycled at 30 Hertz. At each joint, the load was applied directly adjacent to one side of the joint, and displacements were measured by one sensor at the load point and by another 12 inches away on the opposite side of the joint. The relative vertical displacement movement between the two sensor locations is an indication of the load transfer across the joint.

Data from the tests included the displacement readings, which were expressed in units of mils, or thousandths of an inch, at the two sensor locations. Tests were performed on four joints with steel dowels and two joints with FC dowels. The test data supplied by the IDOT is included in Table 2.1.

The two sensor locations are labeled as the loaded and unloaded sides of the joint, and results are included for the two wheel track locations. Of the two, the outside wheel track is located nearest to the shoulder of the roadway.

From the results in Table 2.1, the deflections measured at the two types of joints due to the dynamic loading conditions applied by the Road Rater™ are very similar. The variability in both the measured displacement values and the calculated relative displacement values is most likely due to slight variability in the pavement and subgrade construction. The average values of relative deflection are quite similar for the joints using steel and FC dowels. Assuming that the pavement and subgrade characteristics are approximately equivalent for all of the joints tested, the results indicate that the FC dowels are performing as well as the steel dowels at these locations.

In addition to testing with the Road Rater™, inspection of the pavement slab was performed to determine if the concrete was cracked at the joint locations. By digging the shoulder gravel away from one edge of the pavement adjacent to the joint locations, the pavement was observed to be cracked to its full depth at the joints with FC dowels. A crack at the joint location suggests that the FC dowels are permitting movement of the slab over the dowels due to thermal expansion and contraction.

Table 2.1 Road Rater™ deflection data for pavement joints on U.S. Highway 30

Measured and Relative Displacements, mils (1/1000 in.) Note: Rel. = relative displacement = (Loaded) - (Unloaded)						
Joints with:	Outside Wheel Track			Inside Wheel Track		
	Loaded	Unloaded	Rel.	Loaded	Unloaded	Rel.
Steel Dowels	0.74	0.70	0.04	0.65	0.58	0.07
	0.72	0.69	0.03	0.67	0.63	0.04
	0.72	0.70	0.02	0.69	0.65	0.04
	0.77	0.75	0.02	0.72	0.69	0.03
	Average relative = 0.03			Average relative = 0.05		
FC Dowels	0.76	0.74	0.02	0.72	0.67	0.05
	0.75	0.70	0.05	0.71	0.66	0.05
	Average relative = 0.035			Average relative = 0.05		

CHAPTER 3 COMPUTER MODELING

3.1 Introduction

In the process of evaluating and comparing the performance of FC and steel dowels, the criteria used to compare the two were determined. Possible criteria included: pavement slab displacement under load, load transfer by dowels across pavement joints, and relative displacement across a joint (Teller 1958). All of these criteria were applied during this study.

The selection of the loading to be applied during the testing and modeling was determined from the loading used most commonly to standardize the number of load cycles applied to a highway pavement. Traffic load applications are standardized by the AASHTO to axle loads of 18,000 pounds, or single wheel loads of 9,000 pounds. The 18,000 pound axle load is referred to as an equivalent single axle load, or an ESAL (AASHTO 1986). Standardization of load applications to pavements allows for comparisons of pavement performance, though, no two pavements will experience identical loading conditions during their service life.

Before beginning the experimental study of the performance of FC dowels, computer modeling of an actual pavement using finite element analysis methods was performed for two primary reasons. First, the availability of data

which would give the displacements that an actual concrete pavement system undergoes when loaded in use is very limited. Data indicating such displacements under the loading conditions to be used in this research could not be found. Second, a pavement dowel system using FC dowels that was approximately equivalent to the current standard steel dowel system was unknown. By using the computer model of an actual concrete pavement structure, an approximately equivalent system using FC dowels was determined. The criteria for determination of equivalence were displacements of the pavement structure. One model using steel dowels and a second with FC dowels, both subjected to the same loading, were analyzed.

Actual displacements that a pavement structure undergoes in use were also required in order to design a system of simulated subgrade to be used in the laboratory testing of a full-scale slab. The laboratory setup was to be designed to approximate the loading and displacements that a typical field joint undergoes, which, as mentioned above, was unknown for the loading condition of this research.

Previous finite element analyses of pavement joints have shown that the dowel diameter and the concrete compressive modulus of elasticity, E_c, have a significant effect on dowel deflections and concrete bearing stresses. Subgrade modulus and slab thickness, on the other hand, had less influence on the results (Heinrichs 1989).

3.2 Full-Size Highway Pavement Model

The computer model applied to the analysis of a full-size pavement structure took advantage of several features of finite element modeling and analysis. A plate element was used to model the concrete pavement slab. The selected plate element included the option of an elastic foundation, which was used to model the soil subgrade. To model the soil, a value was needed for the modulus of subgrade reaction, K, in pounds per cubic inch (pci). A conservative value for typical subgrade materials of 100 pci was assumed for K (Pavement). A diagram of the computer model of a full-size pavement, including the slab as a plate and the soil as a uniform elastic foundation, is shown in Figure 3.1. Transverse static loading was applied in the model analysis, with point loads applied at the critical locations on the slab, which were directly adjacent to the joint. The model was symmetric about the joint, so that the loading as shown in Figure 3.1 could also be applied to the opposite side of the joint with the results also being symmetric. Application of point loads simulates the wheel loads applied by a single vehicle axle just before or just after passing over the joint in a static state. A schematic of wheel loading conditions is shown in Figure 3.2.

In order to model the pavement joints, a one-half-inch wide opening between sections of the slab was used at each

joint location. Spanning across each joint opening were the pavement dowels. A beam element was used to model the dowel, with the beam rigidly connected to the two plate elements on each side of the joint, as is shown in Figure 3.3. The full-size model included several joints spaced at 20 feet, which is

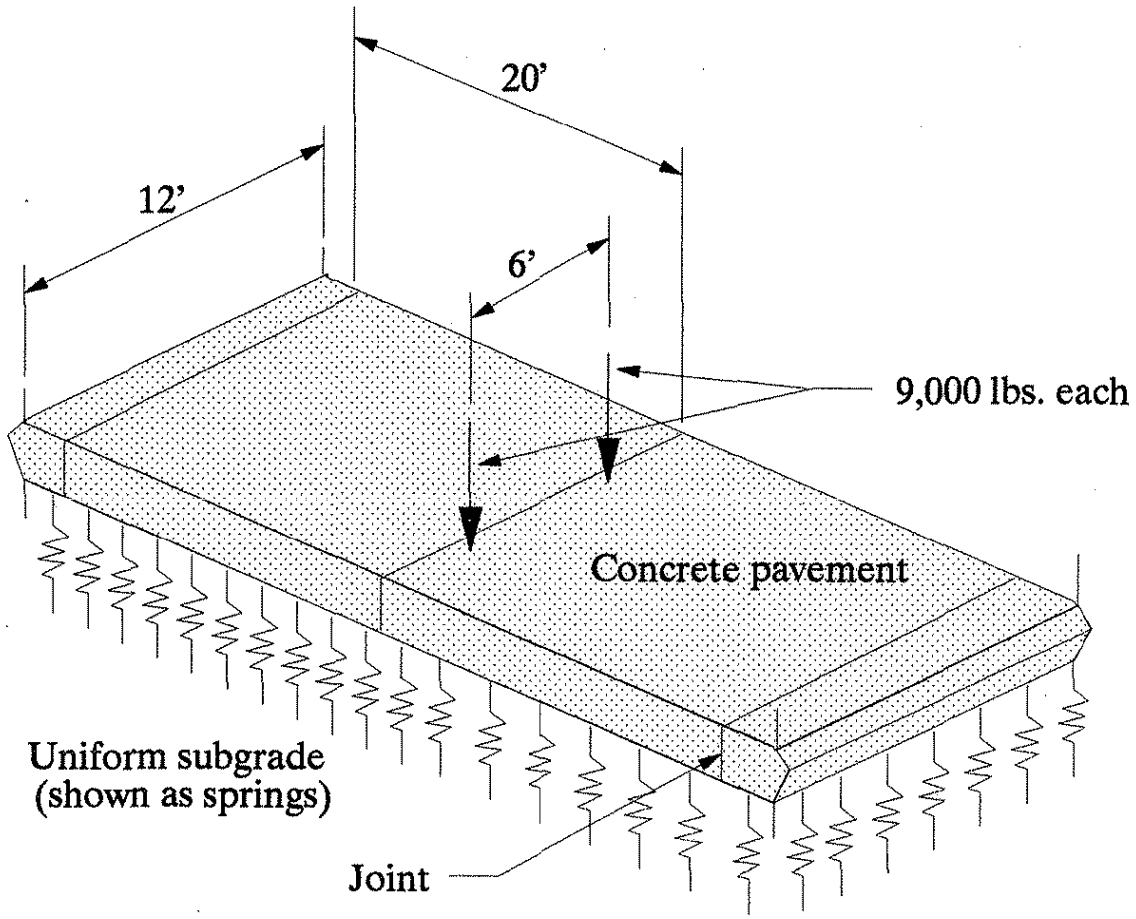

Note: Pavement continues in both directions

Figure 3.1 Computer model of a full-size pavement

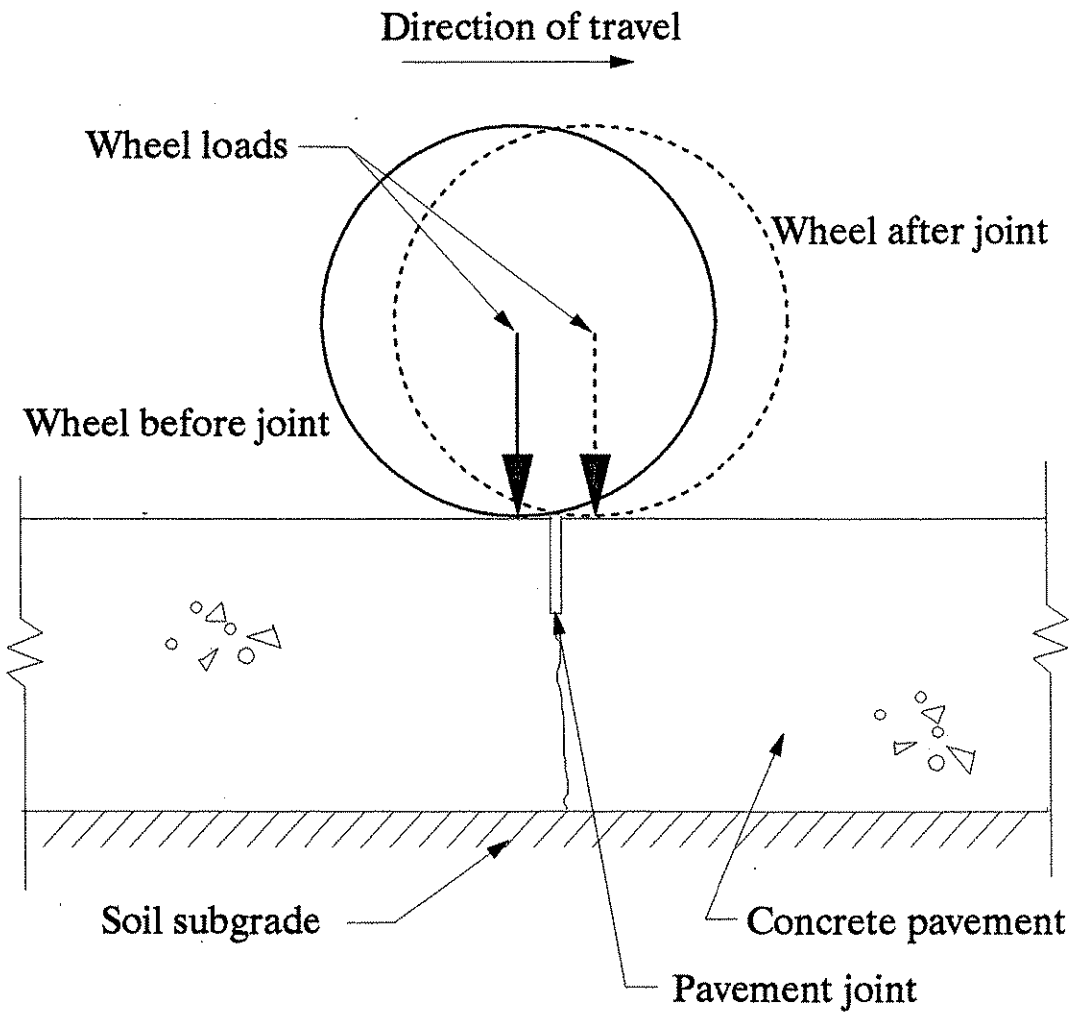

Figure 3.2 Schematic of wheel loads applied to a typical highway pavement joint

the typical spacing for a highway pavement in Iowa. As discussed in Section 2.2, Figure 2.2 includes a diagram of a typical highway pavement, including transverse joints with dowels. The joints in the figure are shown at a skew to the centerline, which is commonly used in highway pavement

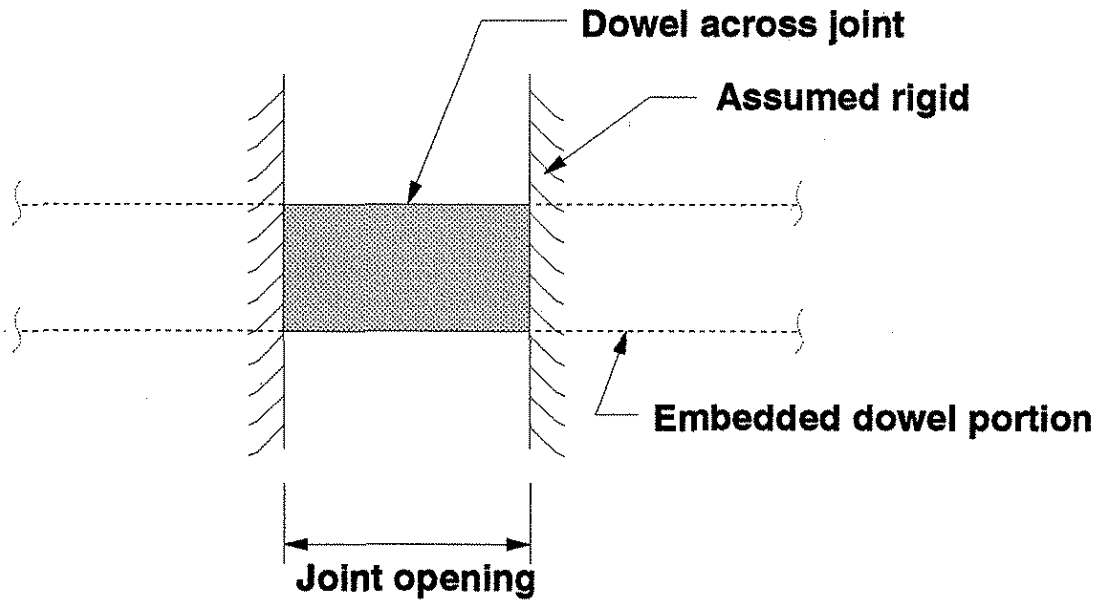

Figure 3.3 Dowel modeled as a beam across a pavement joint

construction in Iowa. A skew of the joint was not modeled in the full-scale laboratory testing because of the difficulty in providing a simulated subgrade at such an angle, and because the authors believed that the performance of the dowels would be sufficiently evaluated without including the skew.

In addition to determining the displacements of a full-size pavement structure model, the computer analysis was used to determine a theoretical equivalent load transfer system using 1.75-inch diameter FC dowels in place of 1.5-inch steel dowels, which are normally spaced at 12 inches. Pavement displacements due to a loading by a standard 18-kip axle, were the criteria for equivalence. Two models, one with FC dowels

and one with steel dowels, were analyzed, with all variables being the same in both models except for the dowel properties and spacing. Through a trial and error process of analysis of the full-size pavement model, an equivalent system was found to require 1.75-inch diameter FC dowels spaced at eight inches center-to-center.

Despite the detail given to the computer modeling, there were several differences between the model and an actual highway pavement structure. In an actual pavement, the supporting foundation does not have properties that are constant over time. With the repeated loading applied by traffic and because of climatic changes, the soil subgrade does not resist applied loads equally at all times. Subgrade failure in a pavement drastically affects the performance of the pavement and its useful life. A computer model of the pavement, on the other hand, did not consider any change in the properties of the subgrade. Therefore, the conservative value for the modulus of subgrade reaction, K, of 100 pci was selected.

As mentioned previously, the dowel was modeled as a beam that was rigidly connected at both ends to the slabs adjoining at the joint. A rigid connection, then, allows no rotation of the dowel, while an actual dowel is able to rotate somewhat at the interface with the concrete. Rotation is possible because the concrete is not a perfectly rigid material.

Another difference between the model and the actual

pavement deals with the joint opening. A joint opening of 0.5 inches was used in the computer model, while an actual pavement has an opening that can vary, dependent upon climate and other variables. For example, in warm weather, a pavement will have essentially no opening, and, in fact, may have aggregate interlock between the two slab sections meeting at the joint. In cold weather, on the other hand, a joint opening as large as one-half-inch can occur, which was the joint width applied in the computer model. These variations greatly influence the type of action applied to the dowels, which is illustrated in Figure 3.4.

3.3 Laboratory Testing Setup Model

After completing the modeling and analysis of the full-size pavement, similar modeling and analysis was applied to a model of the test setup to be used in the laboratory for the experimental fatigue testing of full-scale pavement slabs. The test setup included a simulated subgrade of steel beams in a simple span configuration, so that the system could be designed with the assistance of a computer model. In order to model a concrete slab supported by steel beams, a plate element was again used to model the slab, and "springs" were placed at the locations of the beams, as is shown in Figure 3.5. Using multiple springs to model beams, a linear relationship between the applied load and displacement was

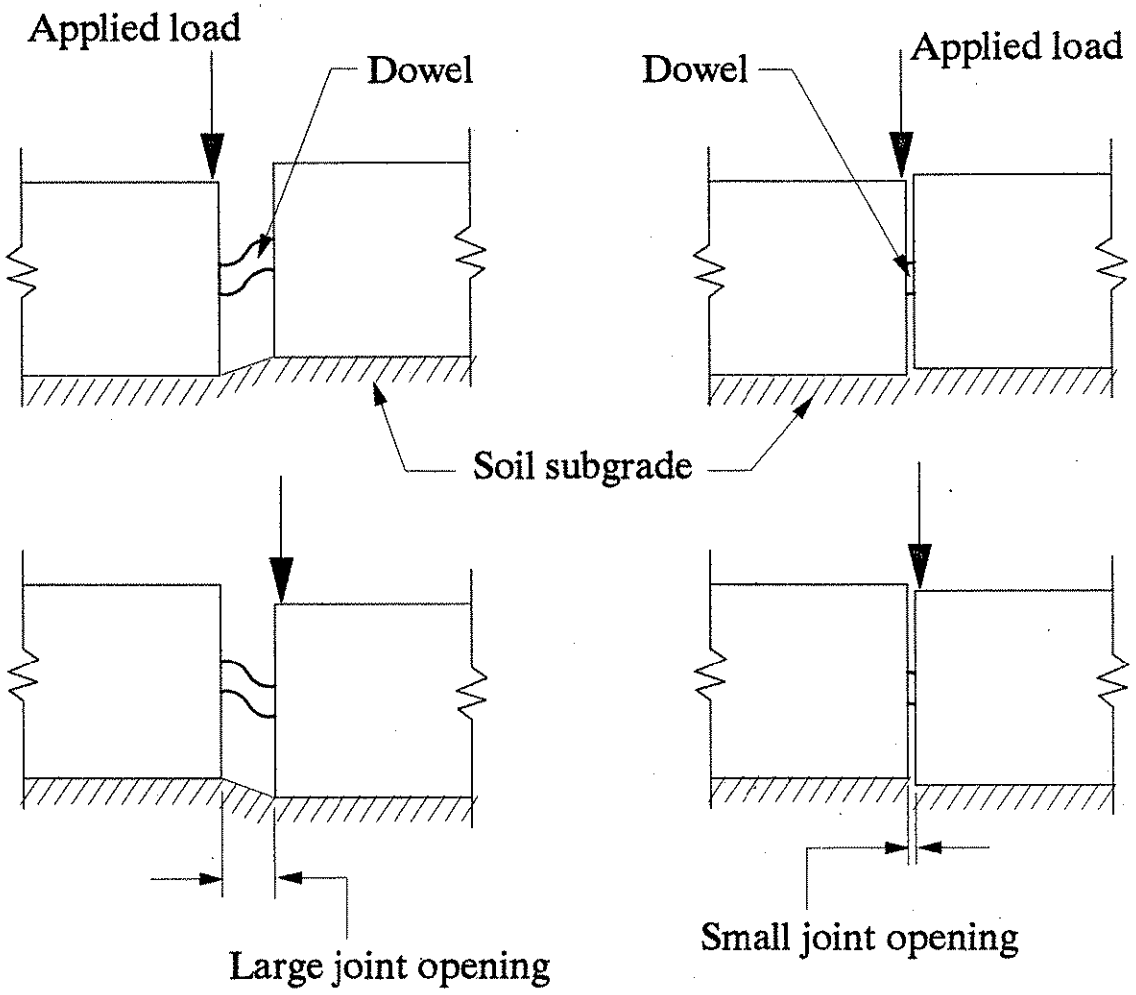

Figure 3.4 Influence of joint opening on dowel action

maintained.

A trial and error process was required to use the model as a tool in the design of the lab setup. Using static loading on the slab, the properties of the springs were adjusted until the displacements in the lab model

approximately matched those of the full-size pavement model. Because of the symmetry of the model, the load shown in Figure 3.5 can be applied to either side of the joint with the results being symmetric. When, after several trials, the displacements were satisfactory, the reaction values in the springs were used to design the beam sections. The reactions experienced by the springs were applied to the simple span supporting beams as an equivalent uniform loading because of the small differences between the spring reactions at each beam location. With these loads applied as shown in Figure 3.6, the supporting beam sections were designed to approximately match the displacements desired for the slab.

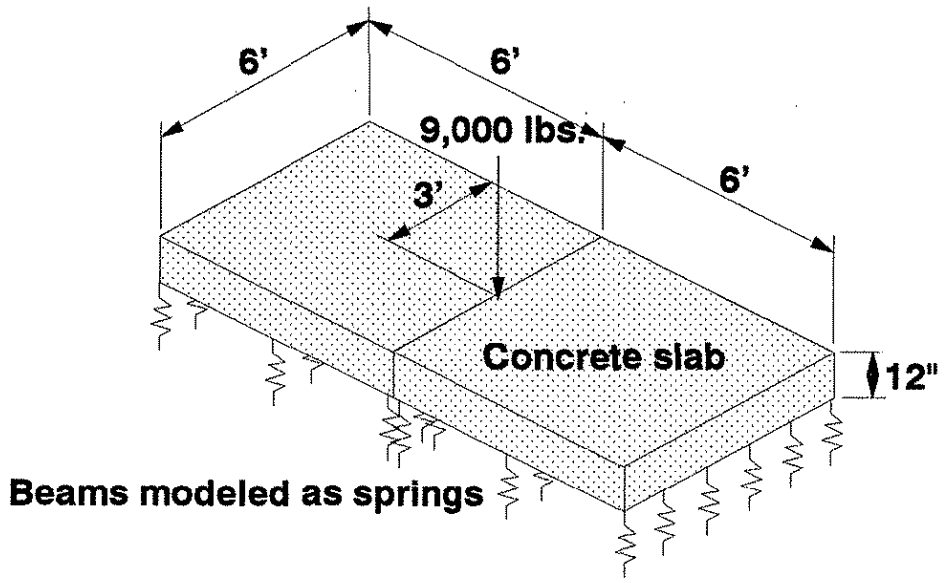

Figure 3.5 Computer model of full-scale slab laboratory testing setup

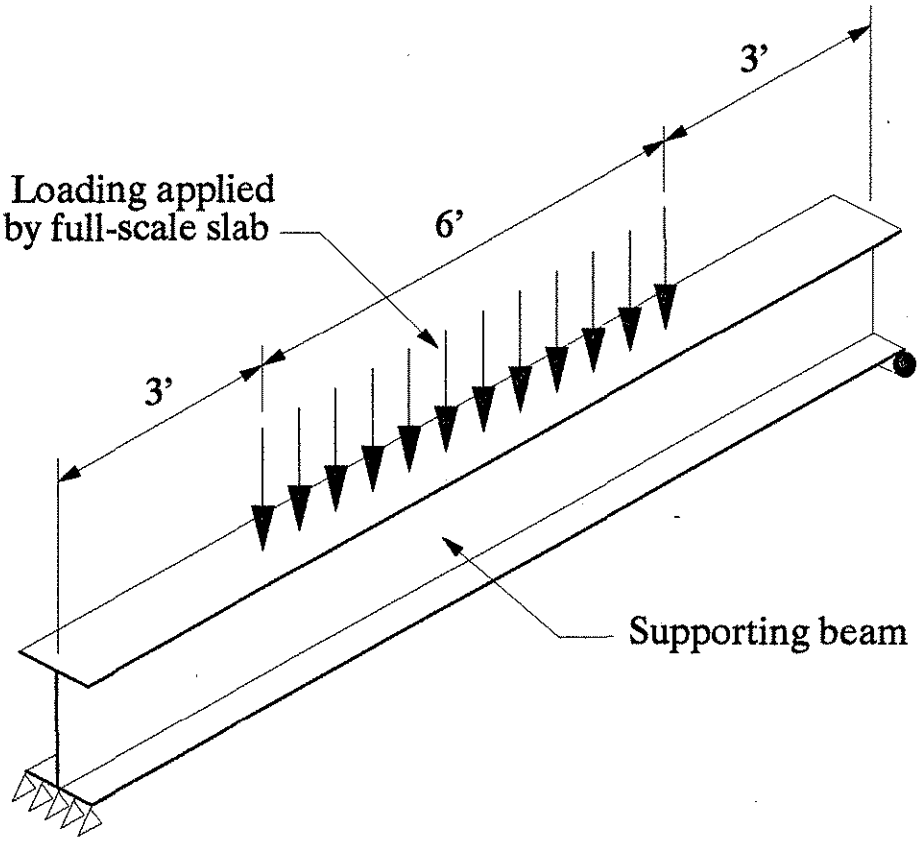

Figure 3.6 Reactions from computer model of full-scale lab setup applied to supporting beams

CHAPTER 4 LABORATORY EXPERIMENTAL INVESTIGATION

4.1 FC Dowel Property Testing

4.1.1 Introduction

In the analysis of highway pavement joints with dowels, the flexural and shear properties of the dowels must be known. Therefore, these properties were investigated, both experimentally and by composite materials theory, for the FC materials studied in this research. Testing of FC materials differs from testing of some other materials, such as steel, because FC materials are anisotropic, and the performance of a particular material is a function of the components of that material.

4.1.2 Proportions of FC components

In order to determine the properties of FC materials by analytical methods of composite materials theory, the proportions of each of the components of the FC must be known. Testing was completed to determine the proportions of E-glass and of vinyl ester resin contained in the material studied in this research.

Samples were taken from the FC dowels studied in this research and were evaluated by a test procedure which included

burning a small sample at a high temperature to destroy the resin contained in the specimen, while leaving the glass. The test procedure is referred to as a "burn-down" test. The procedure followed ASTM D2584-68 (Annual 1991) standard testing practices, and resulted in the proportions of resin and glass by weight, referred to as the weight fractions. Results of the "burn-down" test are shown in Table 4.1, along with the calculated proportions of the two components by volume, or the volume fractions. The calculation of volume fractions were performed while assuming a value for the specific gravity of E-glass, SG_f, of 2.57, which is a median value for such materials (Auborg 1986).

Table 4.1 Weight and volume fractions of FC dowel material

Component	Weight Fraction	Volume Fraction
E-glass	0.76	0.57
Vinyl ester resin	0.24	0.43

In order to determine the volume fraction of each component from the weight fraction, the unit weight of the FC material was needed. The weight of a single FC dowel with a diameter of 1.75 inches and a length of 18 inches was found to be an average of 1,362 grams (3.00 lbs). The following includes sample calculations to determine the volume fractions

of the fibers and the resin.

The volume fraction of fibers is expressed in Equation 4.1 by applying standard relationships between volumes, weights, and unit weights.

$$v_f = \frac{V_f}{V_D} = \frac{\frac{W_f}{\gamma_f}}{\frac{W_D}{\gamma_d}} = \left(\frac{W_f}{W_D}\right)\left(\frac{\gamma_d}{\gamma_f}\right) \qquad \text{Eqn. 4.1}$$

Because the FC material was assumed to contain only glass fibers and resin, Equation 4.2 can be used to determine the volume fraction of the resin matrix.

$$v_m = 1 - v_f - v_v \qquad \text{Eqn 4.2}$$

where,

v_f = volume fraction of fibers
v_m = volume fraction of resin matrix
v_v = volume fraction of voids within the FC material (assumed to be = 0)
V_f = volume of fibers in one dowel (ft^3)
V_D = volume of one FC dowel
= 0.02506 ft^3
W_f = weight of fibers in one dowel (lbs)
W_D = weight of one FC dowel
= 3.00 lbs
γ_f = unit weight of fibers (lbs/ft^3)
γ_d = unit weight of FC dowel material (lbs/ft^3)

The volume of a single dowel, was determined by the relationship for solid cylinders in Equation 4.3.

$$V_D = \frac{\pi d^2}{4} L_D \qquad \text{Eqn. 4.3}$$

where,

d = dowel diameter = 1.75 inches
L_D = dowel length = 18 inches

The volume of a single FC dowel was found to be 43.30 $in.^3$ or 0.02506 ft^3 by substituting the values for diameter and length, 1.75 and 18 inches, respectively, into Equation 4.3. The unit weight of the FC material is expressed in Equation 4.4.

$$\gamma_d = \frac{W_D}{V_D} \qquad \text{Eqn. 4.4}$$

Substituting the measured weight and calculated volume into Equation 4.4, the unit weight was determined to be 119.8 lbs/ft^3. The specific gravity of the FC dowel material, SG_d, was determined by Equation 4.5.

$$SG_d = \frac{\gamma_d}{\gamma_{water}} \qquad \text{Eqn. 4.5}$$

Applying the unit weight of the dowel material and the unit weight of water, γ_{water} = 62.4 lbs/ft^3, to Equation 4.5 results in a specific gravity of 1.92.

From the "burn-down" test, the weight fraction of glass was determined to be 0.76, which can be expressed as shown in Equation 4.6.

$$\frac{W_f}{W_D}=0.76 \qquad \text{Eqn. 4.6}$$

By assuming that the dowel consists of only resin and glass, Equation 4.7 applies.

$$\frac{\gamma_d}{\gamma_f}=\frac{SG_d}{SG_f} \qquad \text{Eqn. 4.7}$$

Then, the results of Equations 4.6 and 4.7 were substituted into Equation 4.1, and the volume fraction of fibers, v_f, was determined to be 0.57. This result was then substituted into Equation 4.2 to determine the volume fraction of resin matrix, v_m, to be 0.43.

4.1.3 Composite materials theory

Properties of unidirectional composite materials can be determined by applying the theory presented by Tsai and Hahn (Tsai 1980), which considers that the composite properties are a function of the properties of each of the components of the composite. For the calculations performed in this investigation, the material was considered as a composite of only E-glass fibers and vinyl ester resin. The proportions of each material, as discussed in Section 4.1.2, were determined experimentally to be 57 percent glass and 43 percent resin by volume. Volume fractions are the proportions applied in the

Tsai and Hahn methods. For this investigation, properties of the two components were those provided by the manufacturer, where possible, or typical properties established for similar materials.

The models applied by Tsai and Hahn to determine the longitudinal modulus of elasticity, E_x, and Poisson's ratio, ν_{xy}, are based on a rule of mixtures approach. The Poisson's ratio, ν_{xy}, is symbolized with two subscripts, the first, x, signifying the direction of applied load. The second subscript, y, signifies the direction of the transverse strain caused by the load. In the case of a unidirectional fiber composite material, the x-axis is parallel to the direction of the fibers. The rule of mixtures approach considers the properties and volume fraction of each component of a composite in order to determine the composite properties. Equations 4.8 and 4.9 (Tsai 1980) were used to evaluate E_x and ν_{xy}, respectively.

$$E_x = V_f E_f + V_m E_m \qquad \text{Eqn. 4.8}$$

$$\nu_{xy} = V_f \nu_f + V_m \nu_m \qquad \text{Eqn. 4.9}$$

where,

v_f = volume fraction of E-glass fibers
= 0.57 (see Section 4.1.2)
v_m = volume fraction of vinyl ester resin matrix
= 0.43 (see Section 4.1.2)
E_f = modulus of elasticity of E-glass fibers (psi)
= 10.5 x 10^6 psi (Fiber 1991)

E_m = modulus of elasticity of vinyl ester resin matrix (psi)
= 0.49×10^6 psi (DERAKANE 1990)
ν_f = Poisson's ratio of E-glass fibers
= 0.22 (Fiber 1991)
ν_m = Poisson's ratio of vinyl ester resin matrix
= 0.30 (DERAKANE 1990)

Substituting the above values into Equations 4.8 and 4.9 result in the values of E_x and ν_{xy} for the fiber composite of:

$E_x = 6.20 \times 10^6$ psi

$\nu_{xy} = 0.254$

To determine properties of the fiber composite material in a direction transverse to the direction of the fibers, a model referred to by Tsai and Hahn as the modified rule of mixtures was applied (Tsai 1980). The modified model considers the properties and proportions of each component, while also applying stress partitioning parameters, which are abbreviated by η and a subscript. These parameters are a measure of the relative magnitudes of average stresses in the fibers and matrix of the composite. When using the modified rule of mixtures, the matrix and fiber materials are both assumed to be isotropic, which allows for the calculation of the shear modulus, G, of each using the relationship involving Young's modulus, E, and Poisson's ratio, ν. Equations 4.10 and 4.11 show these relationships (Beer 1981).

Shear modulus of the resin matrix:

$$G_m = \frac{E_m}{2(1+\nu_m)} \qquad \text{Eqn. 4.10}$$

Shear modulus of the glass fibers:

$$G_f = \frac{E_f}{2(1+\nu_f)} \qquad \text{Eqn. 4.11}$$

Substituting the appropriate values from above for E and ν into Equations 4.10 and 4.11 results in values for the shear moduli of the two components to be:

G_m = 0.188 x 10^6 psi

G_f = 4.30 x 10^6 psi

The transverse modulus of elasticity, E_y, and the transverse shear modulus, G_{xy}, of the fiber composite material were determined by applying Equations 4.12 through 4.15 (Tsai 1980).

$$\frac{1}{E_y} = \frac{1}{V_f+\eta_y V_m}\left(V_f\frac{1}{E_f}+\eta_y V_m\frac{1}{E_m}\right) \qquad \text{Eqn. 4.12}$$

$$\frac{1}{G_{xy}} = \frac{1}{V_f+\eta_G V_m}\left(V_f\frac{1}{E_f}+\eta_y V_m\frac{1}{E_m}\right) \qquad \text{Eqn. 4.13}$$

$$\eta_y = \frac{1}{2}\left(1+\frac{E_m}{E_f}\right) \qquad \text{Eqn. 4.14}$$

$$\eta_G = \frac{1}{4(1-\nu_m)}\left(3-4\nu_m+\frac{G_m}{G_f}\right) \qquad \text{Eqn. 4.15}$$

where,

E_y = transverse modulus of elasticity of the FC material (psi)
G_{xy} = transverse shear modulus of the FC material (psi)
η_y = stress partitioning parameter for transverse modulus of elasticity
η_G = stress partitioning parameter for transverse shear modulus

The known property values for each of the component materials were substituted into Equations 4.14 and 4.15, with the resulting values of η_y and η_G placed into Equations 4.12 and 4.13, respectively. Then, the resulting values for E_y and G_{xy} were determined and are shown, along with the properties determined earlier, in Table 4.2.

Table 4.2 Theoretical properties of the FC dowel material

E_x	ν_{xy}	E_y	G_{xy}
6.20×10^6 psi	0.254	1.55×10^6 psi	0.476×10^6 psi

4.1.4 Flexural testing

4.1.4.1 Introduction

Included in the research was experimental testing to determine structural properties of the FC dowel material, such

as flexural and shear modulus. Several load configurations were applied for flexural testing of FC dowels. Both three-point and four-point bending, which are shown in Figure 4.1, were utilized. The four-point test application was necessary because strain gages were mounted at the center of the span of one dowel. Therefore, the load was to be applied away from the center of the span, so that the gages were not disturbed. No strain gages were placed on specimens tested in three-point bending.

The calculation of the experimental flexural modulus of elasticity of a specimen, assuming pure bending, applies the measured displacements and the corresponding applied loads from a particular flexural test. The relationships between the measured load, measured displacement, beam (dowel) properties, and modulus of elasticity for the two simple beam configurations of Figure 4.1 can be found in most engineering mechanics books, and those applied to this testing are expressed in Equations 4.16 through 4.19 (Load 1986).

For a single concentrated load at mid-span (three-point bending):

$$\Delta = \frac{P_1 L^3}{48 E_b I} \qquad \text{Eqn. 4.16}$$

where,

Δ = deflection at the middle of a simple span flexural test (in.)
P_1 = load applied in three-point bending (lbs)
L = length between supports for a simple span (in.)
E_b = flexural modulus of elasticity (psi)

I = moment of inertia of a flexural specimen
= $\pi d^4/64$ in^4

Solving Equation 4.16 for E_b gives Equation 4.17.

$$E_b = \left(\frac{P_1}{\Delta}\right)\frac{L^3}{48I} \qquad \text{Eqn. 4.17}$$

where,

P/Δ = slope of the load-deflection curve from a flexural test where P is equal to either P_1 or P_2 (lbs/in.)

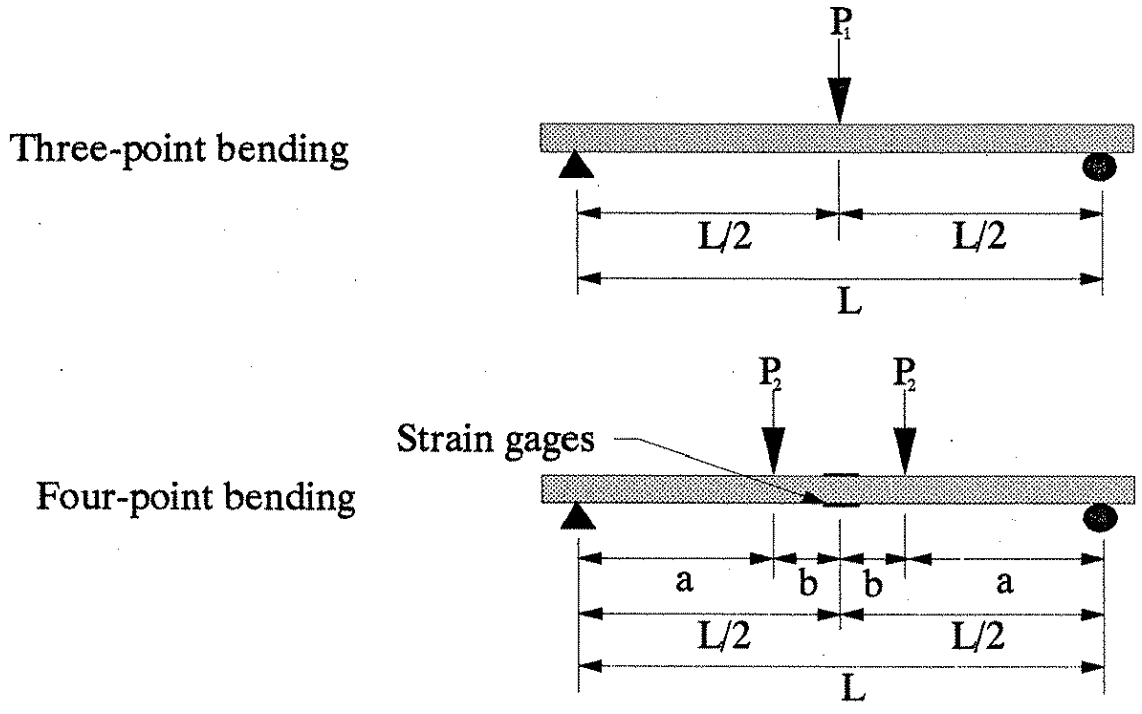

Figure 4.1 **Test setups for three-point and four-point flexural testing of FC dowels specimens**

For two equal concentrated loads symmetrically placed in the span (four-point bending):

$$\Delta = \frac{P_2 a}{24 E_b I}(3L^2 - 4a^2) \qquad \text{Eqn. 4.18}$$

where,

P_2 = loads applied in four-point bending (lbs)
a = distance from a support to the nearest load point in four-point bending (in.)

Solving Equation 4.18 for E_b gives Equation 4.19.

$$E_b = \left(\frac{P_2}{\Delta}\right)\left[\frac{a}{24 I}(3L^2 - 4a^2)\right] \qquad \text{Eqn. 4.19}$$

By solving Equations 4.16 and 4.18 for E_b to get Equations 4.17 and 4.19, respectively, the modulus of elasticity is a function of the quantity of P/Δ. This quantity was then taken to be the slope of the regression line for the load versus deflection data from the flexural tests. The value of E_b was then determined by inserting the experimental values of P/Δ into the expression for the associated test configuration (three-point or four-point bending).

Displacements of the flexural specimens under load were measured, in all cases, at the center of the span by an electronic measuring device called a direct current displacement transducer, or DCDT. These displacements, as well as the load and strain readings, were collected during testing by a personal computer interfaced with a data

acquisition system.

4.1.4.2 Full-size dowel specimens

Unlike common construction materials, such as concrete and steel, the flexural behavior of a fiber composite material is often greatly influenced by the shear properties of the material. In this study, the effects of shear deformation during flexural testing of FC dowels with diameters of 1.75 inches and lengths of 18 inches were found to be significant. Therefore, the analysis of data from flexural testing of full-size FC dowel specimens included shear deformation effects.

Shear properties, such as the transverse shear modulus, G_{xy}, cannot be determined by the flexural test method, but an expression involving G_{xy} and E_y can be developed using equations for deflection which includes both shear and flexural deformation components. In order to determine G_{xy}, separate and independent testing must be performed. The test method recommended by Munjal (1989) in an ASTM publication is the Iosipescu shear test for fiber composites. The Iosipescu method has been applied extensively through testing by Adams, Walrath, and others (Adams 1987; Walrath 1983). Though this method is not yet fully approved by ASTM, the procedure has been shown to be the best means for determining values for shear modulus of FC materials.

Shear deformation was included in the analysis of results

from the flexural testing of full-size FC dowels with the three-point test configuration. Equation 4.16 was modified to include shear deformation for such a load case. The modified form is given in Equation 4.20, and the development of this equation is included in the Appendix, where Equation A7 expresses the relationship in general terms. Equation 4.20 is expressed with the specific variables substituted for E, I, and G.

$$\Delta = \frac{P_1 L^3}{48 E_b I_d} + \frac{P_1 L F}{4 G_{xy} A_d} \qquad \text{Eqn. 4.20}$$

where,

F = form factor, equal to 10/9 for a solid circular section
G_{xy} = transverse shear modulus of the FC dowel (psi)
A_d = cross sectional area of a FC dowel (in^2)

Equation 4.20 indicates that the total deflection at the midspan of a FC dowel tested by the three-point method is the summation of the deflection due to flexure and the deflection due to shear. Solving Equation 4.20 for Δ/P_1 results in Equations 4.21.

$$\frac{\Delta}{P_1} = \frac{L^3}{48 E_b I_d} + \frac{L F}{4 G_{xy} A_d} \qquad \text{Eqn. 4.21}$$

Equation 4.21 was used along with experimental results to develop a relationship involving the flexural modulus of elasticity, E_b, and the transverse shear modulus, G_{xy}. The value for Δ/P_1 was determined from the flexural tests of full-

size dowels to be the inverse of the slope of the regression line for the load-deflection data. Placing the experimental value of Δ/P_1 and the known dowel parameters, L, A_d, I_d, and F, into Equation 4.21, the resulting relationship includes only E_b and G_{xy}. Then, by determining one of these values by an independent test method, the other parameter can be found.

One such independent test is flexural testing using strain gages mounted on a full-size dowel specimen. In order to verify the results of other flexural tests, and to verify the application of strain gages on FC dowels, testing was performed with strain gages placed on a dowel specimen. The dowel was tested using the four-point bending method as shown in Figure 4.1, and two gages were placed 180 degrees apart at the center of the span of the dowel.

Calculation of the value of E_b from the strain gage data was performed using basic principles of engineering mechanics. As mentioned previously, a single FC dowel was instrumented with two strain gages, located at midspan. The strain at the midspan location was determined by averaging the strain values from the two gages. Equations 4.22 and 4.23 are equations relating stress, strain, section properties, and material properties (Beer 1981).

$$\sigma = \frac{Mc}{I} \qquad \text{Eqn. 4.22}$$

$$\sigma = E_b \epsilon \qquad \text{Eqn. 4.23}$$

where,

σ = normal stress (psi)
M = bending moment at a section (in.-lbs)
c = distance from the neutral axis to a point of interest for stress (in.)
I = moment of inertia at the section of interest (in^4)
E_b = flexural modulus of elasticity (psi)
ϵ = strain (in./in.)

For the four-point bending condition used for dowels with strain gages, the moment at the point of interest, which was the center of the span, was equal to the load at one load point, P_2, multiplied by the distance from the load point to the nearest support, a. By applying this relationship, substituting the moment of inertia of a dowel, I_d, for I, combining Equations 4.22 and 4.23, and solving for the modulus of elasticity, the result is Equation 4.24.

$$E_b = \frac{P_2}{\epsilon}\left(\frac{ac}{I_d}\right) \qquad \text{Eqn. 4.24}$$

In Equation 4.24, the quantity of P_2/ϵ is the slope of the regression line of applied load (ordinate) versus strain (abscissa) from the test data. Substituting the experimental value for P_2/ϵ and the known values for a, c, and I_d into Equation 4.24 results in a value for E_b.

4.1.4.3 Reduced-size flexure specimens

Two characteristics of the FC dowels introduced a

significant influence of shear deformation to the flexural testing of the full-size FC dowel specimens as described above. First, the shear modulus of the FC material in a plane transverse to the direction of the fibers was relatively small, which resulted in a relatively great influence of shear. Also, the diameter of the dowel, or the depth of the section during flexural testing, was somewhat large relative to the span between supports. Using a span of 16 inches, the span to depth ratio was 9.14 to 1, which was significantly smaller than the minimum ratio of 16:1 that is recommended by the ASTM in test procedures D4476-85 and D790-86 for flexural testing of similar materials (Annual 1991). To limit the influence of shear deformation while determining the flexural modulus of elasticity, E_b, testing was performed on flexural specimens meeting the geometry recommendations of the ASTM tests mentioned above. Because the value of the flexural modulus of elasticity of the reduced-size specimens was determined independently from other flexural tests, applying the E_b for the reduced specimens to Equation 4.21 as discussed in Section 4.1.4.2 resulted in an independent value for the shear modulus, G_{xy}.

Test specimens, referred to as reduced-size specimens, were cut from a 1.75-inch FC dowel to an approximately square cross-section, one-half-inch on a side, with a total length of ten inches. A span of eight inches between supports was used, resulting in a 16 to 1 ratio of span to depth. Figure 4.2

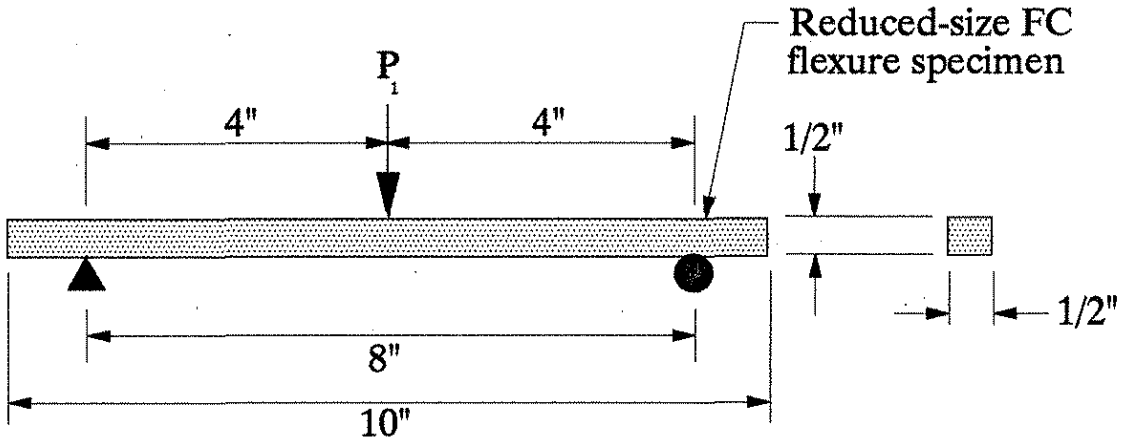

Figure 4.2 **Test setup for flexural testing of specimens cut from FC dowels (reduced-size specimens)**

includes a diagram showing the flexural test setup and the reduced-size specimens.

4.1.5 Results

The influence of shear deformation on flexural testing of full-size FC dowel specimens was found to be significant and can be seen from the test results from several specimens. When determining the flexural modulus of elasticity, deflection due only to flexure was desired. Therefore, to include the shear effects, the amount of shear deformation was subtracted from the total measured displacement, leaving displacement due to flexure alone.

Full-size dowel specimens were tested under three-point

bending, with midspan displacements and load collected with a data acquisition system. The results of the load and deflection data from testing of three separate dowels are shown in Figure 4.3. Included is the average value for the slope of the regression line, P_1/Δ = 30,899 lbs/in. Using the method of calculating the flexural modulus of elasticity discussed in Section 4.1.4.1 and applying Equation 4.17, an average value for the three specimens was determined to be, E_b = 5.73 x 10^6 psi. This value, though, was determined while neglecting any shear deformation of the dowel.

To consider the influence of shear deformation on the results mentioned above, the methods discussed in Sections 4.1.4.2, including Equations 4.20 and 4.21, were applied to the results shown in Figure 4.3. Substituting the inverse of the average regression line slope, P_1/Δ, and the known dowel section properties for a 1.75-inch diameter FC dowel (L = 16 in., I_d = 0.46 in^4, A_d = 2.405 in^2, and F = 10/9) into Equation 4.21, a relationship was developed involving the flexural modulus and the transverse shear modulus of the dowel. The resulting relationship, given in Equation 4.25, is satisfied for a distinct pair of values of E_b and G_{xy}.

$$\frac{185.35}{E_b} + \frac{1.8477}{G_{xy}} = \frac{1}{30,899} \qquad \text{Eqn. 4.25}$$

A full-size dowel was also tested with strain gages mounted at midspan and at the extreme compression and tension

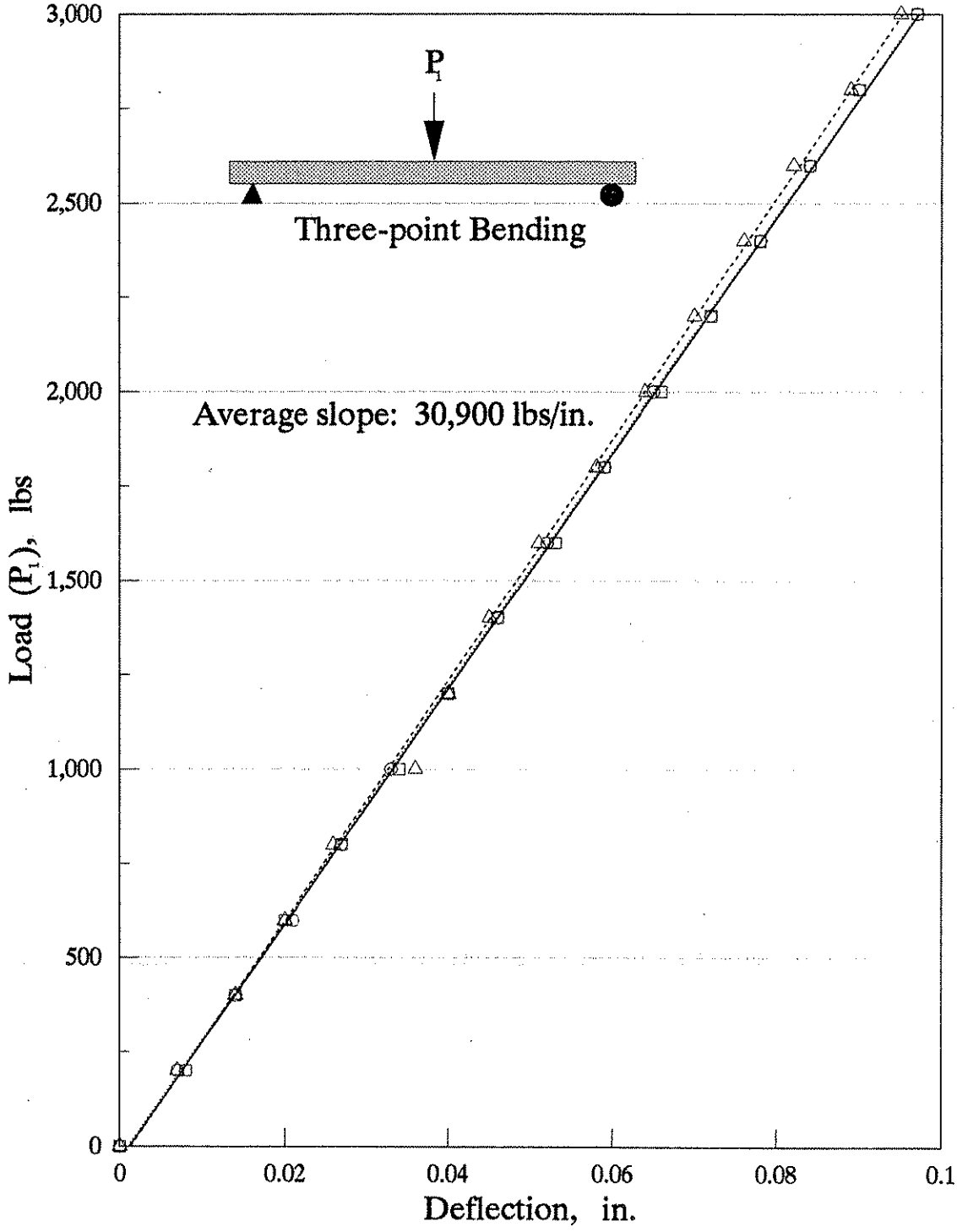

Figure 4.3 Load versus deflection diagram at the midspan of dowels tested by three-point bending

fibers. The results of the full-size flexural tests are shown graphically in Figure 4.4. Strain measurements from both gages are shown to be positive, as their absolute values are plotted. Applying the method discussed in Section 4.1.4.2 for determination of the flexural modulus from measured load and strain values, Equation 4.24 results in a value of, E_b = 6.42 x 10^6 psi. Because this result was determined from actual measured strains at the extreme fibers of the flexural member, this method reflects more closely the actual flexural stiffness of the dowel for this particular case.

A final test method using flexural specimens cut from a FC dowel, referred to as reduced-size specimens as described in Section 4.1.4.3, was applied to determine the modulus of elasticity, E_b, of the FC material. The test followed the method recommended by ASTM for flexural testing of FC materials, using a span to depth ratio of 16:1 and three-point bending. Four specimens were evaluated, with three separate tests performed on each specimen, for a total of 12 tests. During each test, load and deflection data were collected, and the load was applied up to 40 percent of the calculated failure load for the setup. Determination of the modulus of elasticity value followed the procedure described in Section 4.1.4.1, using Equation 4.17. The resulting calculated value was E_b = 6.22 x 10^6 psi. Figure 4.5 includes load-deflection diagrams from the flexural tests.

Values of flexural modulus of elasticity determined

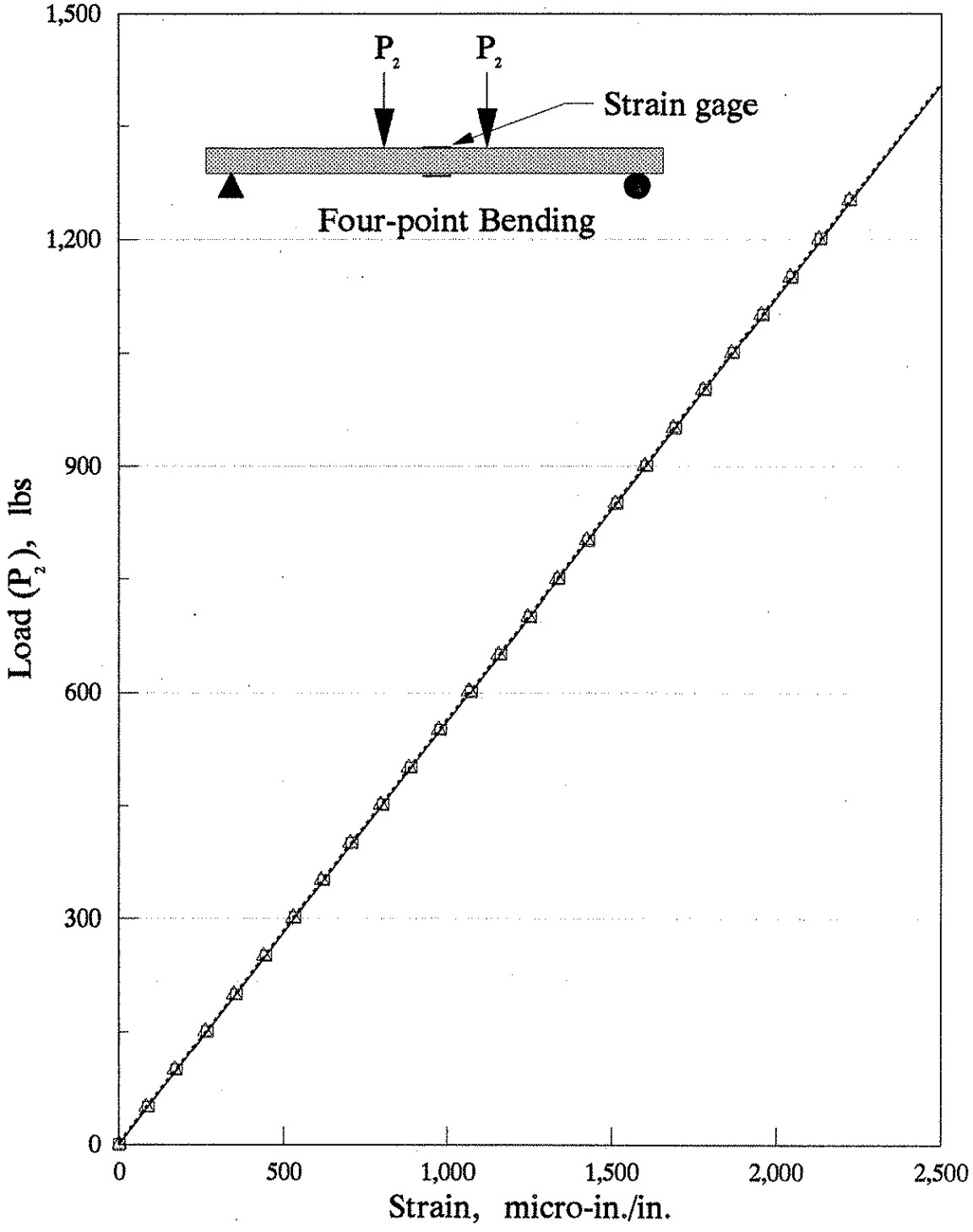

Figure 4.4 Load versus strain diagram at the midspan of a dowel tested by four-point bending

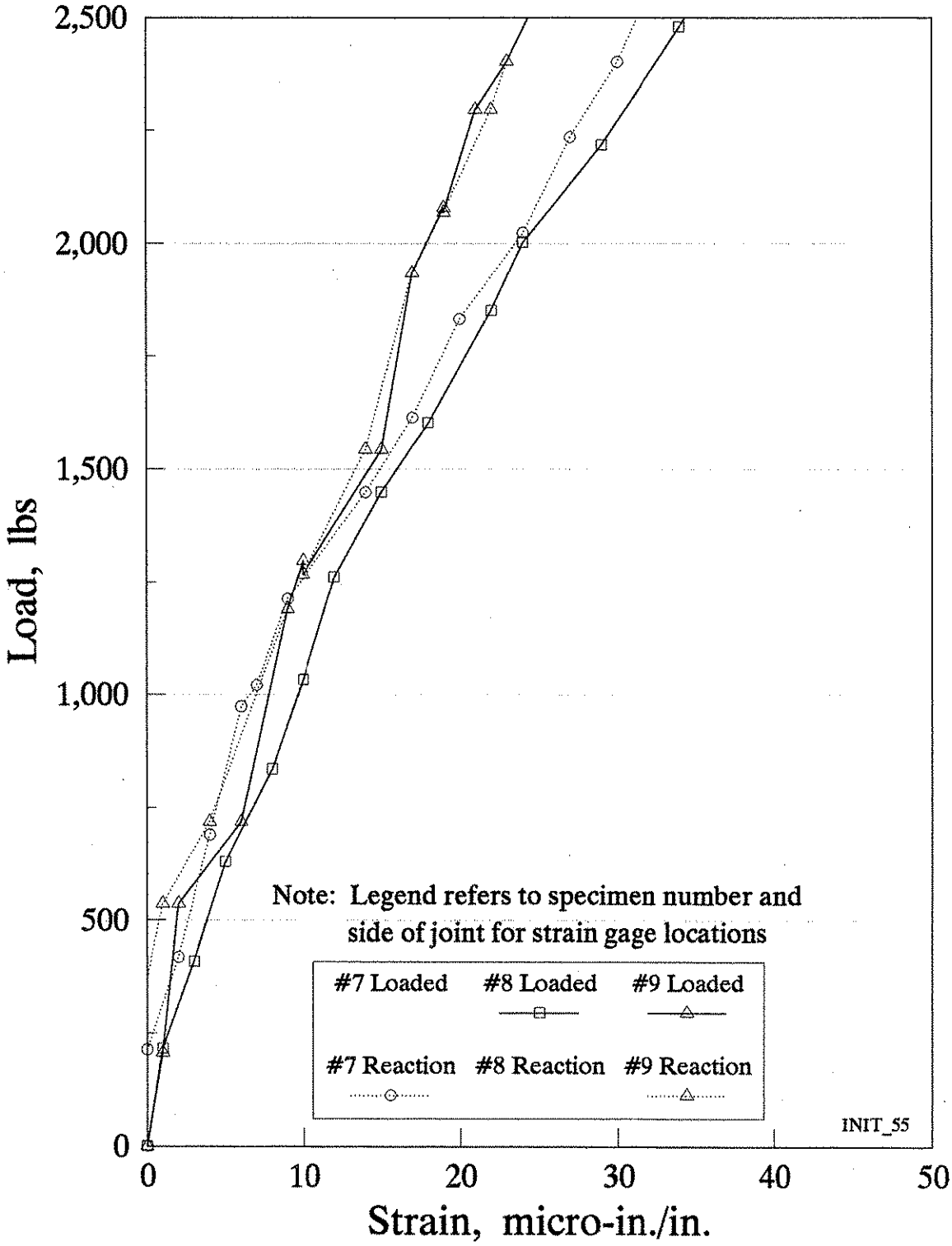

Figure 4.17 Initial load versus strain diagram at 5.5 inches from the joint of FC dowel elemental tests

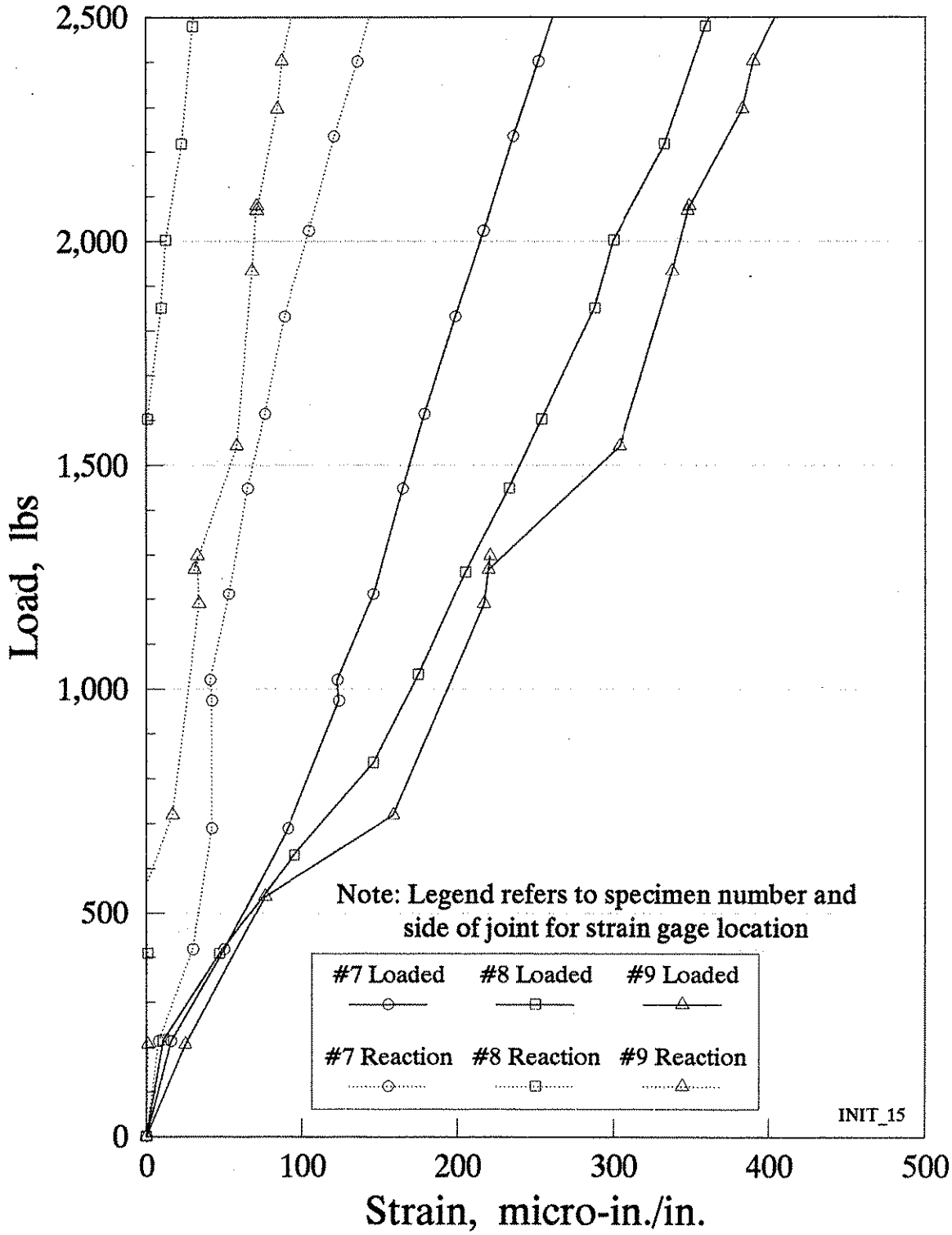

Figure 4.16 Initial load versus strain diagram at 1.5 inches from the joint of FC dowel elemental tests

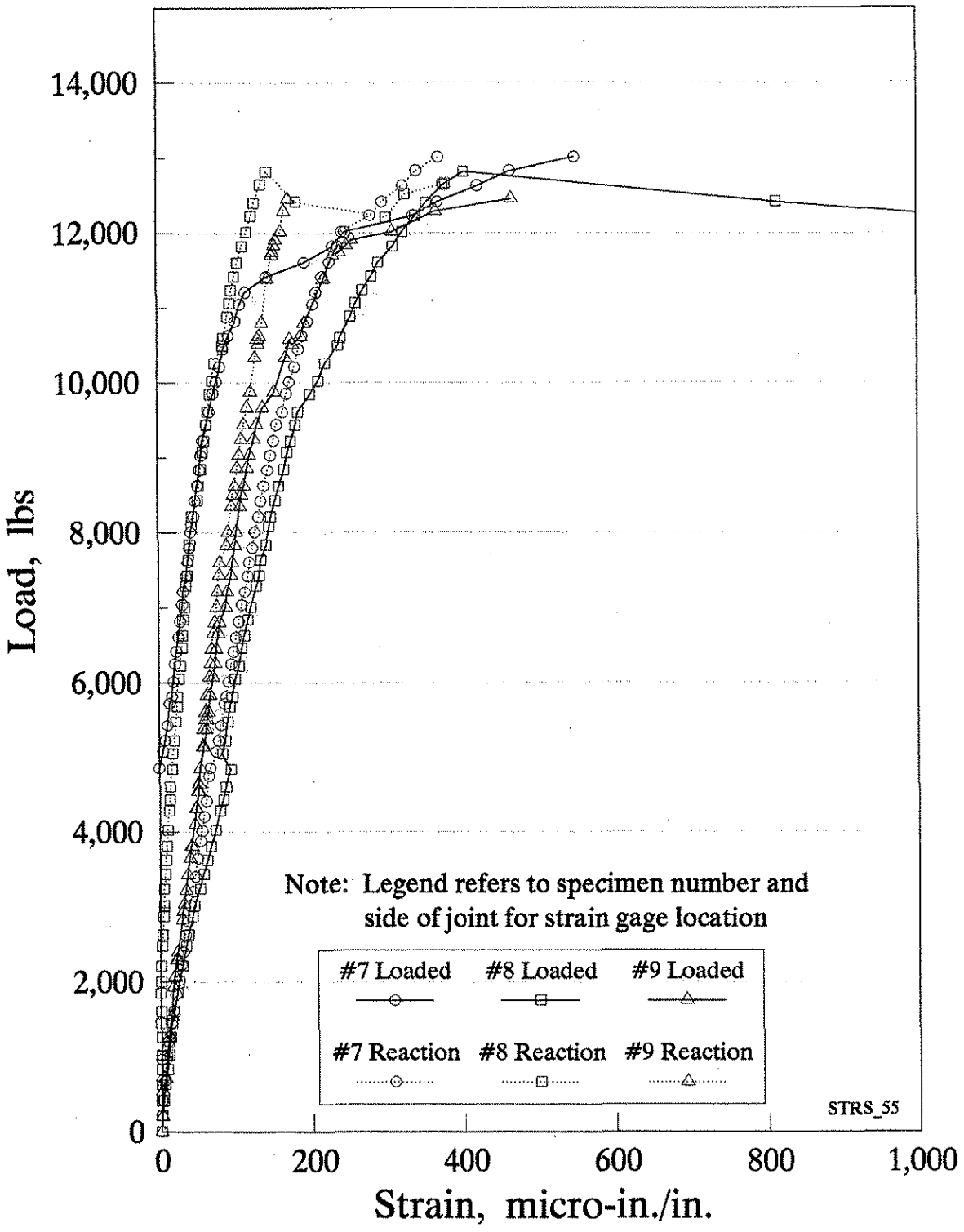

Figure 4.15 Load versus strain diagram at 5.5 inches from the joint of FC dowel elemental tests

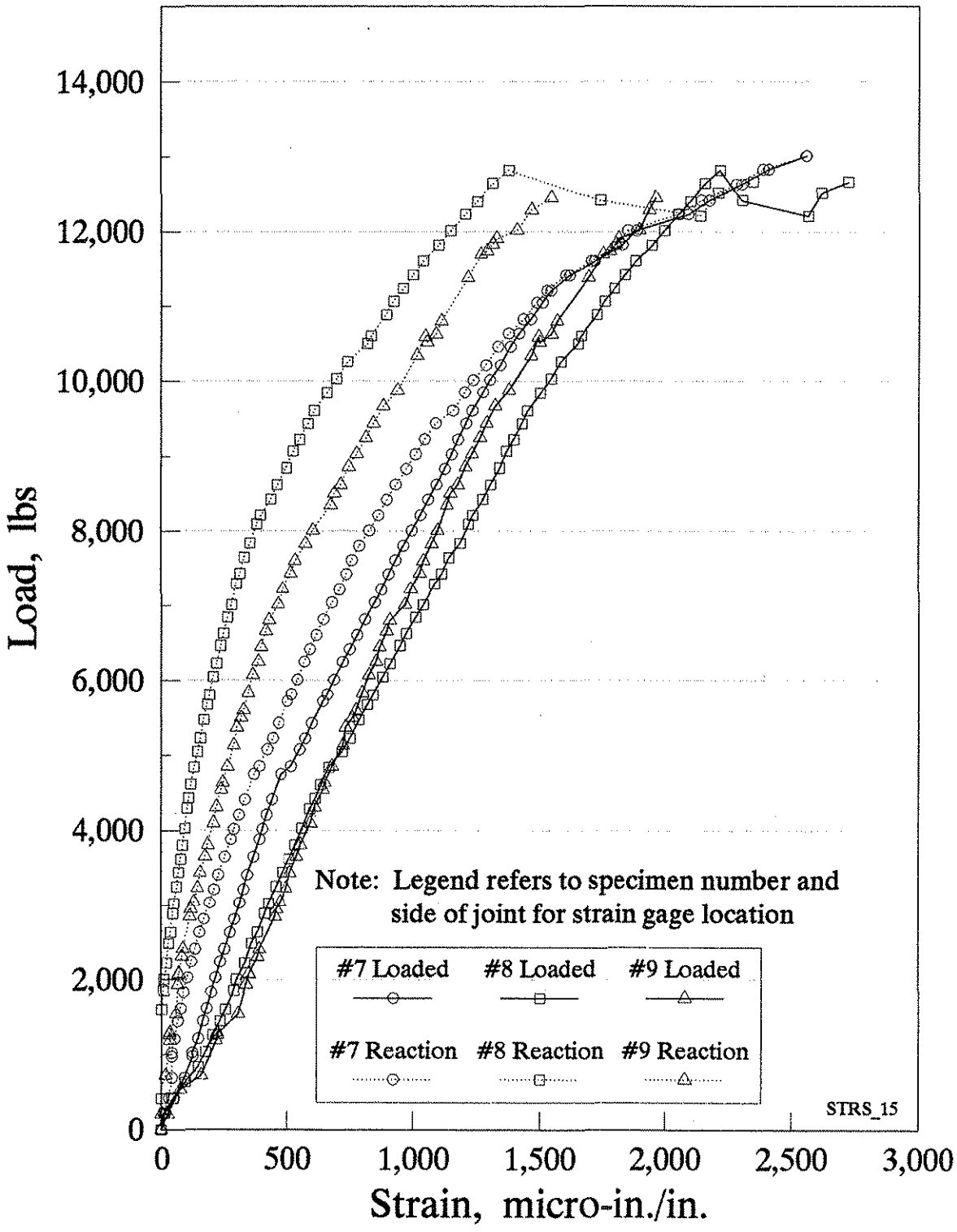

Figure 4.14 Load versus strain diagram at 1.5 inches from the joint of FC dowel elemental tests

4.14 and 4.15, respectively.

Because the range of load transfer for a single dowel that was of most interest in relation to highway pavement dowels is much smaller than the failure loads for the elemental tests, the dowel behavior at relatively small loads must be studied more closely. The strain gage data from the initial stages are shown in Figures 4.16 and 4.17 at the locations 1.5 and 5.5 inches from the joint, respectively. During the initial stages the difference in the strains of the loaded and reaction sides at 1.5 inches is more evident, but also, the linearity of the load versus strain relationship can be evaluated. Also noteworthy in Figure 4.17 is that the strains at 5.5 inches were similar for the loaded and reaction sides as well as being significantly smaller than at 1.5 inches. Further consideration was given to the data for the loaded side strain at 1.5 inches by performing a regression of the combined data from the three tests in the load range of 0 to 2,000 pounds. From the regression of the combined data, a single linear relationship was developed, and is shown in Figure 4.18. The developed regression equation is given in Equation 4.31.

$$P_s = 6.697 S_{1.5} \qquad \text{Eqn. 4.31}$$

where,

P_s = shear in the dowel at the joint (lbs)
$S_{1.5}$ = measured dowel strain at 1.5 inches from the joint on the loaded side (μin./in.)

values for EI and k_o.

The ratio of k_o values is smaller than the ratio of EI values, though the difference is most likely due to the variability of k_o values. Because the only difference between the elemental tests performed on the two types of dowels was the dowel material, the two ratios indicate that the flexural rigidity of the dowels in the elemental test specimens has a direct influence on the resulting values of k_o.

In addition to displacements, data was collected from the strain gages mounted on Specimens 7, 8, and 9 during testing. Results from these specimens indicated several interesting characteristics of the testing. In general, the three specimens behaved similarly with respect to measured strains. As discussed in Section 4.2.4, the gages were placed at four locations on each dowel specimen, with two instruments diametrically opposed at each location. The load was applied by the load ram through the mobile member to one side of the joint, referred to as the loaded side, while the other side was held rigid, referred to as the reaction side. One characteristic of the behavior of all three specimens was that of a significant difference in strain values between the loaded and reaction sides at 1.5 inches from the joint. Because of the pure shear conditions, the flexure of the dowel was expected to be approximately symmetric about the joint. Plots of load versus strain at 1.5 and 5.5 inches from the joint on the loaded and reaction sides are shown in Figures

determined for a load transfer of approximately 2,500 pounds.

As a comparison, the values for k_o determined by others using the same experimental procedures were considered. A value of k_o = 650,000 pci was determined for a 1.5-inch steel dowel bar in concrete with f'_c = 7,090 psi (Lorenz 1993). Testing of a 1.25-inch FC dowel bar, which was made of E-glass and a polyester resin, in concrete with f'_c = 8,000 psi resulted in a k_o of 148,000 pci (Porter 1990).

The difference in modulus of dowel support values for the elemental tests with 1.5-inch steel and the 1.75-inch FC dowels in concrete of the same strength (f'_c = 7,090 psi) is most likely related to the difference in structural stiffness, EI, of the two dowels. Table 4.5 includes values of the modulus of elasticity, moment of inertia, EI, and modulus of dowel support for the FC and steel dowels tested in the elemental specimens. Also given are the ratios of steel to FC

Table 4.5 Comparison of relative stiffness and k_o values for dowels tested in elemental specimens (f'_c = 7,090 psi)

Type of Dowel	Modulus of Elasticity, E (psi)	Moment of Inertia, I(in.^{2})	EI (lbs-in.^{2})	Modulus of Dowel Support, k_o (pci)
Steel	29×10^6	0.25	7.21×10^6	650,000
FC	6.20×10^6	0.46	2.85×10^6	358,000
Ratios: (i.e. EI_{steel}/EI_{FC})			2.53	1.81

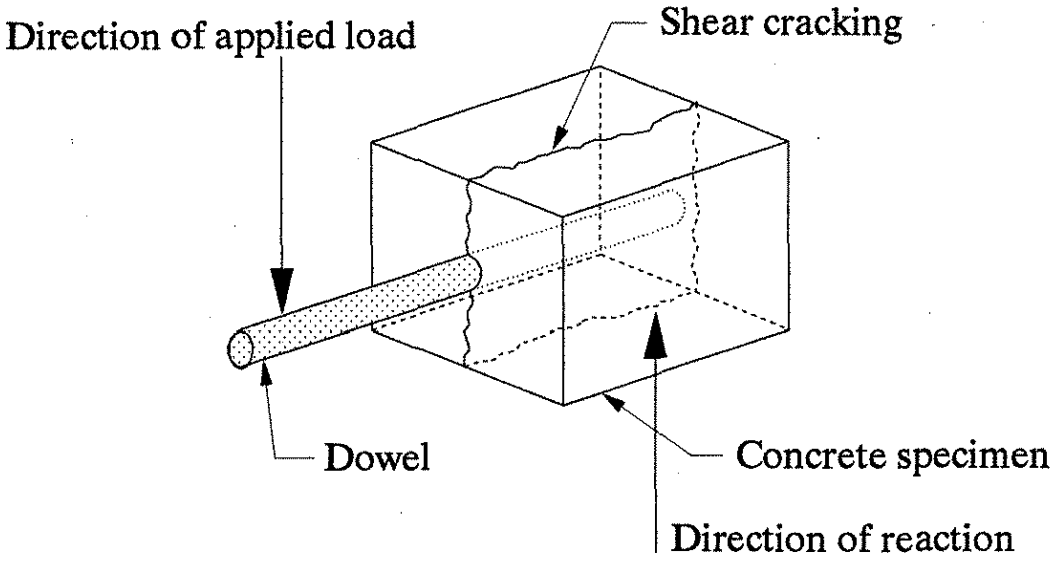

Figure 4.13 Typical shear splitting failure mode of elemental specimens with 1.75-inch FC dowels

specific to the particular dowel/concrete systems evaluated in this research, which includes a 1.75-inch diameter FC dowel embedded in concrete with a compressive strength, f'_c, as shown in Table 4.4.

In the analysis of the elemental specimens, the value of k_o determined from the load and deflection data was found to vary greatly dependent upon the load and deflection values that were used in the analysis. In previous work by Lorenz, k_o was calculated for a load transfer of 10,000 pounds and the associated experimental displacement (Lorenz 1993). Such a magnitude of load, though, is much larger than the service level conditions of an actual pavement dowel. Therefore, for this research, the values of the modulus of dowel support were

be due to the lower concrete strength or the absence of shear reinforcing in the second group. For the second group, the type of failure was consistent with results of previous work with this test method. All of the test specimens failed due to shear splitting of the concrete. The shear crack was formed in the same plane as the applied load, where previous test specimens had steel reinforcing placed across the expected crack. Figure 4.13 includes a diagram of how the shear failure mode occurred. As discussed in Section 4.2.3.3, no reinforcing was provided in the elemental specimens, so a shear splitting mode of failure was expected to occur.

One of the primary reasons for performing the elemental testing was to determine the value of the modulus of dowel support, k_o. The method for determining k_o was described in Section 4.2.6, using the experimental load transfer and displacements. Applying the analytical method to the results from the two groups of elemental specimens, the values of k_o as shown in Table 4.4 were determined. These values are

Table 4.4 Experimental values for modulus of dowel support for 1.75-inch FC dowels

Group	Number of Specimens	Concrete Compressive Strength, f'_c (psi)	Modulus of Dowel Support, k_o (pci)
1	3	7,090	358,000
2	6	5,090	247,000

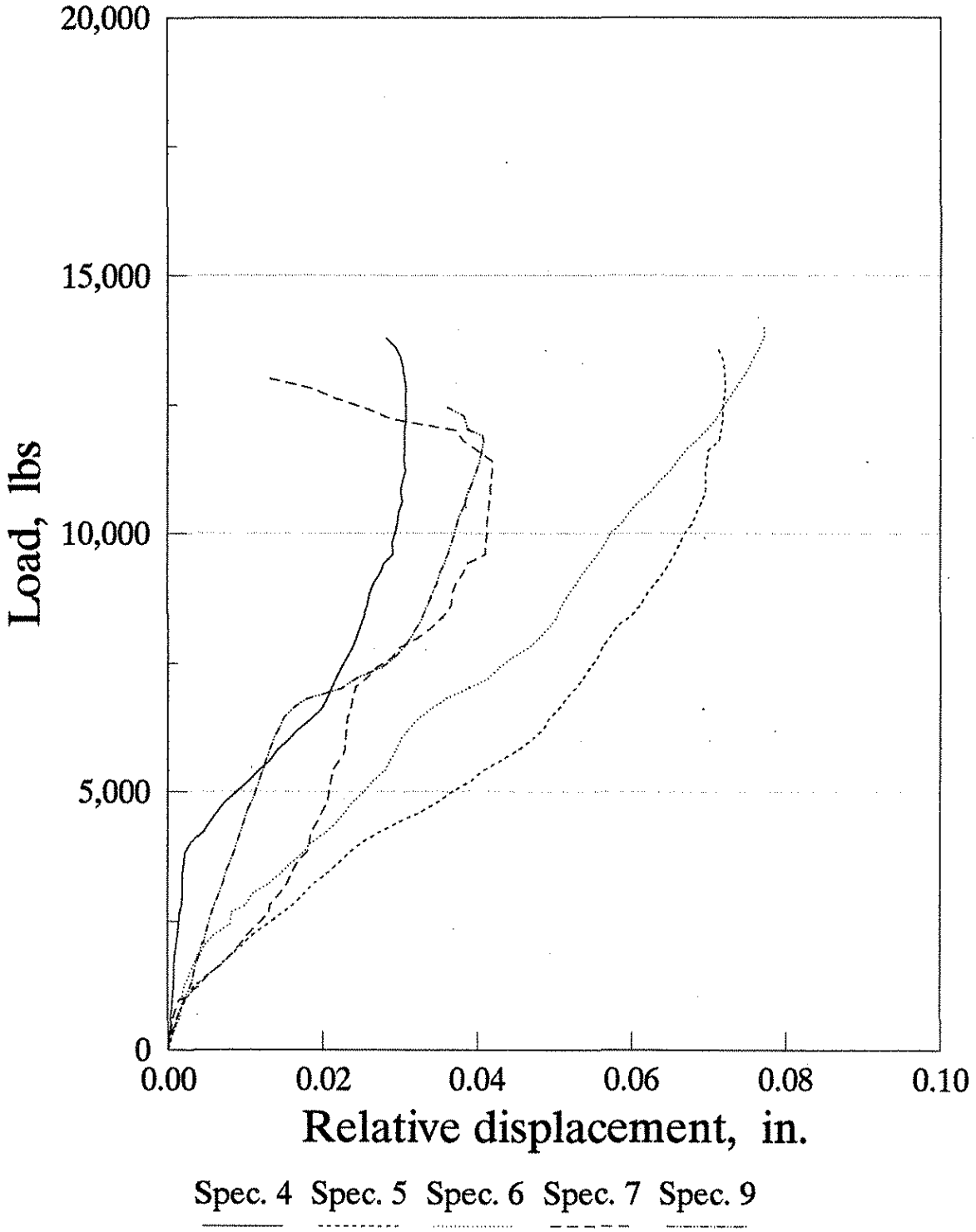

Figure 4.12 Load versus deflection diagrams from the second group of elemental specimens with 1.75-inch FC dowels

versus deflection for the group is shown in Figure 4.12. As mentioned in Section 4.2.4, three of the six specimens in the second group had strain gages placed on them. In Figure 4.12, the three are labeled as Specimens 7, 8, and 9, while Specimens 4, 5, and 6 had no strain gages. General behaviors of the two types of specimens differed in terms of load and deflection at failure, as well as the load versus deflection relationships at smaller loads. From the plots in Figure 4.12, Specimens 5 and 6 appeared to be less stiff than those with strain gages on the dowels, but failed at higher loads. The three specimens without strain gages (4, 5, and 6) failed at very consistent loads.

Specimens numbered 4, 7, and 9 behaved in similar manners during the test, with an initial linear segment, followed by a segment where the stiffness decreased and a final segment before failure when the stiffness increased. Because the final segment was quite linear before failure, the drop in stiffness could result from the final "seating" of the dowel within the concrete. Near the point of failure, the apparent decrease in displacement is due to instrument bias resulting from the rotation of the specimens at the large loads. Similar behavior was noted in the results of Specimen 2 from the first group of specimens (shown in Figure 4.11).

The loads at failure for the second group of specimens were also noted to be quite consistent and generally smaller than those for the initial three tests. Such a difference may

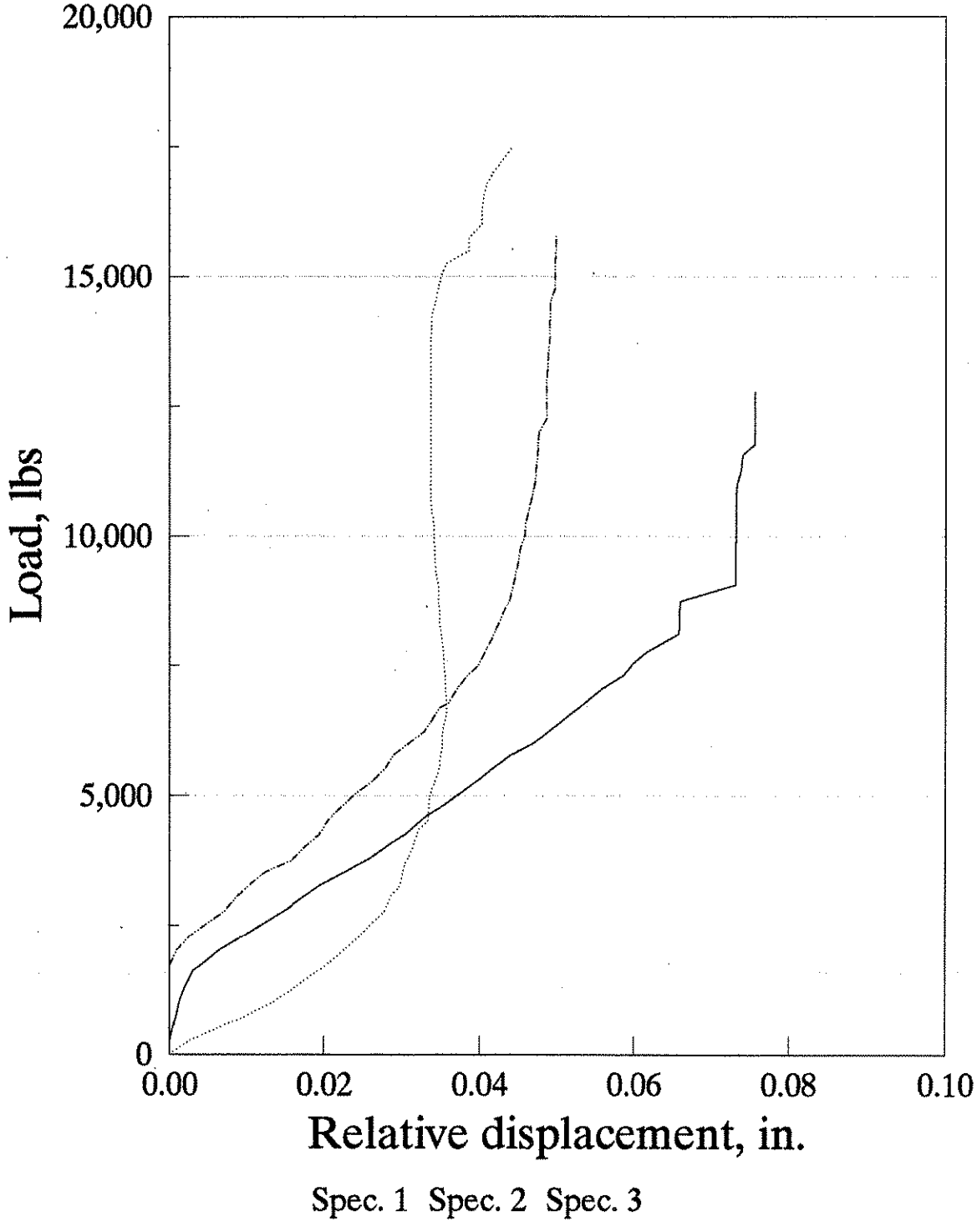

Figure 4.11 Load versus deflection diagrams from the first group of elemental specimens with 1.75-inch FC dowels

with strain gages at three locations, were tested with only the resulting load and deflection data being of use. Figure 4.11 includes the load versus deflection diagrams for the three specimens. The loads and measured displacements at failure for the three specimens vary rather significantly. The general trend in the load versus deflection data is an initial stiffness of the system that is rather constant, until a point when the stiffness increases up to a sudden failure. Two of the three specimens in the first group, labeled as Specimens 1 and 3 in Figure 4.11, followed a rather linear relationship after the initial stage and until approximately 7,500 pounds, when the system stiffened. The behavior of Specimen 2 was somewhat different, possibly because of an initial slip of the dowel within the concrete. Because of this behavior, consideration should be given to applying several cycles of a small load to each specimen before performing the test. Pre-loading would eliminate initial slip of the dowel occurring during the test, so that each specimen would perform more consistently. The apparent decrease in displacement of Specimen 2 as the load increased approximately from 6,000 to 14,000 pounds was due to displacement instrumentation bias. Rotation of the specimen due to applied load resulted in what appeared to be decreasing displacement at the instrument location.

From the data of the six specimens in the second group, several interesting trends were observed. A diagram of load

where,

F = form factor; 10/9 for solid circular section
P_s = dowel shear (lbs)
L_s = dowel shear span across the joint opening (in.)
A_d = cross sectional area of dowel (in^2)
G_{xy} = transverse shear modulus (psi)

In addition to the previous method of analysis, the elemental specimen behavior was studied by placing strain gages on the dowels within three of the elemental test specimens in the second group. The strain gage placements are discussed in Section 4.2.4. From the strain gage data, experimental moments in each dowel were determined at two locations on each side of the joint. The dowel moment values could then be analyzed and compared in order to indicate the flexural behavior of the dowels within the concrete specimens.

4.2.7 Results

Testing was carried out on the two groups of elemental specimens separately, with three specimens tested initially, and followed by testing of the six others. The differences between the two groups of specimens are described in Section 4.2.3.3 and include the concrete compressive strengths and the reinforcing placed in the specimens. Because of these differences, variations in the results were noticed between the two sets.

The first group of three specimens, which were equipped

that is a function of k_o, the distance from the joint along the length of the dowel, x, and the displacement of the dowel relative to the concrete at the face of the joint, y_o. Because k_o was to be determined for the system using an experimental value of y_o, a trial and error process was followed in order to find a solution. A value of x = 0 was substituted into the expression, which considers the specific location of the joint. Then, values for k_o were substituted into the expression and the resulting values for displacement, y_o, were determined. Successive values of k_o were applied until the calculated displacement was approximately equal to the experimental displacement at the joint. The final value of k_o was then taken as the experimental modulus of dowel support.

Experimentally, the value of y_o is expressed as:

$$y_o = \frac{(\Delta_r - \delta)}{2} \qquad \text{Eqn. 4.29}$$

Values for Δ_r come from experimentation and are the relative displacements measured between the two sides of the joint. The shear deformation, δ, was calculated by Equation 4.30 (Young 1989).

$$\delta = \frac{FP_s L_s}{A_d G_y} \qquad \text{Eqn. 4.30}$$

$$\frac{d^2y_o}{dx^2}=\beta^2e^{\beta x}(-2A\sin\beta x+2B\cos\beta x)+\beta^2e^{-\beta x}(2C\sin\beta x-2D\cos\beta x) \quad \text{Eqn. 4.27}$$

$$\frac{d^3y_o}{dx^3}=2\beta^3e^{\beta x}[-A(\cos\beta x+\sin\beta x)+B(\cos\beta x-\sin\beta x)]$$

$$+2\beta^3e^{-\beta x}[C(\cos\beta x-\sin\beta x)+D(\cos\beta x+\sin\beta x)] \quad \text{Eqn. 4.28}$$

where,

$$\beta=\sqrt[4]{\frac{k_od}{4EI_z}}\,(in.)^{-1}$$

y_o = deflection of a dowel within the concrete (in.)
x = distance along the length of the beam (in.)
k_o = modulus of dowel support (pci)
EI_z = flexural rigidity of a finite beam (lb-in^2)
A, B, C, D= constants in the solution for deflection of the dowel in concrete

Experimental relative displacements and the corresponding applied load, or load transfer, were used to determine the modulus value for the system. Four boundary conditions were required in order to solve for the deflection, shear, pressure, and moment diagrams along the length of the dowel. Load transfer at the joint is equal to the shear at that point, and the load transfer multiplied by ½ the joint opening gives the moment at the joint. Besides these two boundary conditions, the shear and moment values must be zero at the end of the dowel, giving the other two boundary conditions required. Solving the four equations results in an expression

value is specific to the particular dowel properties and concrete strength included in the testing. The theoretical model for analysis of pavement dowels within concrete was developed based upon theory originally presented by Timoshenko (1925; 1976). In the previous work by Lorenz, the dowel was modeled as a finite beam resting on an elastic foundation, which is shown in Figure 4.10. Relationships for the bending moment and shear along a finite beam were developed by the second and third differentials respectively, of Timoshenko's general solution for a beam on an elastic foundation. The general solution is an expression for the displacement along the length of the beam and is presented in Equation 4.26. The expressions for bending moment and shear along the beam are given in Equations 4.27 and 4.28, respectively.

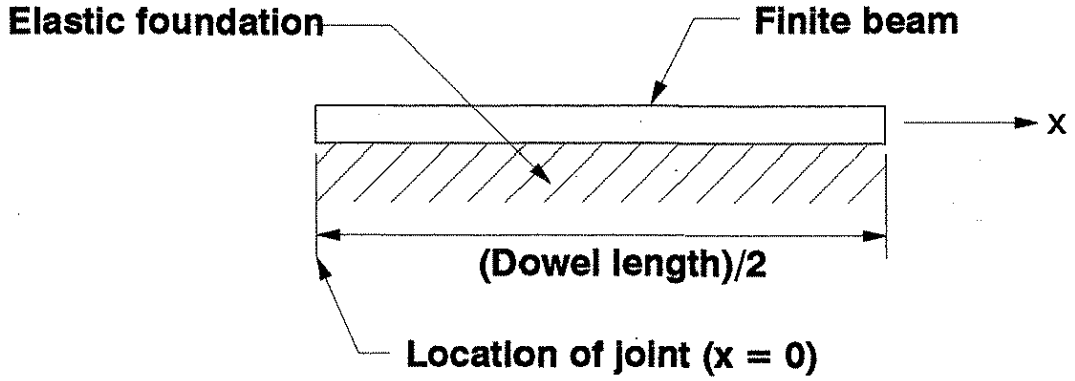

Figure 4.10 Beam on an elastic foundation (Lorenz 1993)

$$y_o = e^{\beta x}(A\cos\beta x + B\sin\beta x) + e^{-\beta x}(C\cos\beta x + D\sin\beta x) \qquad \text{Eqn. 4.26}$$

test frame, and the restraining rods were tightened to hold the specimen in place. Instrumentation was connected to a data acquisition system (DAS) which was interfaced with a personal computer. Before beginning load application to the specimen, the data collection was begun to measure initial conditions. Then, load was applied using a manual hydraulic pump connected to the hydraulic ram. The applied load was constantly monitored by the computer system, and readings of all the instrumentation were automatically taken at a predetermined interval of load set into the controlling program.

The test was continued until failure of the specimens. Failure was defined as a severe drop in the measured load while the relative displacement increased. Major cracking of the concrete usually indicated the point of failure of the specimen. The measured load could possibly increase after initial failure, but an increase would be due to restraint of the specimen due to the steel rods. Of course, behavior after failure would not indicate the performance of the dowels, so data beyond the initial failure was not considered.

4.2.6 Analytical investigation

Elemental testing was completed in order to experimentally determine the value of the modulus of dowel support, k_o, for a particular dowel/concrete system. This

approximately 1.5 inches from the joint, which was assumed to be near the point of maximum moment in the dowel. The second location was at approximately 5.5 inches from the joint, which was intended to give a general indication of the moment diagram along the dowel. These instruments provided a means of determining the flexural performance of the dowel within the concrete while load was transferred across the joint. Results of the strain gage data can then be compared to the theoretical results determined using only the load and displacement data.

Placement of strain gages on steel dowel specimens was found by Lorenz (1993) to influence some of the test results. Steel dowel specimens with gages in place were found to fail at a lower load than those without strain gages. Data collected during the elastic region of the shear testing, though, was found to be unaffected by the placement of strain gages. Because highway pavement dowels experience stresses only in the elastic range during their useful service life, this research was most interested in the dowel performance in the elastic region. For this reason, the use of strain gages on the FC dowels was judged to be acceptable for this research.

4.2.5 Test procedure

Each elemental specimen to be tested was placed in the

of dowel support, K_o, additional instrumentation was applied in an attempt to verify the results. All three of the dowels in the first group of specimens had strain gages placed on them. These were intended, as stated above, to verify the results from the load and deflection data. Problems with the strain gage instrumentation and data collection, though, prevented strain data from being collected during the testing of these three specimens. On three of the elemental specimens in the second group, strain gages were placed on the FC dowels at two locations on either side of the joint. Locations of the strain gages are shown in Figure 4.9, and, at each location, two strain gages were placed 180 degrees apart, both measuring longitudinal strain. One location was at

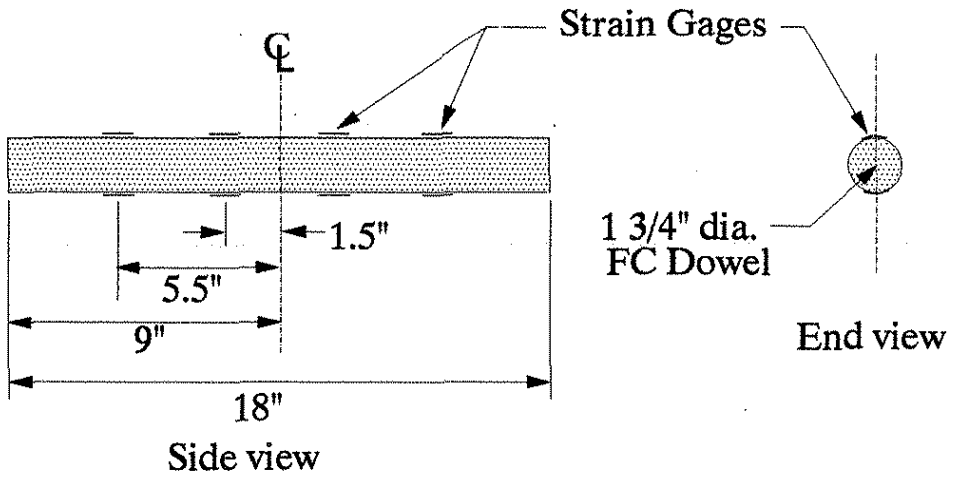

Note: Location of strain gages is symmetric about C.L.

Figure 4.9 **FC dowels used in elemental shear testing, showing strain gage locations**

splitting failure.

Determination of the modulus of dowel support, k_o, was performed using the data from the elastic portion of the shear performance of the elemental specimens. The vertical shear failure mode, for which previous research provided reinforcing, occurred outside of the range of the elastic portion. Therefore, the second group of six elemental specimens constructed for this research did not include shear reinforcing.

4.2.4 Instrumentation

The data measurements of interest during this testing were the displacements of the loaded side of the specimen relative to the reaction side and the corresponding applied load. A load cell was placed between the hydraulic ram and the mobile portion of the frame to record the applied loads. Displacements were measured with a DCDT, which was anchored to one side of the specimen and measures the relative movement of the two sides of the joint. Though a single DCDT would be sufficient to determine relative displacements between the two sides of the joint, two such instruments were used in order to monitor the rotation experienced by the specimen due to the applied load.

Though the load and displacement data collected as described above can be used to determine a theoretical modulus

total of nine specimens, in two groups, all using 1.75-inch FC dowels, were constructed and tested. The first group consisted of three, while the second included six elemental shear specimens. Steel formwork was used to form the specimens, and 1/8-inch plexiglass was used to form the joint opening. Concrete strengths were determined experimentally by making standard 6- by 12-inch concrete cylinders at the time the specimens were cast, and testing the cylinders at the time of the shear tests. A minimum of three cylinders were tested at each time, and the results were averaged to determine the concrete compressive strength, f'_c. Measured strengths for the concrete were quite different for the two groups. The first group of three used concrete with a compressive strength of approximately 7,090 psi, while the second group had a concrete strength of approximately 5,090 psi.

From the previous research by Lorenz (1993) on similar specimens, a shear failure mode was noted that could occur during the tests. The failure mode, referred to as vertical shear or concrete splitting, is not common in an actual pavement because of the restraint provided by the large amount of concrete surrounding the dowel, and because fatigue of the concrete will usually control failure of the concrete surrounding the dowel. During previous testing, steel reinforcing was placed vertically in the specimens on the unloaded side of the dowel for shear strengthening. The initial group of three specimens was reinforced for the

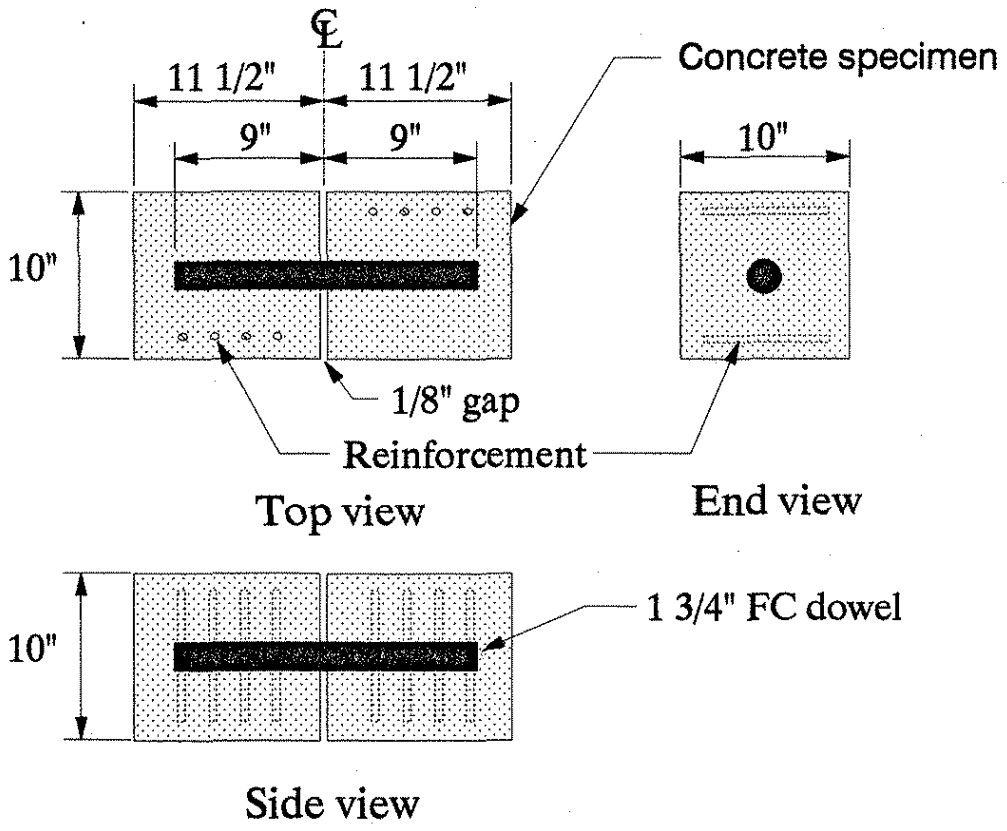

Figure 4.8 **Elemental dowel shear test specimens (Lorenz 1993)**

length provided sufficient cover over the ends of the dowel, while allowing loads to be applied without excessive rotation of the specimen. A joint width of 1/8-inch assured that the shear transfer was limited to the dowel alone, while not introducing significant effects due to bending of the dowel over the joint opening.

For the elemental testing portion of the research, a

frame considered the possibility that the restraining rods confine the concrete surrounding the dowel specimen and, therefore, influence the results. Results of the previous testing indicated that the confinement does not influence the results until after the initial failure of the specimen has occurred. Because only the data before failure was of interest in this study, the modified Iosipescu test method was determined to be appropriate (Lorenz 1993).

4.2.3.3 Test specimens

Two requirements were to be met by the test specimens used in this study. First, they must provide a good approximation of the conditions experienced by a dowel placed in a highway pavement joint. Second, the specimens must be able to be tested by the modified Iosipescu shear method. Figure 4.8 shows a diagram of the elemental test specimens, which had outside dimensions of 10 by 10 by 23 inches. These dimensions provided a dowel embedded in a mass of concrete sufficient to approximate field conditions in such a way that the dowel was able to displace within the concrete. Consideration of dowel displacements within the concrete stems from the assumption of an elastic foundation provided by the concrete. Displacements were assumed to be related to the foundation stiffness, and a slight rotation of the end of the dowel was assumed to occur within the concrete. The specimen

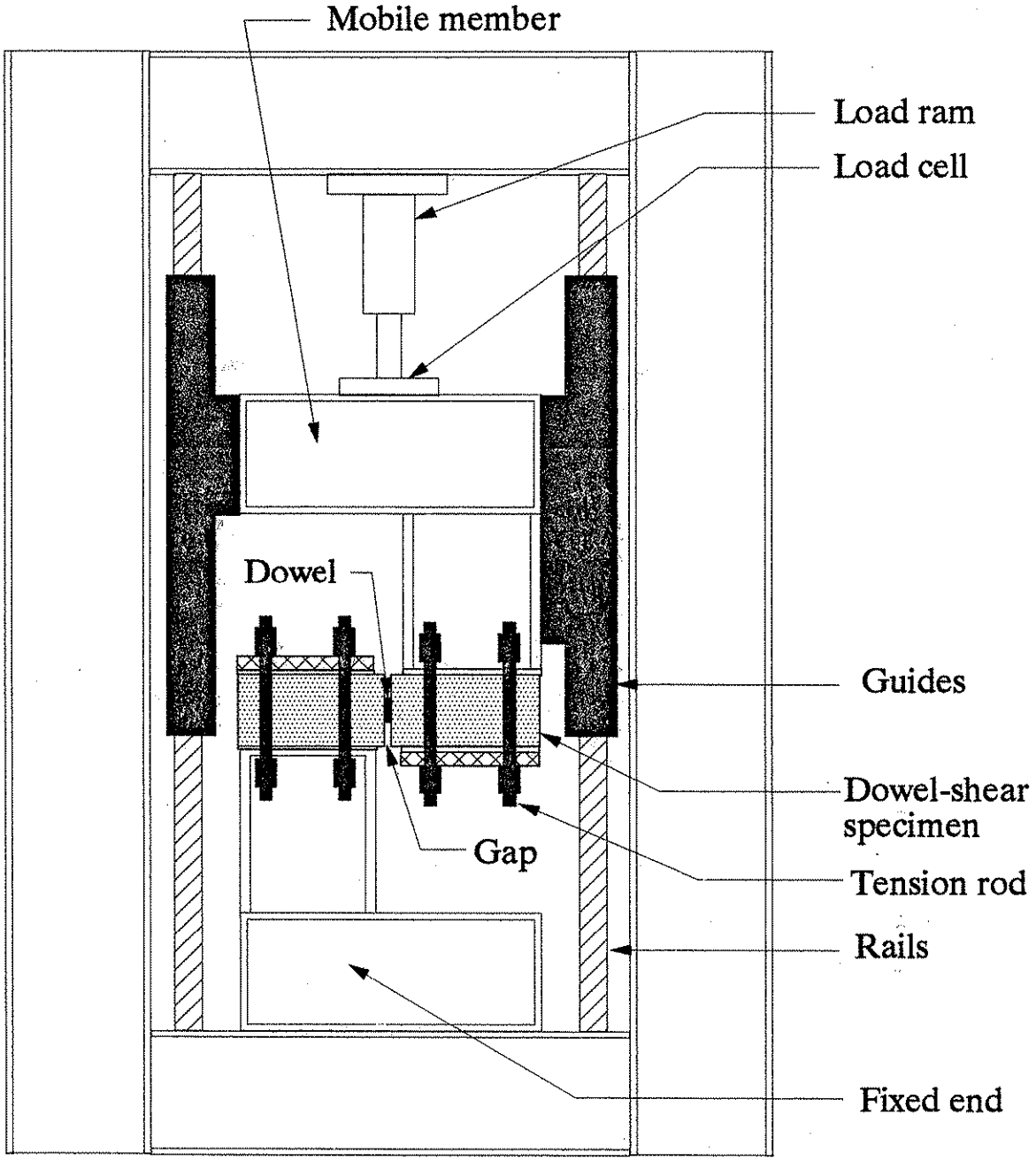

Figure 4.7 Elemental dowel shear, or modified Iosipescu, testing frame (Lorenz 1993)

applied to a specimen such that there is maximum shear and no moment at the test section. As the Iosipescu test method applies to the elemental test specimens included in this research, one side of the specimen joint, referred to as the reaction side, is held in a rigid position, while load is applied to the other side of the joint, referred to as the loaded side. In effect, the elemental specimen joint approximates the notch that is present at the test section of the Iosipescu specimens.

4.2.3.2 Testing frame

A load frame was previously built for the modified Iosipescu test method using structural steel members and plates. The frame, shown in Figure 4.7, lies horizontally, and uses a single hydraulic ram to apply the load to the specimen. The load ram lies between one end of the test frame and a mobile member which applies load to one-half of the specimen. Guide rails direct the mobile portion in a linear movement. Because rotation of the specimen results from the applied load, restraint of the specimen was necessary. Restraint was provide by four threaded rods placed on each half of the specimen, two near the top and two near the bottom. The nuts on the rods bear on steel plates which distribute the restraint to the specimen through thin neoprene rubber pads. A previous study by Lorenz using the same test

determined, as discussed in Section 4.1.4, through experimental and analytical methods.

4.2.3 Test setup

4.2.3.1 General

In order to determine the shear resistance properties of the FC dowel and concrete system, the test must apply only shear loading to the test specimen. The shear testing method selected for this research was a modified version of the Iosipescu pure shear test, shown in the schematic of Figure 4.6 (Walrath 1983). By the Iosipescu method, a shear load is

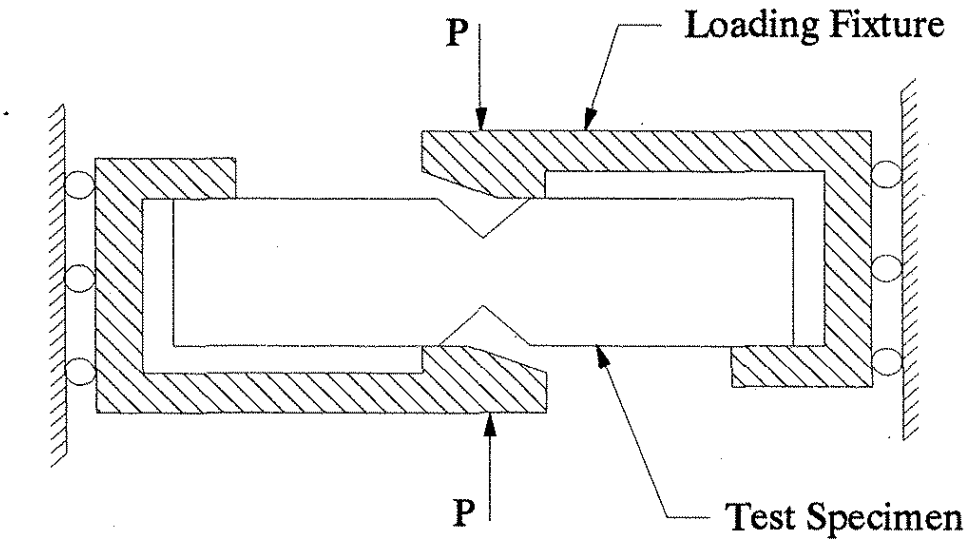

Figure 4.6 **Schematic of the Iosipescu shear test method (Walrath 1983)**

dowel and the concrete related to the displacement by a constant. The constant, called the modulus of dowel support, k_o, is fixed for a particular dowel/concrete system. Testing was performed by Lorenz in order to determine k_o experimentally. During the work by Lorenz, a test method referred to as a modified Iosipescu shear method (Lorenz 1993) was designed and verified for shear testing of a single dowel specimen cast in concrete. Testing by the modified Iosipescu method was previously performed with both 1.5-inch steel and 1.25-inch FC dowels.

The same method of experimental evaluation that was used by Lorenz for testing of FC dowels was applied here. As in the previous work, determination of a value of k_o was desired for the particular dowel/concrete system studied, which included a 1.75-inch diameter FC dowel.

4.2.2 Materials and specimens

The FC dowels tested in the elemental shear specimens were the same dowels as those evaluated by the methods described in Section 4.1, and also fatigue tested in the full-scale pavement slabs. The components of the composite material were E-glass fibers in a vinyl ester resin, with properties and proportions as discussed in Section 4.1.2. Dowel dimensions include a diameter of 1.75 inches and a length of 18 inches. Properties of the FC dowels were

independently were substituted into Equation 4.25, resulting in a theoretical value for the shear modulus of the FC material. The values of E_b of the dowel, determined previously by several methods, resulted in the values of G_{xy} given in Table 4.3.

Table 4.3 Experimental and theoretical flexural and shear modulus values for a FC dowel

Method of Determining E_b	Flexural Modulus of Elasticity, E_b, (psi)	Theoretical Transverse Shear Modulus, G_{xy}, (psi)
Full-size dowel flexure testing w/ strain gages	6,418,600	529,960[a]
Composite materials theory	6,195,700	754,900[a]
Reduced-size flexure specimen testing	6,217,504	723,880[a]

[a] value determined by applying the value of E_b to Equation 4.25

4.2 Elemental Dowel Static Shear Testing

4.2.1 Introduction

The method of evaluating a dowel in concrete, developed through work by Lorenz (1993) and based on work by Timoshenko (1925; 1976), considered a pavement dowel as a finite beam on an elastic foundation, with the bearing pressure between the

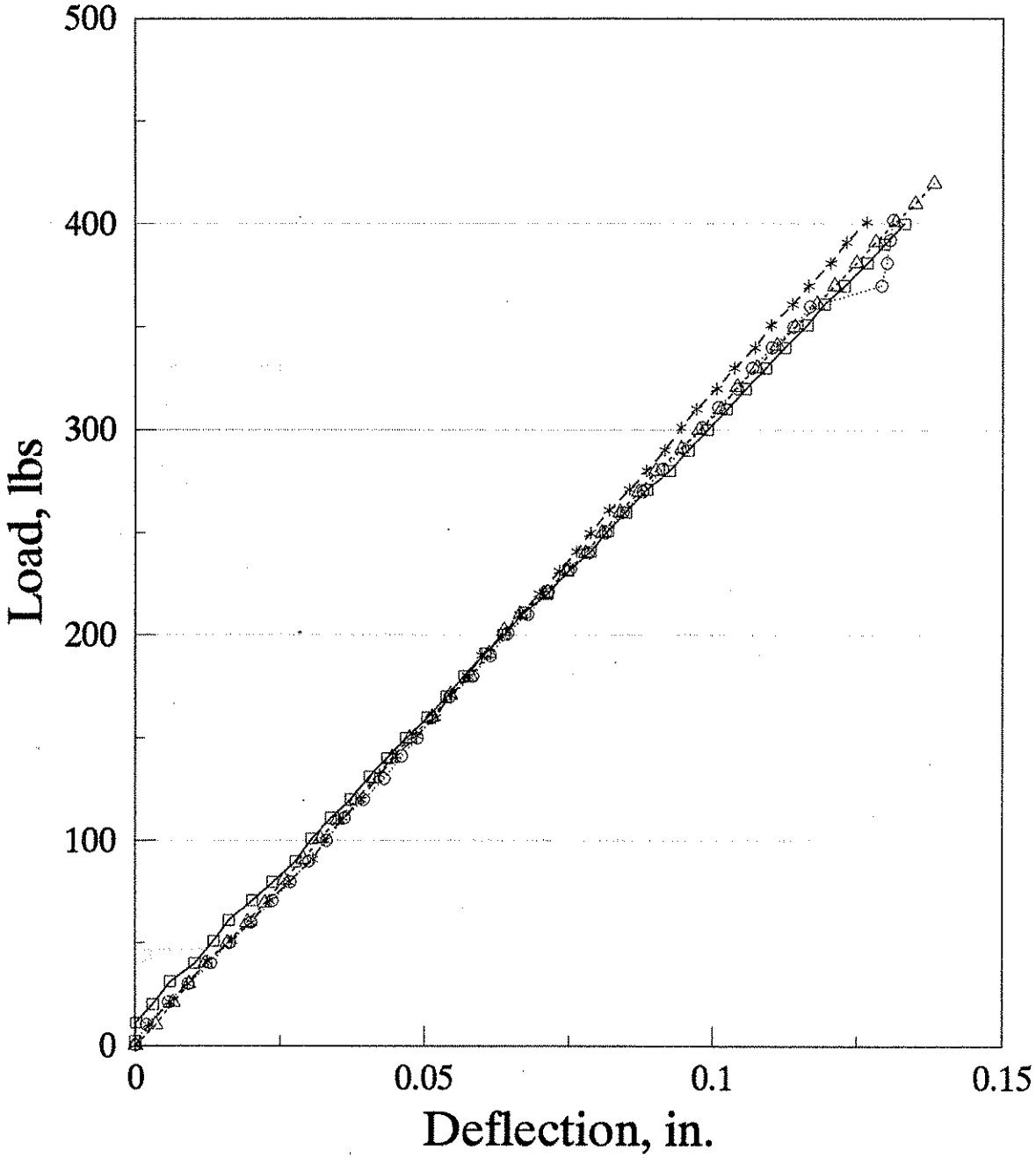

Figure 4.5 Load versus deflection diagram from testing of reduced-size FC flexure specimens

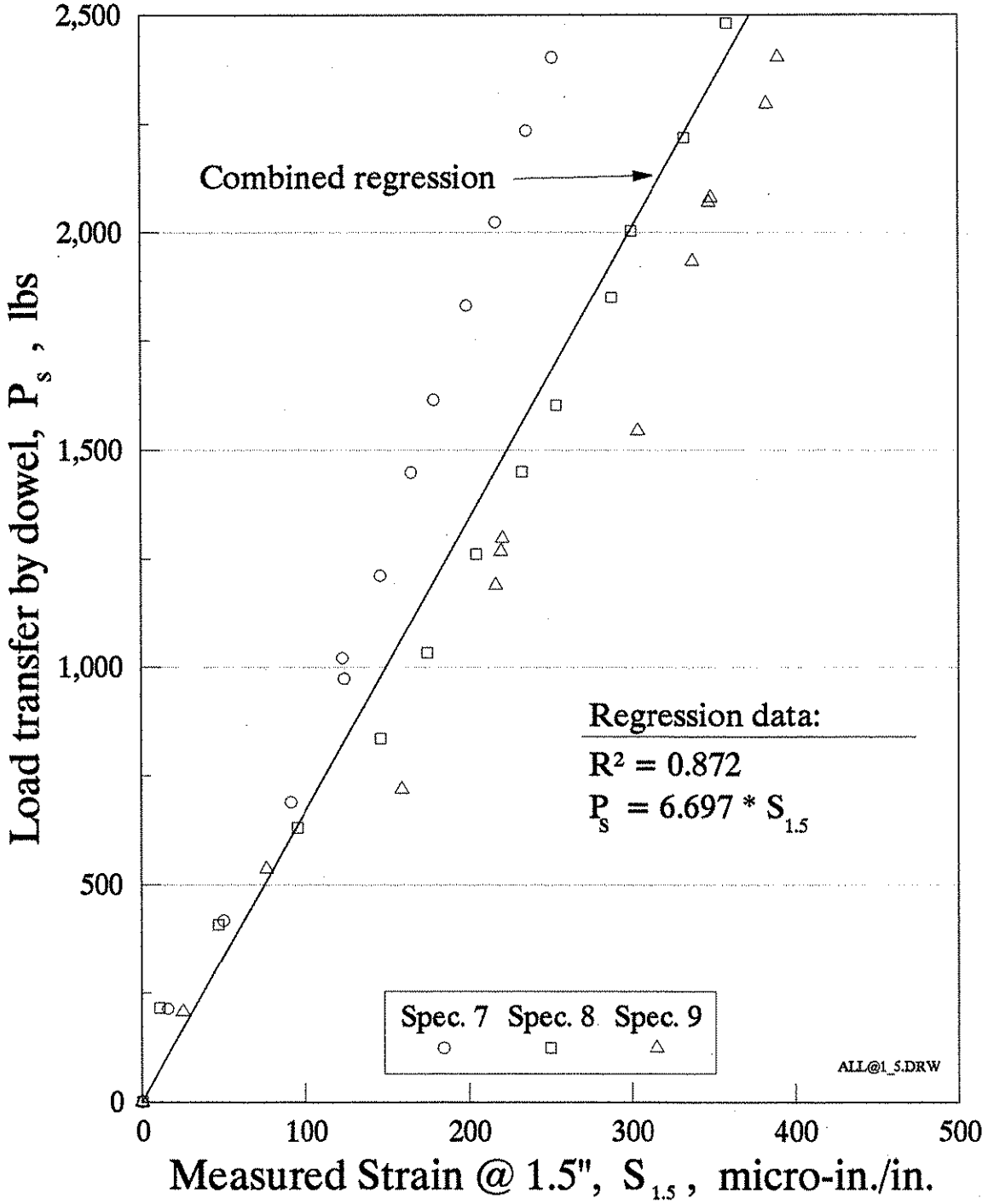

Figure 4.18 Regression of load versus strain data at 1.5 inches from the joint of FC dowel elemental test specimens

4.3 Full-Scale Fatigue Slab Testing

4.3.1 Introduction

Efficiency of a highway pavement joint is determined by monitoring two parameters: relative displacement between the two sides of a joint and load transfer across the joint. To compare the performance of steel and FC dowels as load transfer mechanisms in pavement joints, these two parameters must be measured when a joint is loaded. Because an actual pavement joint is repeatedly loaded and unloaded while in service, the fatigue due to cyclic loading must be considered when evaluating the relative displacement and load transfer performance of a joint. The number of repeated load applications may be from 10 to 100 million during a design period of 20 to 40 years for a high volume roadway (Heinrichs 1989). In this research, a method of laboratory testing that monitors the performance of doweled pavement joints while undergoing cyclic loading was developed.

When a doweled pavement joint is in service, the fatigue caused by cyclic loading applied by vehicle traffic is expected to affect the performance of the joint. Fatigue of the joint and dowels will then reduce their efficiency in transferring load (Teller 1958). An indication of reduced efficiency is, first, an increase in the relative displacement of the two sides of the joint, and, second, a decrease in the

fraction of load that is transferred across the joint, as the number of load cycles increases. Therefore, testing in this research included monitoring those parameters for a doweled pavement joint under cyclic loading which was modeled by a laboratory setup.

Often, when performing a fatigue study, a stress versus cycles, or S-N curve is developed. Such a relationship is determined by testing many specimens to failure at differing stress levels. Each failed specimen, then, creates a point on the S-N curve. Such a method of study was not followed for the laboratory fatigue testing of full-scale pavement slabs in this research. The purpose of the fatigue portion of this research was to compare the performance of FC and steel dowels under conditions which simulated those of an actual highway pavement joint. As a results of testing the dowels, the feasibility of using FC dowels as load transfer devices was studied. Because failure of an actual dowel/concrete system is difficult to define and rarely occurs, the S-N curve approach was not applied to this study. In addition, the time and cost of such a program for the full-scale study would be quite extreme.

4.3.2 Materials and specimens

Test specimens used in the fatigue testing of pavement dowels were full-scale concrete slabs with dowels placed in

the slabs at a joint that was formed in the specimens. Each slab was cast-in-place in the laboratory on top of steel supporting beams, with a thickness of 12 inches, a width of 6 feet, and a length of 12 feet. Between the steel beams and the slab were 0.25-inch thick neoprene rubber pads which acted to distribute the loading evenly as well as to separate the slab from the beams. Steel forms were used to form the outside of the slab, while wood falsework was used to support the concrete between the beams. Each dowel was placed in the slab at the middle of the thickness with one-half of its length on each side of a formed joint.

Because the laboratory testing was meant to simulate an actual pavement slab, the concrete used was a C-4 mix, which is a mix design commonly used by the IDOT in the construction of new interstate highway pavements (McWaters 1992). Two local concrete companies supplied the concrete, with the same mix requested from each. A minimum of 21 days of curing was allowed before beginning cyclic loading of the slab specimens. The reason for this length of time was that the concrete strength needed to have stabilized before beginning the load cycling. The cyclic loading was applied over a period of up to four weeks, and, if the strength was not stabilized before beginning, the concrete strength would be changing during the cycling, which would influence the results.

Concrete strength was determined using the standard 6- by 12-inch test cylinders for compressive strength, f'_c, and

standard 6- by 6-inch beams for modulus of rupture, f_r. Compressive strength testing was performed at 7, 14, 21, and 28 days in order to determine when the concrete strength had stabilized. Beam testing to determine the modulus of rupture was performed only at 28 days of curing. The strengths determined at 28 days curing for the test specimens are shown in Table 4.6.

Table 4.6 Compressive strength and modulus of rupture values of concrete corresponding to full-scale slab specimens

	Compressive Strength f'_c, (psi)		Modulus of Rupture f_r, (psi)	
Slab #	North	South	North	South
1	5,370	5,370	---	---
2	6,819	7,051	553	585
3	5,476	5,517	485	462
4	7,031	6,373	647	518

In Table 4.6, notation is used to differentiate between the two halves of the slabs. The two sides are referred to as North and South sides, and this notation will be used when necessary throughout the discussion of results of the full-scale testing. Labeling the two sides was necessary in order to maintain consistency when referencing the performance of the test slabs. Further discussion of the labeling of the two sides will be included in later sections.

4.3.3 Test setup

4.3.3.1 Test slabs

The first slab specimen was cast using 1.5-inch diameter steel dowels spaced at 12 inches center-to-center along the joint. In order to create the equivalent of a crack at the location of the joint, a piece of heavy plastic sheeting was placed vertically at the location of the joint. The dowels passed through the sheeting, and directly above the center of the dowels, a 0.375-inch wide joint was formed into the slab. The joint was formed to a depth of one-third of the thickness of the slab, which is the joint size in current practice for such pavements (McWaters 1992). A formed joint was used in place of the sawed joint that would be found in an actual pavement and was chosen because of the difficulty in sawing such a joint in the laboratory.

Because of problems resulting from the method of forming the crack used in the first specimen, a different method was applied in subsequent specimens. During the casting of the first slab the plastic sheeting placed at the joint did not remain vertical as the concrete was placed against it. As unequal amounts of concrete were placed on each side, the plastic was pushed slightly to one side. The result was a curved "crack", with approximately one-half-inch of deviation from a vertical plane. Since the interest during the testing

was to isolate the dowels for transfer of the load across the joint, a crack located at the joint that was not vertical was not desirable. In effect, the curvature created a mechanical method of load transfer by the concrete.

A second slab specimen was again formed and cast-in-place in the laboratory, but using 1.75-inch diameter fiber-composite dowels in place of steel dowels. A dowel spacing of eight inches center-to-center along the joint was used, which was determined by the computer model to be equivalent to using 1.5-inch steel dowels at 12 inches. A 12-inch spacing was also used in the field placement of FC dowels, as discussed in Section 2.2. Because of the problems experienced with creating the crack in the first specimen, a different method of forming the crack was developed. The solution was to cast the slab in two halves on consecutive days. One half of the length of each dowel was embedded in the first pouring, with a cold joint created at the location of the desired crack. The cold joint takes the place of the crack that is assumed to be created at the location of the dowels and the sawcut in an actual pavement. At the cold joint very little interlock between the two halves was desired, but a formed gap was also not desirable. Therefore, the face of the joint was greased when the formwork (with a formed saw cut) was removed from the first half, and when the second half was poured against the face, there was no bonding of the concrete at the joint.

The third slab was formed in the same manner as the first

two, using 1.5-inch diameter steel dowels with 12-inch spacing. For Slab 3, the method of forming the crack at the joint that was developed for the second slab was applied. The fourth slab specimen was prepared exactly like the third slab, but using 1.75-inch diameter FC dowels.

Concrete strengths for the specimens after the first slab were determined at 7, 14, 21, and 28 days from the time that the second half of the slab was cast. Because the two halves were poured only one day apart, the final strengths of the two halves differed by very little as seen in Table 4.6.

4.3.3.2 Simulated subgrade

In the design of the testing setup, several options were considered for the type of subgrade to use in the laboratory testing. The options included using an actual soil subgrade or using a simulated subgrade with steel supporting beams. A simulated subgrade was chosen because of advantages in the ease of construction and the reduced laboratory space that was required. A test method including a simulated subgrade was previously applied in testing by Teller and Cashell (Teller 1958) on pavement dowels in a concrete pavement.

The discussion of the computer modeling of the laboratory test setup in Section 3.2 covers the procedure used to determine the loads for designing the supporting beams. As mentioned earlier, the reactions in the springs from the

computer analysis were used as applied loads in the design of the beams. Several configurations for the beams were considered with the length of the span between simple supports and the number of beams varied. The criteria used for the beam designs were the displacements at the center of the span and at three feet on either side of center, which would be the locations of the edges of the slab. Displacements at these locations were to be as close as possible to those determined from the computer modeling of a full-size highway pavement. Other considerations in the selection of the beams were the depth of the steel beam sections and their weight. Also, the span length of the beams was to be selected to fit into limited lab space while minimizing the beam curvature when loaded. The final beam design resulted in a span of 12 feet with standard steel sections selected to be W14x38, W21x44, and W14x68. The layout of each of the beam sizes and the names by which the beams will be referred can be seen in Figure 4.19.

By using steel beams to simulate a soil subgrade, several differences between the two were considered. The simulated subgrade was a non-uniform and non-continuous support system, unlike a soil subgrade, which is normally considered to be uniform and continuous. Another difference mentioned earlier is that the simulated subgrade was constant over time, despite being subjected to cyclic loading during the testing. Properties of an actual subgrade change over time due to

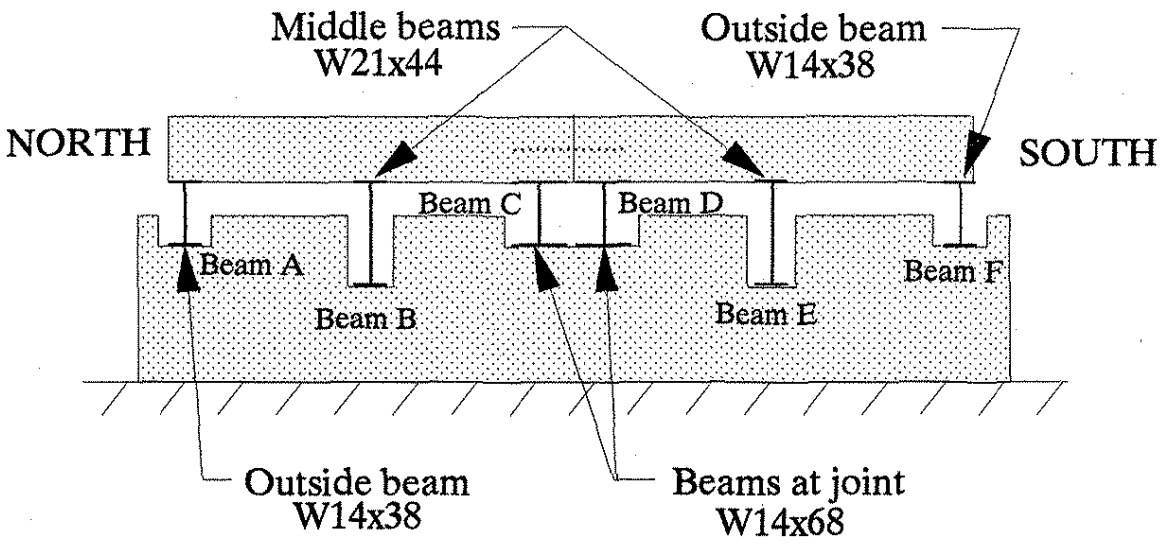

Figure 4.19 **Supporting beams for full-scale pavement slab testing**

climatic conditions, settling and compaction. For example, a subgrade may fail in a small region under the pavement, which greatly influences the performance of the pavement as well as the stresses exerted on the pavement dowels.

4.3.3.3 Loading system

This research consisted of observing the behavior of dowel bars in a full-scale pavement slab as they were loaded repeatedly to a very large number of cycles. Therefore, simulation of the loading experienced by a highway pavement is important, but the specimen must be subjected to these cycles in a reasonable amount of time. To limit the time required, a

loading system that can provide the desired loads at a high frequency in a laboratory setting was needed.

In the ISU Structural Engineering Laboratory, a MTS Service Corporation servo-controlled dynamic loading system was used. The system used two hydraulic actuators and a dynamic controlling system which was capable of loading as described above. Several load diagram shapes were available through the system, including: sinusoidal, square, and linear. For this research, the sinusoidal load diagram was selected because of the assumption that the sinusoidal shape most closely simulated the loading of a truck tire upon a joint. The actuators may be controlled by several variables, including stroke or load control. Since this research called for a maximum load of 9,000 pounds to be applied to the specimen throughout the test, load control was selected.

Load cells were integral with the actuators, located between the piston and the base. The load cells were constantly monitored by the controlling system in order to provide the same desired load with each stroke. The load magnitude as well as the frequency of the loading was set at the controller. Between the actuators and the test specimen were placed three-inch thick neoprene pads, which are shown in Figure 4.20. The pads served to "soften" the load applied to the slab, much like the suspension of a truck.

The actuators were mounted to a large steel load frame which was tied down to the floor of the laboratory. A mobile

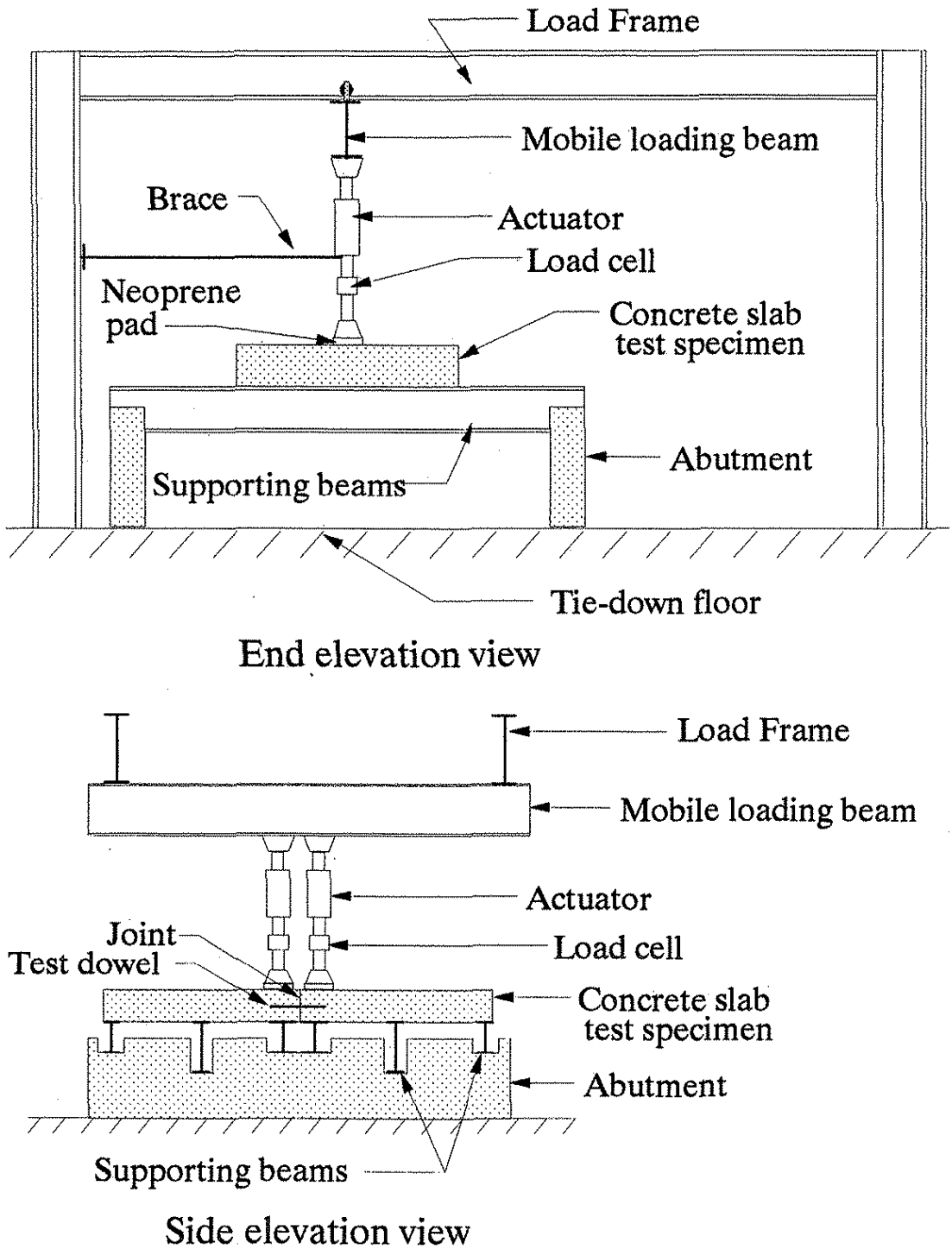

Figure 4.20 Laboratory setup for full-scale pavement slab fatigue testing

member transferred the load from the actuators to the structural frame and could be moved on wheels resting on the flanges of the frame. The actuators, then, could be moved from their location while testing the slabs to a location to the side while the slabs were being constructed. In addition, because of the vibration of the actuators while cycling, a bracing frame was constructed to brace the actuators horizontally to the frame. A diagram of the laboratory testing setup is shown in Figure 4.20.

4.3.4 Instrumentation

4.3.4.1 Displacement measurement

Relative displacements at the joint could be determined by two methods. One method included using a single DCDT at the location of displacement desired with the instrument fixed to one side of the joint and the measuring stem resting on the other side. With a single instrument, only relative displacements could be measured. A second method would require displacements to be measured on both sides of the joint with respect to a datum outside of the slab. Then, the relative displacements at a particular point would be the difference between the two measured values.

In this research, the latter alternative was chosen because of the need to verify that the actual displacements

during the testing were comparable to the values that were used in the design of the test setup. To measure displacements relative to an external datum, a reference frame was built to which all of the displacement instrumentation on top of the slab could be attached during the test.

Because of differences in the spacing used for FC and steel dowel bars, the displacement instrumentation locations were different for each slab. For each of the slabs, DCDT's placed at the joint for monitoring the relative displacements were located on top of the test slabs, directly above each dowel bar location. The instruments were placed as close to the joint as possible, with the DCDT stem resting on small plastic or glass plates glued to the concrete to guarantee a flat surface. In addition to the instruments on either side of the joint, DCDT's were placed above the locations of the middle beams on both sides of the joint.

For the first full-scale test specimen, a total of 22 DCDTs were in place on top of the slab, with 20 measuring vertical displacements and two placed horizontally to measure the change in joint opening. A diagram showing the DCDT layout is given in Figure 4.21. With six dowels placed at the joint in this specimen, a total of 12 DCDTs were placed to determine absolute and relative displacements at the joint. At each of the middle supporting beam locations, three DCDTs were placed in a line corresponding with the centerline of the beam. The final two instruments on top of the slab were

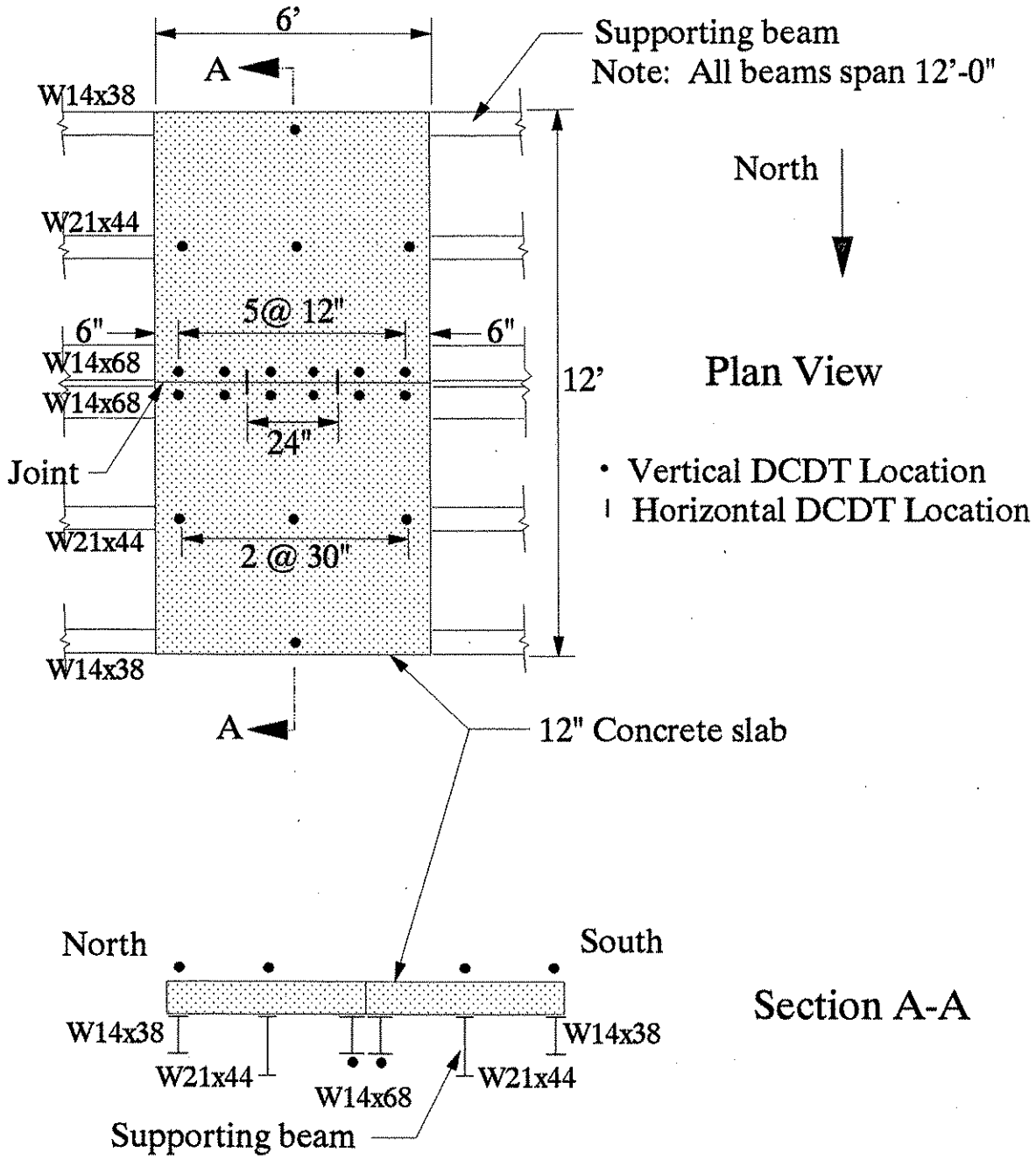

Figure 4.21 Displacement instrumentation for first full-scale fatigue test slab (with 1.5-inch steel dowels at 12-inch spacing)

located directly above the centerline of the outside supporting beams at midspan. In addition to those on top of the slab, two DCDTs were placed at midspan and underneath the two supporting beams at the joint. These were meant to determine whether the thin neoprene placed between the slab and the beams had an influence on the displacements.

Because the FC dowels used in the second slab were placed at a spacing of eight inches, a total of nine dowels were placed at the joint. Therefore, the placement of displacement instrumentation differed from the first slab. Also, because of a limited amount of instruments available, measurements from the first test slab that proved to be insignificant were eliminated. Measurements taken at the outside supporting beams were found to be small enough to be considered insignificant. Monitoring of the horizontal displacement at the joint was also found to be unimportant because of the small movements and little importance to analysis. These changes then allowed for DCDTs to be placed at all dowel locations as well as over the middle beams on both sides. The layout of the instruments for the second slab is shown in Figure 4.22. Because one dowel was located directly below the point of load application, DCDTs were again placed underneath and at midspan of the beams at the joint.

Since the third and fourth slab specimens again used a dowel spacing of 12 inches along the joint, the displacement instrumentation used in these slabs was very similar to that

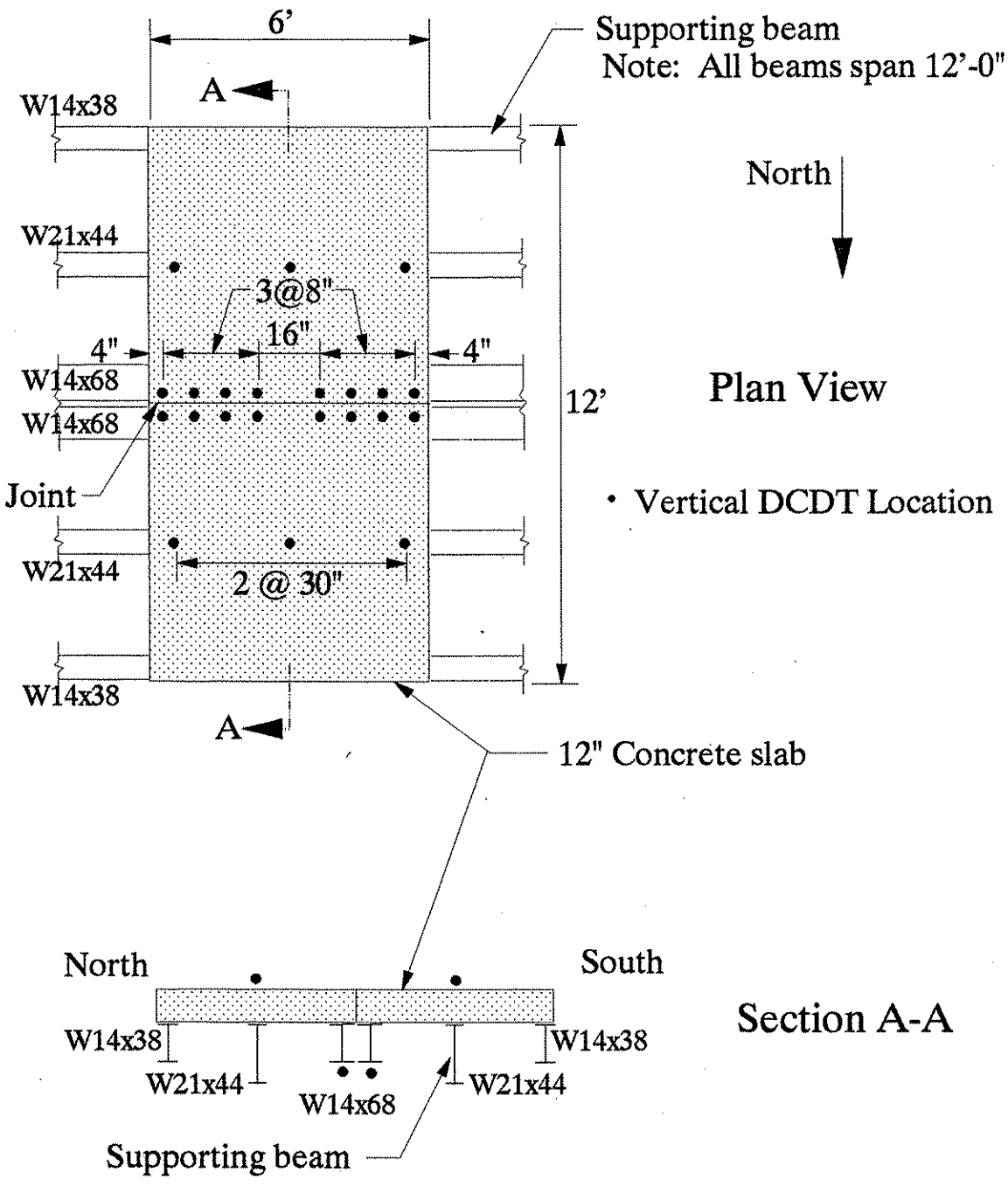

Figure 4.22 Displacement instrumentation for second full-scale fatigue test slab (with 1.75-inch FC dowels at 8-inch spacing)

used in the first slab. The only difference being that DCDTS were not placed above the locations of the outside supporting beams and were not placed to measure horizontal displacements at the joint. A diagram of the DCDT locations for the third and fourth slabs is shown in Figure 4.23.

4.3.4.2 Load transfer

The second variable requiring monitoring and measurement during the static load testing was the load transferred across the joint by the dowels. Determination of the load transfer had to be accomplished in a less direct manner than for displacements. Strain gages were mounted on the steel supporting beams underneath the test specimens, from which the strains were measured and the moment and the load applied to each of the beams could be calculated. Loads were applied to the supporting beams through the concrete slab which was six feet wide and rested in the middle of the 12-foot span of the supporting beams. Strain gages were placed at three locations along the span, which are shown in Figure 4.24. One location was at the middle of the span, and the other two were below both edges of the slab, three feet on either sides of the midspan. At each location, four strain gages were placed on the beam, as is shown in Figure 4.24 for each of the three beam sections used. The method used to determine the load transferred to each beam involved the development of

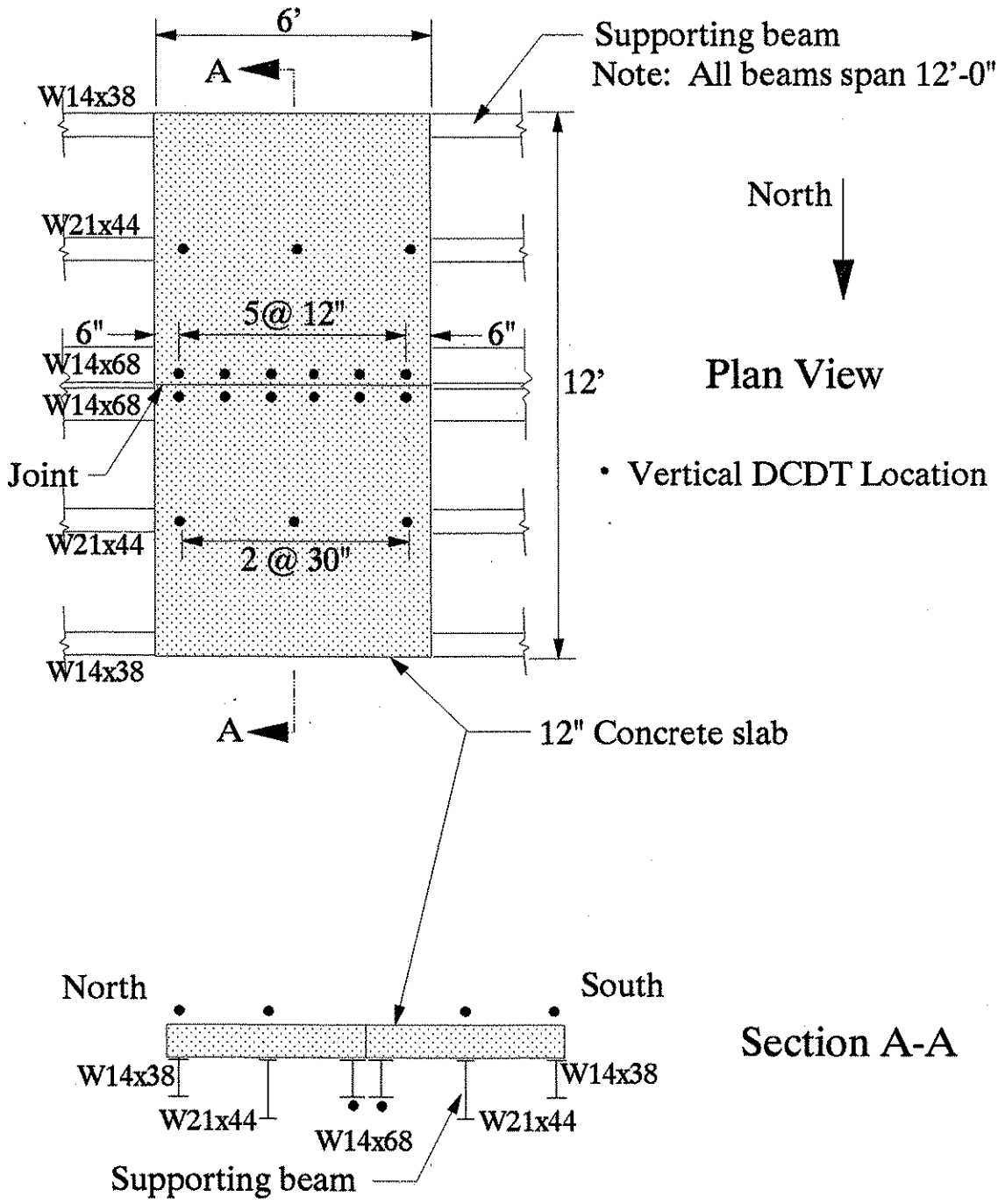

Figure 4.23 Displacement instrumentation for third full-scale fatigue test slab (with 1.5-inch steel dowels at 12-inch spacing)

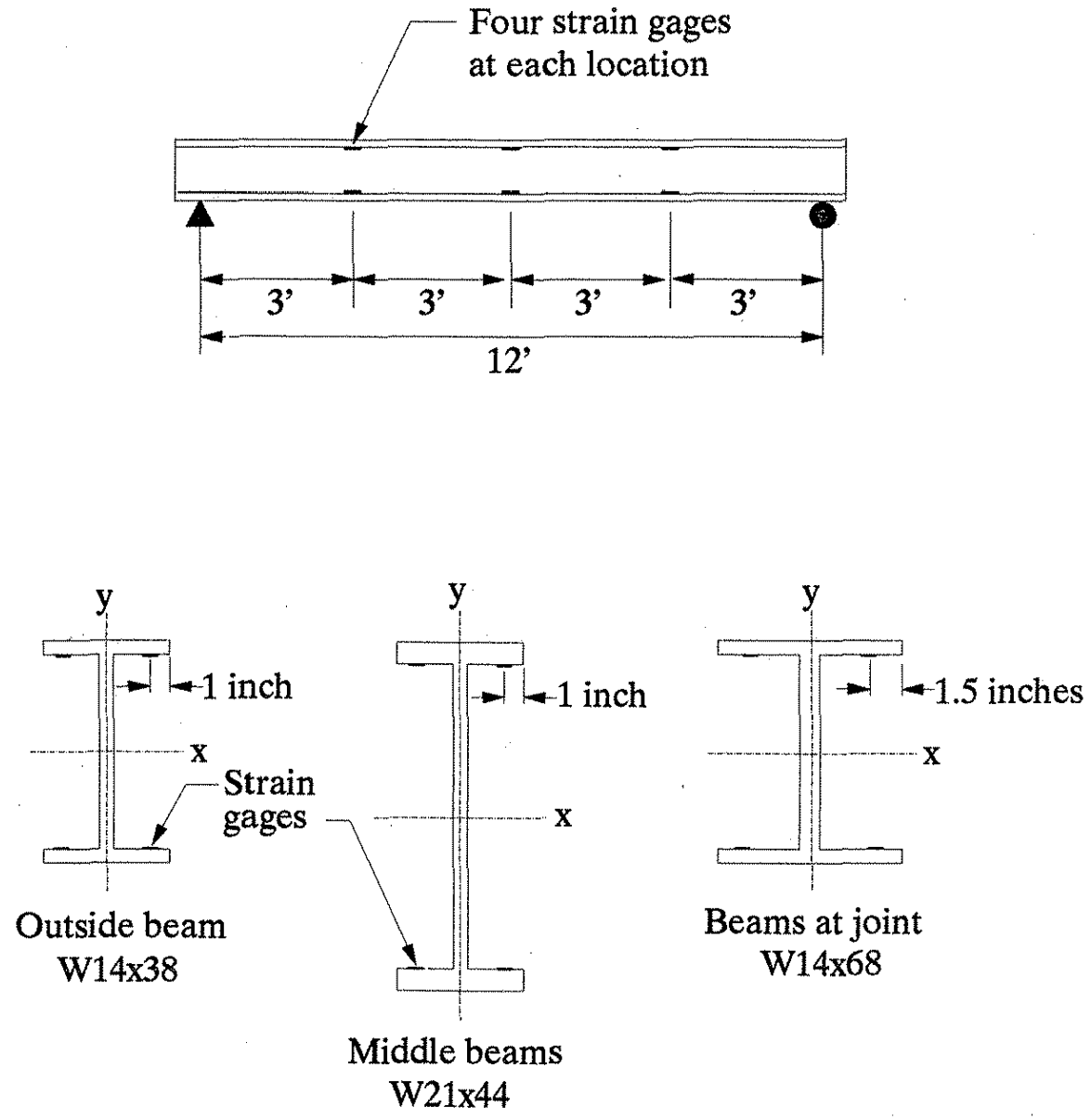

Note: All strain gages are placed symmetrically about the x- and y-axes

Figure 4.24 Locations of strain gages placed on supporting beams

calibrations between a known applied load and the resulting measured strains in the beams. After conducting load tests of each beam individually, linear relationships were developed from the data. Then, during static load testing of the slabs, the load applied to each beam was determined by applying the calibration to the strains measured in the beams. Load testing of the supporting beams is discussed further in Sections 4.3.5.2 and 4.3.6.1.

As an additional means of monitoring the load transfer through the dowels, strain gages were mounted directly on the dowels. In the second slab, strain gages were mounted on the three center dowels, which were 1.75-inch diameter FC rods placed at an 8-inch spacing. These three dowels were selected because the majority of the load was transferred through the dowels which were located near the point of load application (Heinrichs 1989). On each half of each dowel, the gages were placed at two locations, the first at 1.5 inches, and the second at 5.5 inches from the center of the dowel. Figure 4.25 shows the gage locations on the dowels. At each of the locations, two gages were mounted, each diametrically opposite the other. The bending of the dowel was determined by averaging the two values of strain. When placed in the slab, care was taken to guarantee that the dowels were oriented so that all of the gages lied in a vertical plane.

Again, for the third slab, strain gages were placed on the dowels closest to the load application, which included the

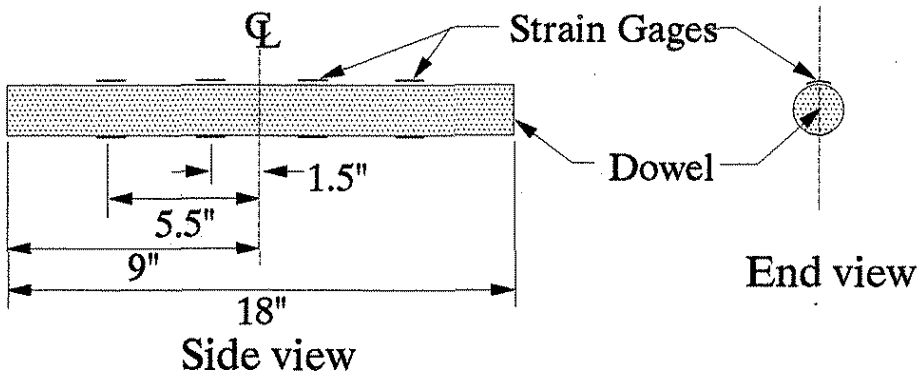

Figure 4.25 **Dowel (FC or steel) showing strain gage locations as placed in second and third full-scale pavement test slabs**

middle two 1.5-inch diameter steel dowels. The gages were placed at the same locations along the length of the dowels as were used in the previous slab (1.5 and 5.5 inches from center). Figure 4.25 shows the strain gage locations for the dowels used in the third slab specimen.

Strain gages were also placed on the 1.75-inch FC dowels of the fourth slab. As with the third slab, the middle two dowels closest to the application of load were selected for mounting the strain gages. These dowels were placed on either side of the center line of the test slab at a distance of 6 inches from the center line. Accordingly the locations of the instrumented dowels will be referred in this report as 6 inches east or 6 inches west of the center line.

The number of strain gages on the dowels of the fourth slab was increased in order to get three data points on each

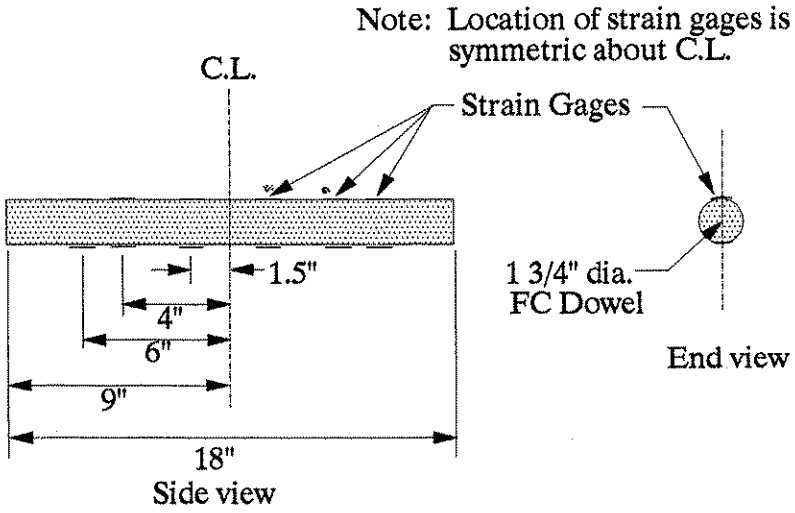

Figure 4.26 **FC dowel showing strain gage locations as placed in fourth full-scale pavement test slabs**

side of the dowel for observing the distribution of moment along the length of the dowel. Strain gages were placed at three locations (1.5, 4.0, and 6.0 inches) on the dowels of the fourth slab. Figure 4.26 shows the details of the instrumentation on the dowels of the fourth slab specimen.

4.3.5 Test procedure

4.3.5.1 Introduction

The initial step in the test procedure was to perform load tests of the supporting beams, which was then followed by testing of the full-scale slab specimens under static and cyclic loading. In general, the full-scale slab testing procedure involved subjecting the specimen to cyclic loading,

and, at times during the cycling, stopping to test the slab under static loads equivalent to those during cycling. Data was collected only during the static load tests performed on the slabs. For example, during the testing of the first specimen, which used 1.5-inch steel dowels, static tests were performed at the completion of the following numbers of load cycles, in thousands: 0; 50; 100; 200; 300; 400; 500; 750; 1,000; 1,500; and 2,000.

Before the full-scale concrete slabs were cast, the supporting beams were tested with strain gages in place. Using beam test results, calibrations were determined between the applied load and the measured strains in the beams. The calibrations were used in the analysis of the load transfer across the joint, and will be discussed in more detail in Section 4.3.6.

4.3.5.2 Supporting beam load tests

As discussed in Section 4.3.4.2, strain gages were placed on the supporting beams in order to monitor load transfer across the joint as load was applied to the slabs during static load tests. Using the strains measured as load was applied during a static test, the magnitude of the load distributed to each supporting beam could be determined by applying the section properties of the beams. The beam properties, though, were assumed to not match exactly those

specified for the particular section designation, such as W14x38. Therefore, load tests were conducted on each of the supporting beams with the strain gages in place in order to determine calibrations between load and strain values.

The procedure for the tests involved applying a load at the middle of the span while the beams were simply supported in the same manner as when in place under the slab. Then, as load was applied at intervals, the measured strains were collected using the same data acquisition system used during the static load testing.

4.3.5.3 Cyclic loading

During the cyclic loading of the specimens, load was applied to both sides of the joint in order to simulate truck traffic passing over the joint. The two electronically controlled hydraulic actuators, which were discussed in Section 4.3.3.3, applied the loads. The load was applied by each actuator in a sinusoidal-shaped function, with the two functions 180 degrees out of phase. Therefore, when one of the actuators was at the maximum load on one side of the joint, the second was at the minimum load on the other side. For each actuator, a maximum of 9,000 pounds, and a minimum of 200 pounds were applied during the cyclic loading. Load diagrams for the two actuators are shown in Figure 4.27. The minimum load was required only during the cyclic loading so

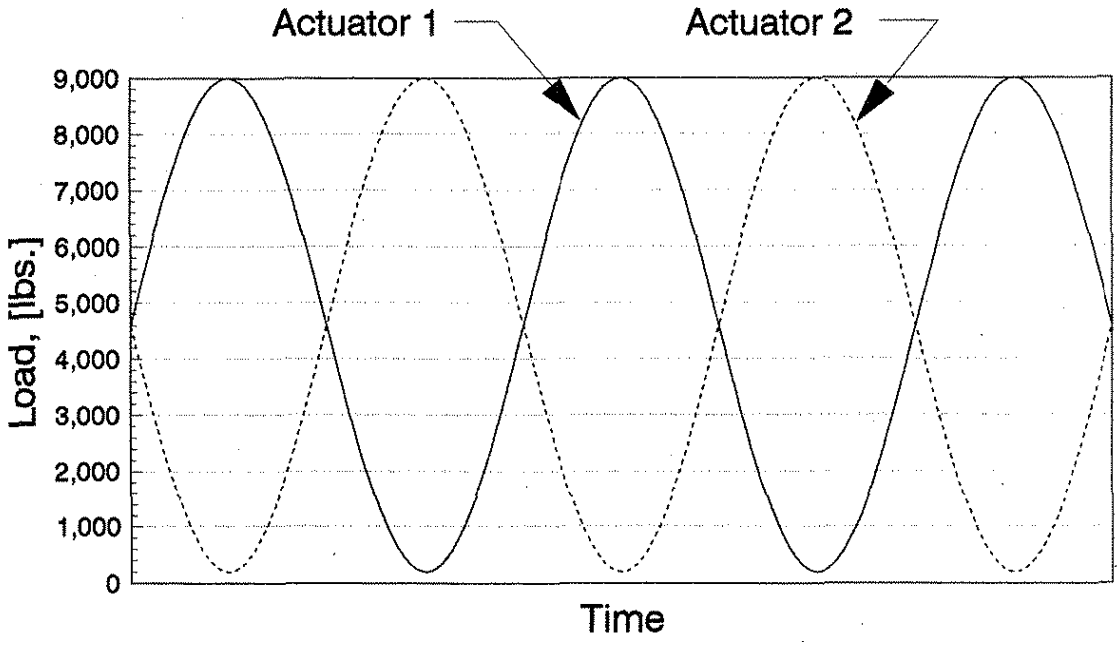

Figure 4.27 Typical load diagrams for two actuators during cyclic loading

that the actuators stayed in contact with the slab at all times. Therefore, summing the load applied by both actuators, the specimen was loaded with a net load of approximately 9,200 pounds at all times during the load cycling.

While the joint was never unloaded during the cycling, the action that the dowel underwent was of the most interest. The dowel experienced a full range of load transfer reversal during the repeated loading. Relative displacement across the joint cycled between the maximum when one side was loaded, to the same maximum when the other side was loaded. Movement such as this subjected the dowel/concrete system to the most

extreme fatigue loading conditions that an actual system would be subjected to with the same magnitude of load. In fact, the relative movement of the two sides of the slab while cycling was visually observed at the edges of the slab specimens.

The loading frequency used during the cycling was approximately five Hertz. Adjustments were made to the frequency at the beginning of the cyclic loading program of the first slab so that there was not excessive vibration of the loading frame. At the beginning of the cycling program for each of the following test specimens the frequency was set at five Hertz, and the system was examined for vibrations of the loading frame. If necessary, adjustments were made to the frequency, though, the frequency remained very near five Hertz for all tests.

A maximum of two million load cycles were applied to the first two slab specimens. The first using 1.5-inch steel dowels at a 12-inch spacing and the second using 1.75-inch FC dowels at an eight-inch spacing. Ten million cycles were applied to the third and fourth slabs having 1.5-inch steel and 1.75-inch FC dowels respectively, spaced at 12 inches.

4.3.5.4 Static load testing

Static load tests were performed using the same hydraulic actuators as were used in the cyclic loading. During the static tests, though, the load was applied using the manual

controls instead of the electronically controlled system. The static tests were performed so that instrumentation could be read while applying the loads that were applied during the fatigue or cyclic loading. At the beginning of each test, readings of the instrumentation were taken with no load applied, giving the baseline for readings to follow. Then, the static load was applied to one side of the joint at a time in many load step intervals. At each load step the instrumentation data was collected as the load was increased to a maximum of 9,000 pounds and decreased, again at intervals, until no load was applied. The same procedure was then followed as the other side of the joint was loaded.

During the tests conducted on the first specimen, a load interval of 500 pounds was followed while loading to the maximum load and while unloading. Reading the instrumentation at the 500-pound interval resulted in an excessive amount of load points, since the behavior of the specimen was quite constant over the range of load. Therefore, for the testing of the second slab, the number of load steps was reduced by adjusting the load intervals used. While loading the slab, an interval of 500 pounds was used up to 4,000 pounds. Then, from 4,000 to 9,000 pounds, a 1,000-pound interval was applied. When unloading, the load was decreased at steps of 1,000 pounds from 9,000 pounds to zero load. These changes reduced the amount of data collected for each test, while still providing 14 data points as the load increased. An

additional change was made to the procedure between the testing of the first two specimens. From the first slab tests, the results indicated that a large part of the degradation of the dowels in the slab occurred during the first 200,000 load cycles. Therefore, collection of more data during that time was desired so any possible critical time during the degradation was not overlooked. A total of 14 static load tests were run, compared to 11 for the first test. Additional tests were carried out at the end of 25, 75, and 150 thousand cycles.

4.3.5.5 Dynamic load testing

While the static load test method documented the performance and degradation of the dowel/concrete system as the number of load cycles increased, the performance of the system during the application of the cyclic loading required further investigation. To monitor the system during cycling, a signal recorder was used to obtain a paper printout of the data from several instruments in the test setup. Output voltages from both load cells, and from two DCDTs were recorded simultaneously as cyclic loading was applied. Load cell voltages were directly proportional to the applied load, and the output voltages from the DCDTs were directly proportional to displacements. The dynamic testing was performed on the third full-scale test slab, which contained

1.5-inch steel dowels, after the completion of 10 million cycles of loading.

Because the testing resulted in a printed output of the load and displacement voltages in a graphical format, the results only indicated a representation of what the slab was experiencing during the cyclic loading. Included in the output were plots with time on the abcissa and output voltages as the ordinate. Any numerical analysis had to be performed using values measured from the plots. Also, the results only indicated a range of movement or load while cycling. From the dynamic evaluation, though, the response of the full-scale slab due to the dynamic loading was observed, along with the consistency and uniformity of the loading curve.

In order to determine the effect of the cyclic loading frequency on the performance of the dowel/slab sytstem, the output voltages were recorded while the dynamic actuators cycled at several frequencies. The loading applied during the dynamic testing was the same as that applied during the cyclic loading, as shown in Figure 4.27, with a maximum of 9,000 pounds and a minimum of 200 pounds. The response of the system was expected to vary upon the frequency at which the load was applied.

4.3.6 Analytical investigation

4.3.6.1 Supporting beam load tests

One method to observe load transfer across the test joints included an analysis of strain gage data from the supporting beams. The amount of load distributed to each beam was calculated for each static load test of a slab specimen. Load tests of the supporting beams were performed in order to relate the load applied to each beam and the strains measured by strain gages mounted on the beam flanges. Discussion of how these results were used to determine load transfer is included in Section 4.3.6.3.

Because of the simply supported configuration of the supporting beams, a direct relationship between the measured strain in a beam and the load applied to that beam was developed. The test procedure is discussed in Section 4.3.5.2, and results from the tests were in the form of load and strain data at the three strain gage locations on the beams. Considering only the locations on the beams that were directly underneath both edges of the slab, or the quarter points of the 12-foot span, a linear relationship was developed between load and strain. By performing a linear regression of strain at the quarter-point versus load applied at the mid-span of the beam, an equation relating the two was determined for each supporting beam.

4.3.6.2 Relative displacements

Relative displacements across the joint were determined by observing the measured displacements on both sides of the joint during static load testing of the slab. These values were collected at each of the dowel locations as one side was loaded at a time. Then, the relative displacement was determined at each dowel location by calculating the difference between the measured displacements of the two sides. The critical relative movement was that which occurred at the maximum applied static load of 9,000 pounds. As discussed earlier, one indication of the degradation of load transfer is an increase in the relative displacement at a joint. By observing these values from each static load test, the load transfer behavior of the dowels was examined as the number of load cycles increased.

4.3.6.3 Load transfer

Measurement of load transfer included monitoring both the load distributed to each of the supporting beams and the flexure in the dowels within the slab. For both methods, strain gage data was collected and analyzed.

Calculation of the load transferred to each supporting beam was performed by using the measured strains at the quarter-points of each beam during the static load tests and

the relationship between measured strain and applied load developed for each beam. For the simple span configuration of the supporting beams, the strain in the beams at the quarter points was directly proportional to the applied load. The loading condition for the supporting beams during a static load test was assumed to be a symmetric distributed load applied between the quarter points, as is shown in Figure 4.28. Therefore, the total load applied to each supporting beam through the slab can be determined by applying the appropriate relationship determined from the beam load tests.

When the portion of the applied load that was distributed to each of the beams was determined, these values were summed on each side of the joint, with the total being the portion of the applied load resisted by each side. When a load was applied to one side of the joint, the sum of loads resisted by the beams on the other side of the joint was equal to the load transferred across the joint by the dowels. Of course, the full sum for both sides must be equal to the total of applied load, which was a maximum of 9,000 pounds during a static load test.

Applying the above method to determine load transfer, though, did not indicate the portion of the load transfer carried by each of the dowels in the slab. Therefore, the strain gage instruments placed on the dowels were valuable in the analysis of the system. By relating the measured strains in the FC dowels from the elemental testing with the measured

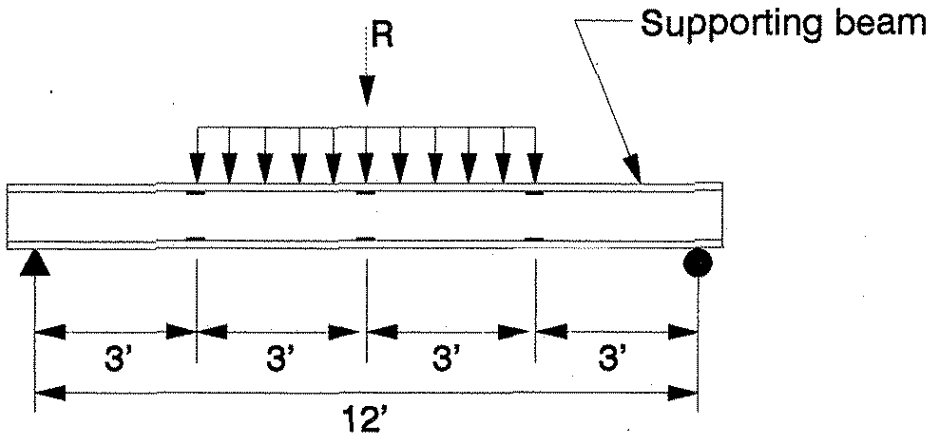

Note: R is the resultant of the distributed load

Figure 4.28 Supporting beams load configuration during static load testing of full-scale slabs

strains in the FC dowels in the full-scale slab specimen, the load transferred by each dowel was determined. This analysis will be discussed in further detail in Section 5.2.

4.3.7 Results

4.3.7.1 Supporting beam load tests

As discussed in Section 4.3.6.1, load tests were conducted on the supporting beams in order to determine calibrations between the strain values measured on the beam flanges during static load testing of the slabs and the amount of load applied to each beam. The objective was to determine the load transfer across the test joint by measuring the

amount of load applied to the supporting beams.

Tests were performed on the two middle supporting beams, referred to as Beams B and E, and the two beams at the joint, or Beams C and D (see Figure 4.19). No tests were performed on the two outside beams, referred to as Beams A and F because the measured strains in those beams during static load testing were considered to be too small for consistent results.

Results of the beam tests are shown in Figure 4.29 for the four beams tested. The resulting regression equations relating strain and applied load are included in the figures. As expected, all of the relationships are quite linear, and were applied effectively to determine load transfer during the static load tests.

4.3.7.2 Static load tests of full-scale slabs

While the data collected from the testing of the initial full-scale slab specimen was not valuable in the analysis of the performance of the pavement dowels, several concepts were studied during the test. Because of the problems experienced with the formed joint, the results from the tests on Slab 1 were not considered in the analysis, but by running the first complete test, the procedure for future testing was fully developed. Also, the first test provided a check of the laboratory setup design, including the performance of the supporting beams as a means of providing a simulated subgrade.

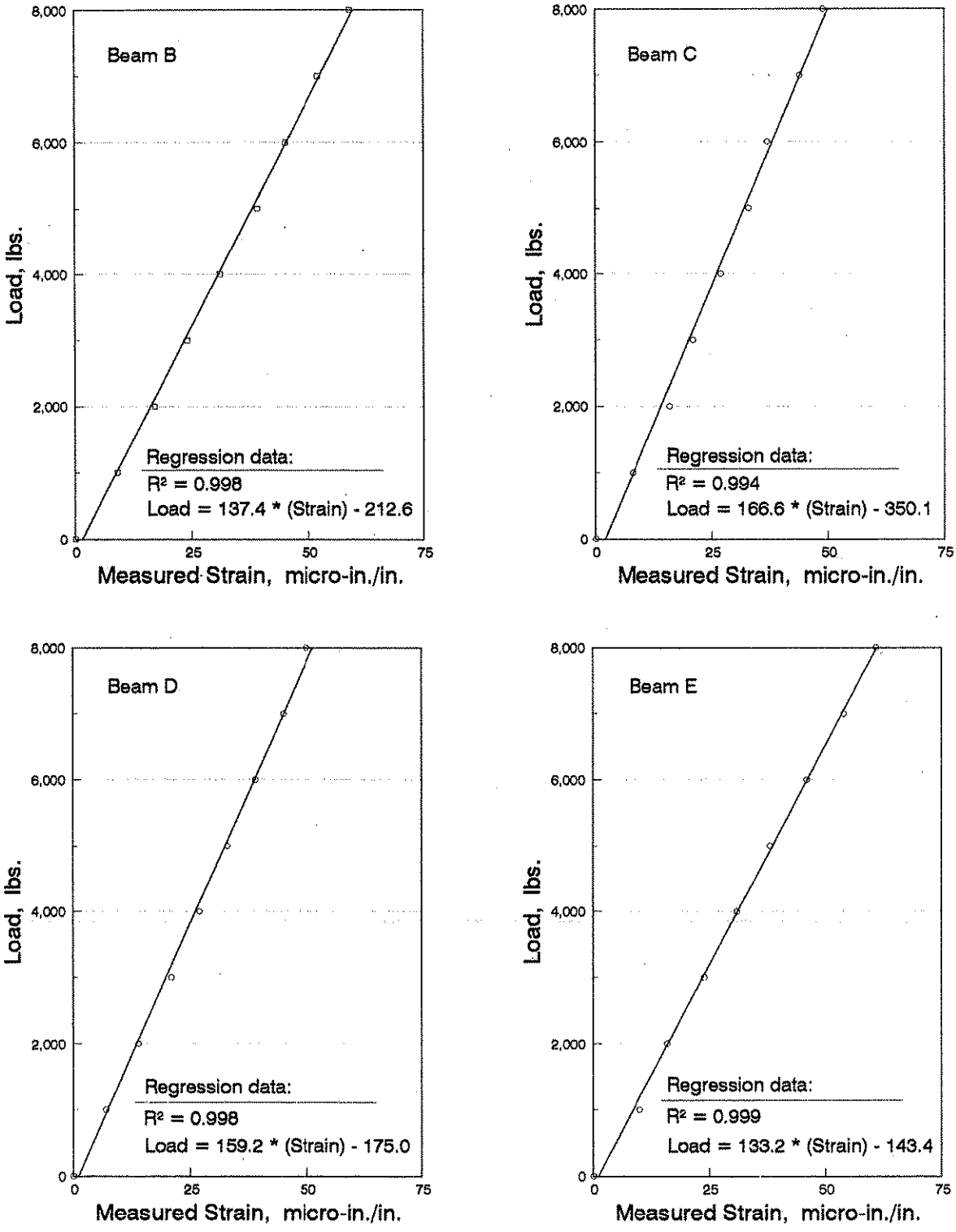

Figure 4.29 Load versus strain diagrams for quarter points of supporting beams

The second slab fatigue testing procedure was much the same as for the first slab, with some adjustments made to the static load testing procedure, as discussed in Section 4.3.5.4. Both the first and the second slabs were subjected to a maximum of two million cycles. The changes between the two slabs included decreasing the number of readings of the instrumentation during each static test, and, also, performing additional static load tests during the first 200,000 load cycles.

As discussed in Section 4.3.3.1, the method of forming the pavement joint in the test specimens was changed after completing the original slab. Casting the specimen in two halves on consecutive days isolated the dowel for the transfer of load by eliminating aggregate interlock across the joint. The difference in concrete strengths between the two sides was found to be minimal when the fatigue testing was begun.

In general, the measured displacements on top of the slab were expected to be quite linear with respect to the applied load. The linearity was anticipated because the displacements were a function of the support provided by the supporting beams, which were simply supported members. Displacements are proportional to the applied load in such a case, and this was found to be the case for displacements measured at the joint. Figures 4.30, 4.31, and 4.32 show graphs of load versus measured deflection at the joint for typical static load tests on the second, third, and fourth slabs, respectively. Each

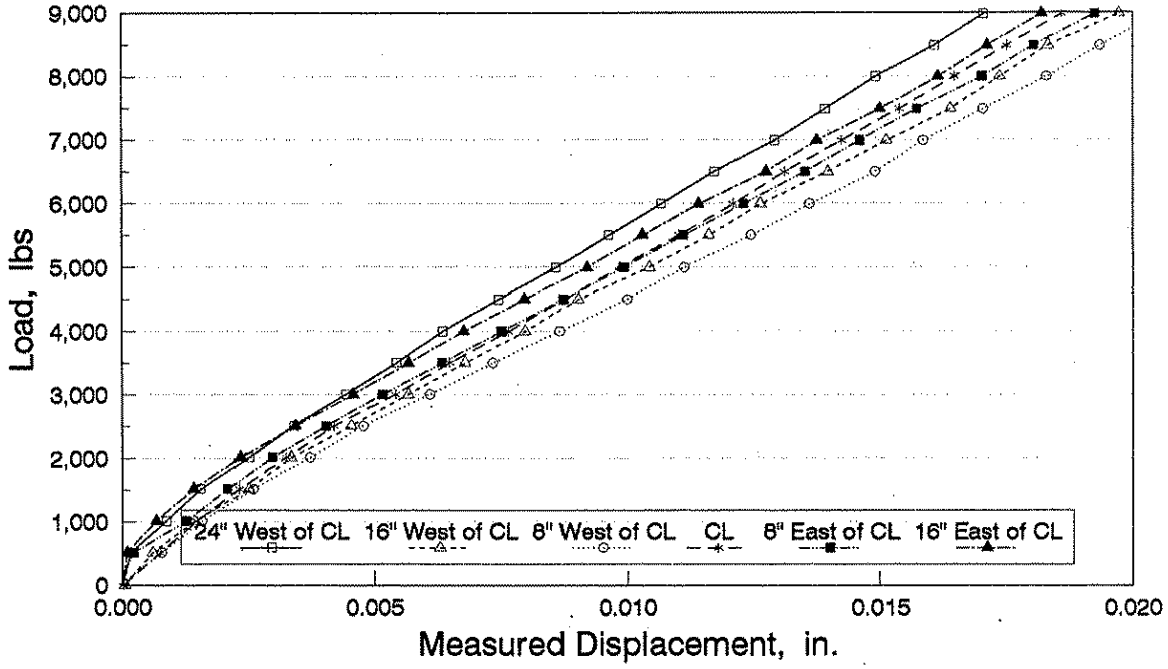

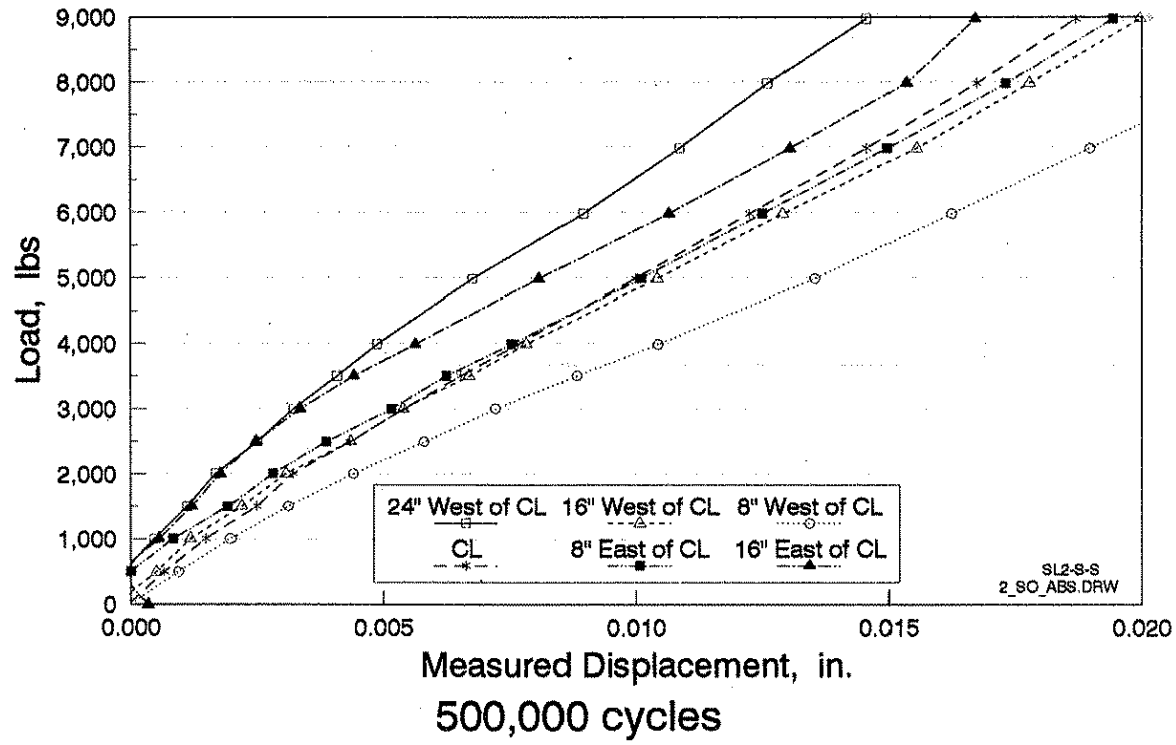

Figure 4.30 Typical load versus displacement diagrams at locations along the joint for Slab 2

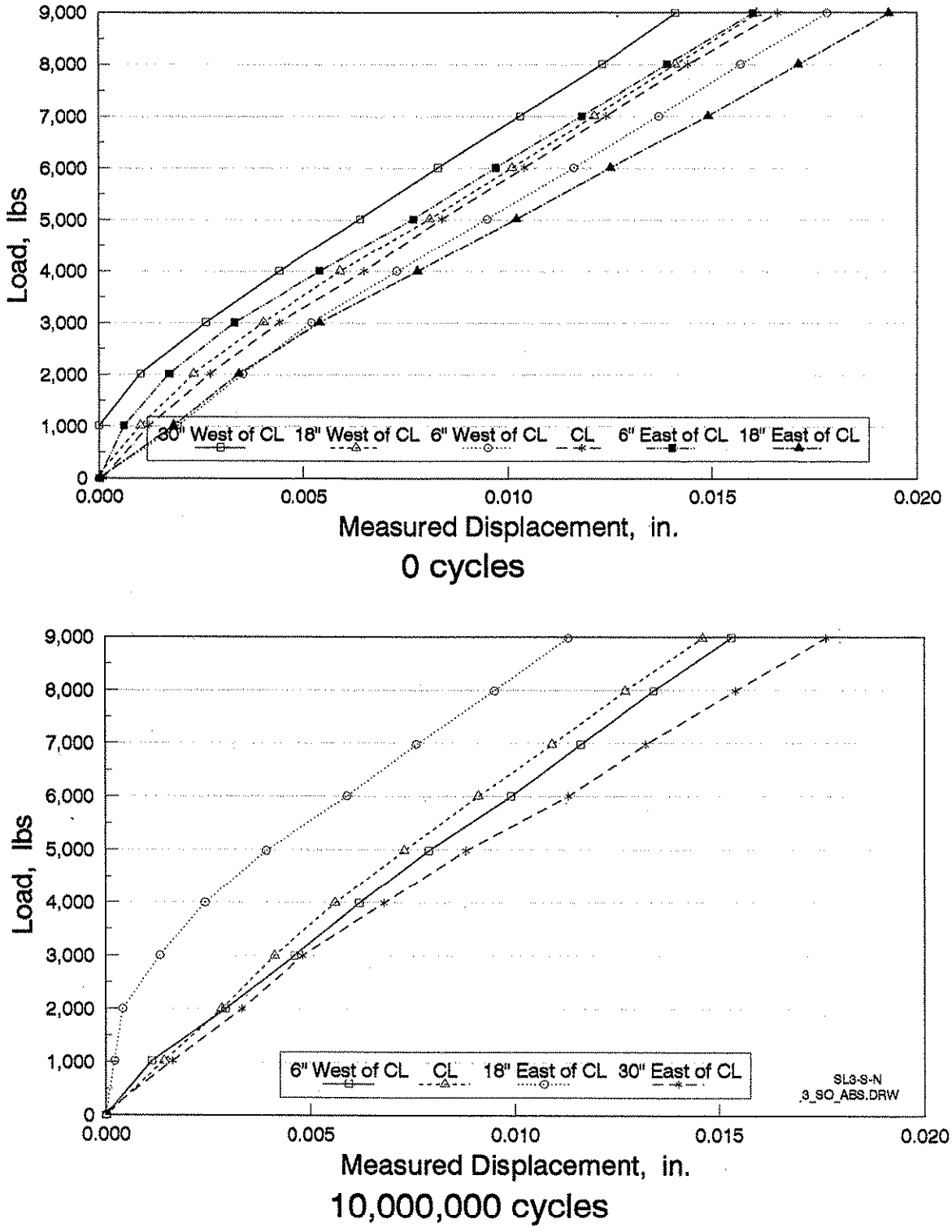

Figure 4.31 Typical load versus displacement diagrams at locations along the joint for Slab 3

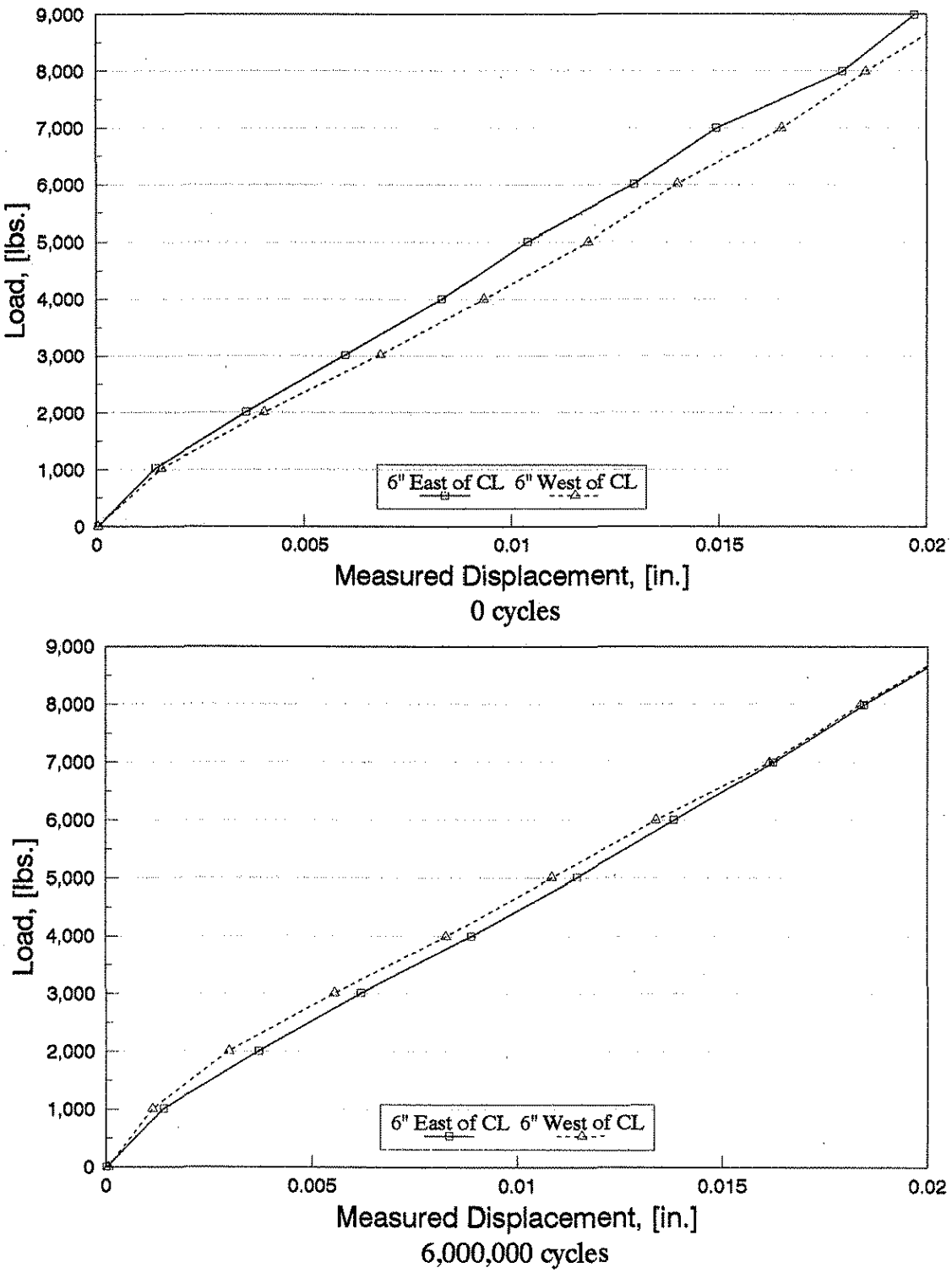

Figure 4.32 **Typical load versus displacement diagrams at locations along the joint for Slab 4**

figure includes two diagrams, one from the results at zero fatigue cycles, and the second at a later number of applied cycles, as indicated in each figure. Because the measured displacements were largely a function of the supporting beams, which were the same for all slabs, the diagrams for the three slabs were very similar in appearance. Plots in Figures 4.30 thru 4.32 are shown for several instrumentation locations along the joint, each following a similar relationship.

The overall behavior of the three slabs was observed to follow the expected performance during the fatigue testing. All the three test slabs tended to follow the anticipated trend of degrading efficiency of the dowelled joint as the number of applied load cycles increased. Degradation of efficiency of the joint was investigated by observing the relative displacements at the joint, load transfer across the joint, and measured strains in the dowel bars.

In terms of relative displacements at the joint, the performance of the test slabs were evaluated by two methods. One method was to observe plots of the maximum relative displacements, due to 9,000 pounds applied to one side of the joint during a static load test, versus the logarithm of the number of applied load cycles at the particular load test. A second method involved monitoring plots of relative displacement versus applied load for particular static load tests, and comparing these results at increasing numbers of load cycles. Both of these methods were applied in this study

to evaluate dowel performance.

For all of the slab specimens, the maximum relative displacements at the joint during the static load tests tended to increase as the number of cycles of fatigue increased. Results from Slab 2 indicated an increasing trend in Figure 4.33 for the locations of the two dowels adjacent to the point of load application. Relative displacements in Figure 4.33 were measured above the dowels which were eight inches on either side of the center dowel. Figure 4.33a shows data which is more consistent than that in Figure 4.33b, which is related to the resolution of the instrumentation used to measure deflections. Because the relative displacements were quite small, the DCDT resolution, which was a maximum of approximately 0.0005 inches, influenced the consistency of the results. The instruments used to collect the data shown in Figure 4.33a had a smaller resolution, resulting in more consistent data. Though the data in Figure 4.33b has more scatter of the results, the plots still indicated a trend of increasing relative displacements with applied load cycles.

An additional observation to be made from Figure 4.33 is that of two data sets plotted for each location. One set of data is for the North side loaded, and the second is for the South side loaded during the static load testing. The difference between the two plots, though, is quite small. Results from other locations on Slab 2, and also from the testing of Slabs 3 and 4, verified that very small

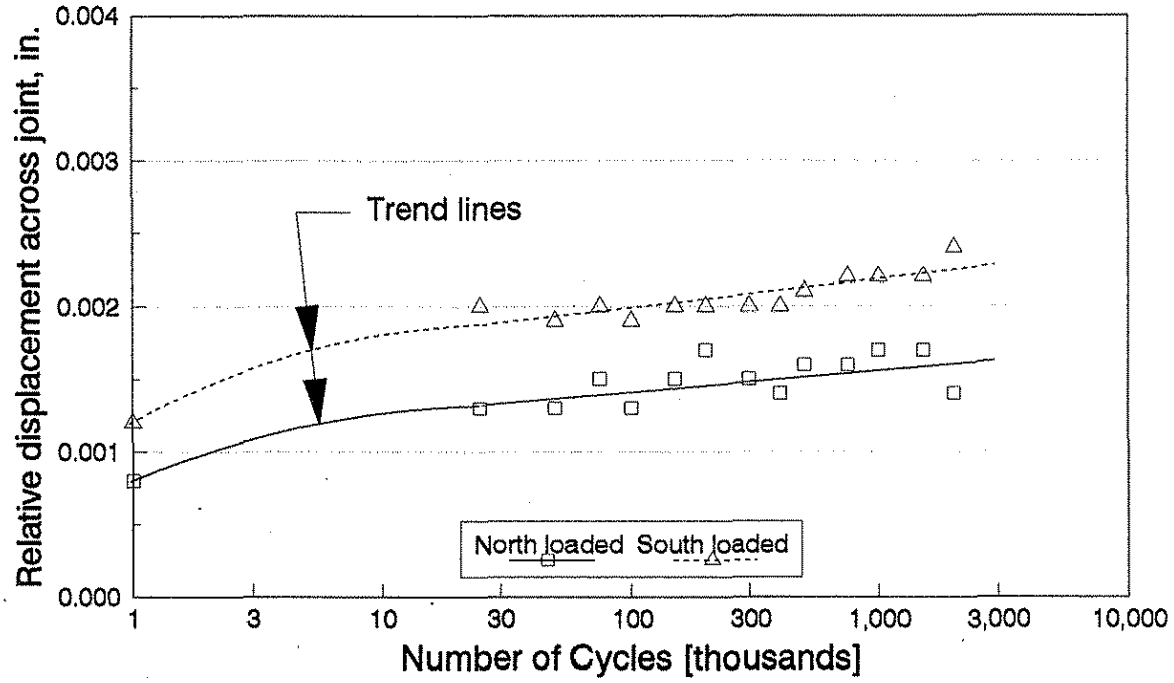

a. FC dowel located eight inches East of center dowel

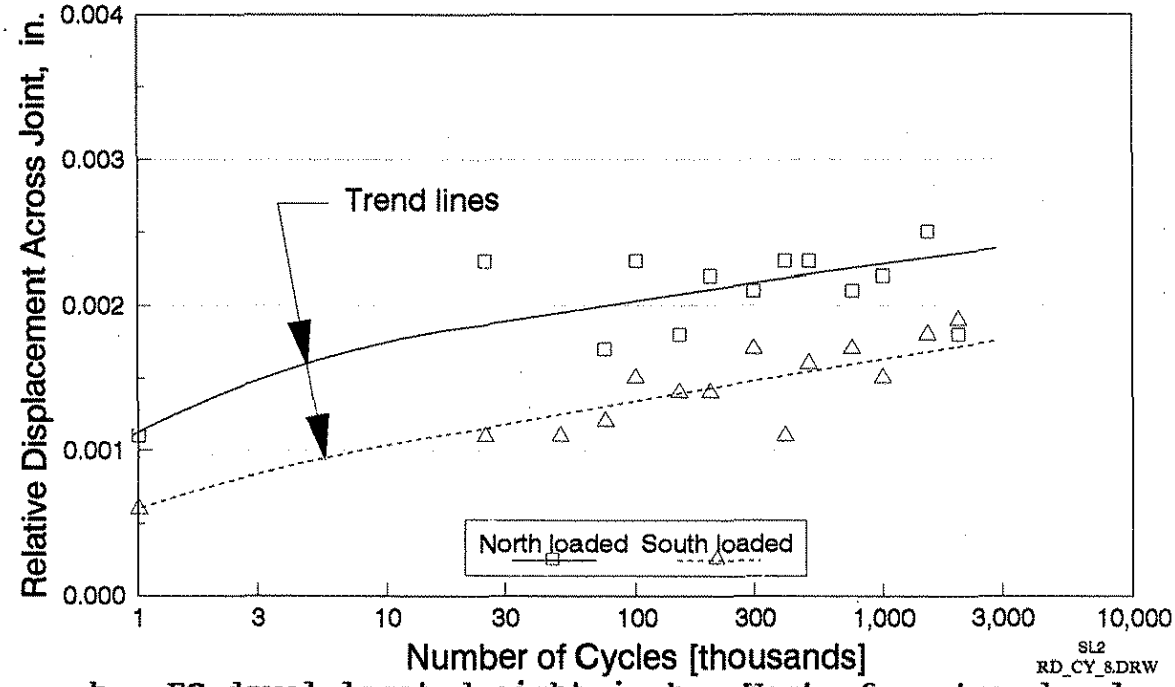

b. FC dowel located eight inches West of center dowel

Figure 4.33 Relative displacement versus number of load cycles (log) at dowels in Slab 2

differences existed between relative displacements when the two sides of the joint were loaded. A difference between the two diagrams of Figure 4.33 is that the loaded side causing the largest relative displacements is reversed for the two dowels adjacent to the load. The largest relative displacement in the dowel eight inches East of center occurred when the South side was loaded, while the North loading caused the maximum value for the dowel eight inches West of center.

Because the variation in relative displacements when the two sides were loaded were quite small, the difference of behavior for the two dowels appears to be insignificant. While idealized behavior would be symmetric, or not depend on the side which was loaded, variations such as those observed are possibly due to slight deviations from ideal conditions, such as in specimen construction. Also, the greatest interest was in the most severe condition experienced by a dowel, which was indicated by the largest relative displacement under loading. Whether the largest relative displacement occurred when the North or South side was loaded was not of importance while considering dowel behavior.

For clarity and ease in the discussion of results, future plots will present the data set, for either North or South side loaded, that has the largest relative displacements. Thus indicating the critical load condition, or the most severe degradation, at each dowel location.

Shown in Figure 4.34 are the relative displacement

results from Slab 2 for the center three FC dowels. Included in Figure 4.34 are one plot from each of Parts a and b in Figure 4.33 with the largest displacements, as well as the data for the location of the center FC dowel. The center FC dowel was located directly underneath the load point, and indicated larger relative displacements than the two adjacent dowels. As observed for the two adjacent locations, the relative displacements at the center tended to increase with the number of cycles. The rate of increasing relative displacements, which indicates the rate of efficiency degradation, appears to be approximately the same for all three locations.

Presented in Figure 4.35 are the relative displacements for Slab 3 measured at dowels located at 6 inches on either side of the load point. Since the 1.5-inch steel dowels used in Slab 3 were spaced at 12 inches, the dowels located at a distance of 6 inches on either side of the load were the two dowels nearest to the load. Thus, the Figures 4.34 and 4.35 depict the maximum relative displacements that the slabs experienced. Similarly Figure 4.36 demonstrates the maximum relative displacements for the Slab 4.

Relative displacements at the FC dowels of Slab 2 located 16 inches away from the center yielded data with a large scatter. Instrumentation problems because of the small displacements produced this scatter. The relative displacements at the locations 16 inches from center appeared

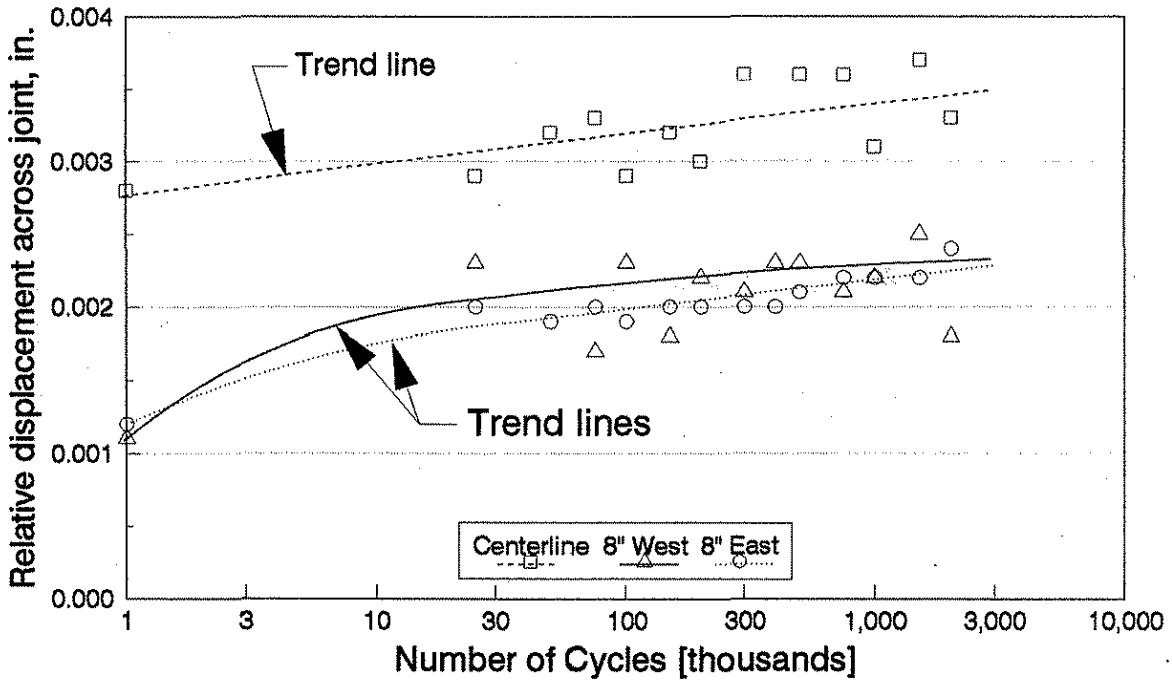

Figure 4.34 Relative displacement versus number of load cycles (log) for slab 2

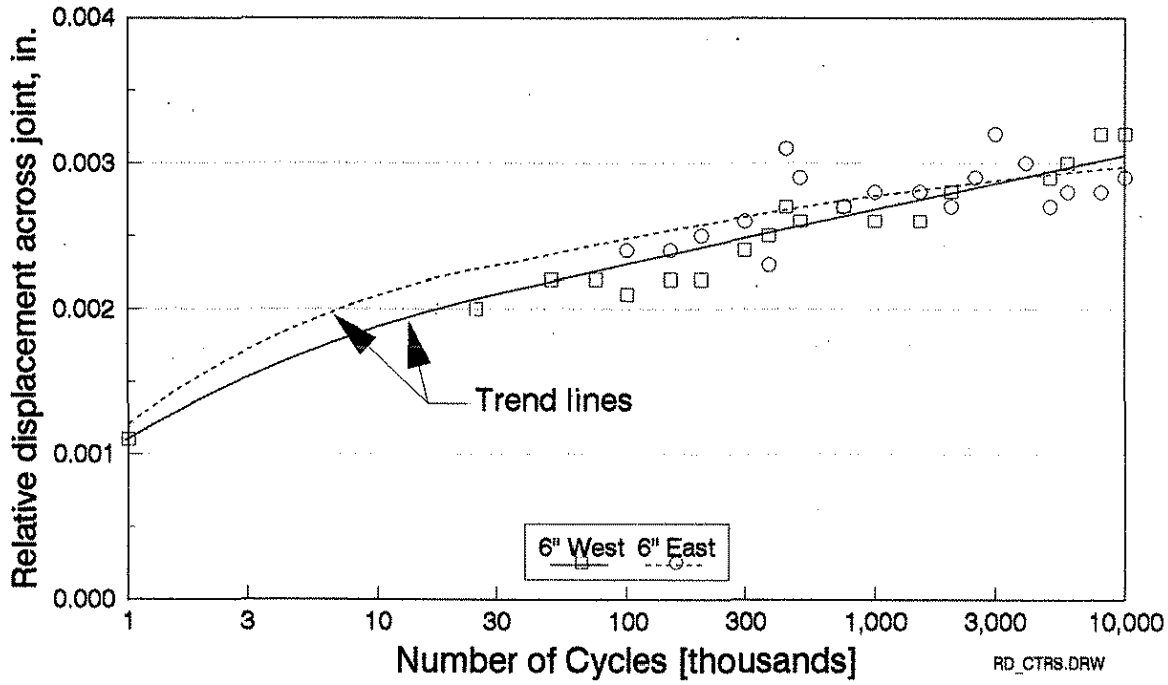

Figure 4.35 Relative displacement versus number of load cycles (log) for slab 3

to be much smaller than those for dowels eight inches from center. The majority of load transfer, indicated by the relative displacement at each location, appeared to be carried by the three dowels which were located within eight inches on either side of the load point. Thus, load transfer and relative displacements at the dowels 16 inches away from the load were significantly reduced.

A very similar trend to that observed in the relative displacements for Slab 2 occurred in the results of Slab 3. Figure 4.37 include relative displacements measured at dowels located 18 inches on either side of the load point. The scatter of the relative displacement is very similar to that of the Slab 2. Because of the more pronounced scatter and less expected dowel loads at the locations other than the nearest dowel locations, the results at the far off dowels were not included.

The differing distribution of relative displacements of the Slab 2 from those of the other two slabs indicated that the dowel located underneath the load point acted to reduce the relative displacements at the adjacent dowels. This behavior displays the importance of the assumption that the critical wheel loading at a joint is directly over a dowel.

A behavior of the slabs, which is demonstrated in Figures 4.33 through 4.37, was that the most significant change in the relative displacements occurred during the first 100,000 to 200,000 cycles. The increase in relative displacements during

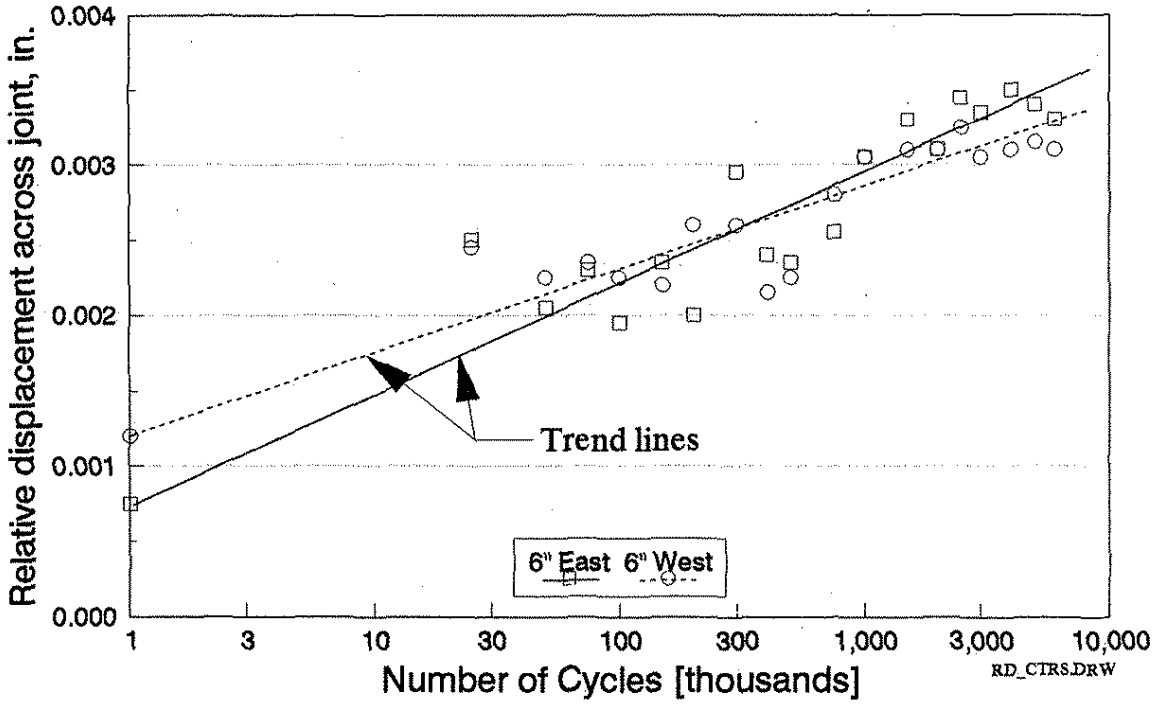

Figure 4.36 Relative displacement versus number of load cycles (log) at the FC dowels 6 inches from the center of Slab 4

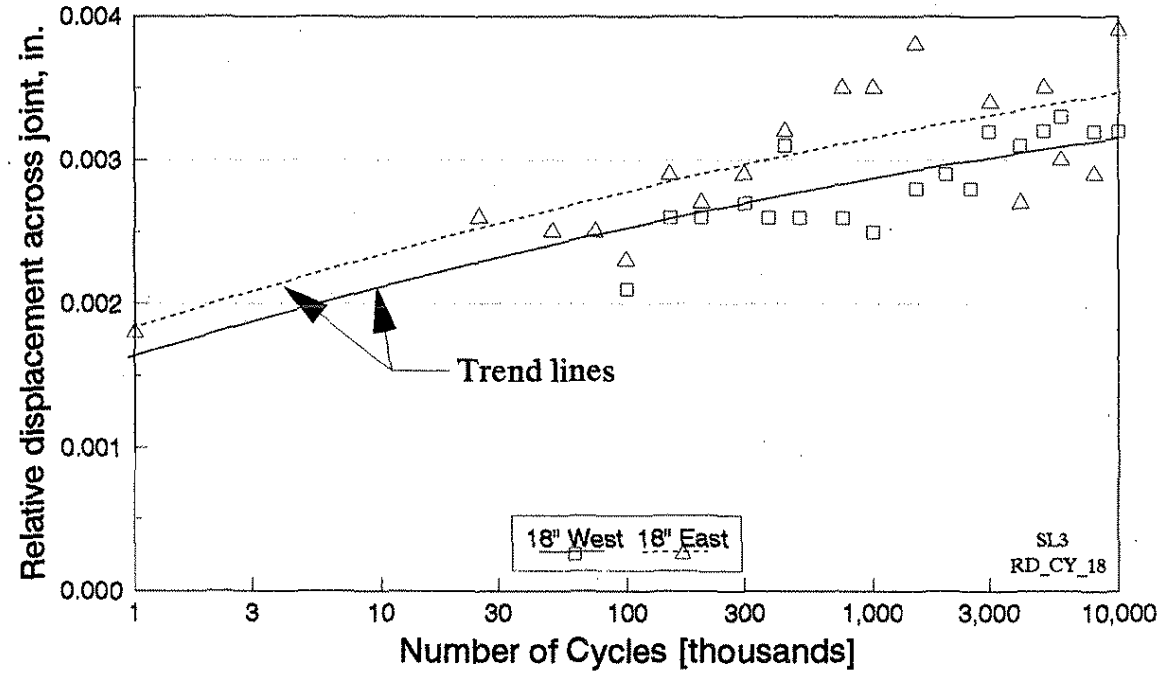

Figure 4.37 Relative displacement versus number of load cycles (log) at the steel dowels 18 inches from the center of Slab 3

the first 200,000 cycles was approximately equivalent to that occurring beyond that point. Behavior such as this indicated that the long-term performance of a pavement dowel system should be evaluated only after a large number of load cycles have been applied. For example, the performance of doweled joints of a newly constructed concrete pavement should be evaluated after approximately one-quarter of a million load applications. Evaluation before this number of cycles may give results that exaggerate the long-term performance of the joints.

An alternative method of observing the influence of the load cycles on the relative displacements at the joint is to compare plots of load versus relative displacements at the joint for individual static load tests. Results from testing of the three slabs showed that, as the number of applied cycles increased, the plots of load versus relative displacements changed. At the beginning of the test program for each slab, or zero fatigue cycles applied, the load versus relative displacement plot was rather linear at all displacement locations. As the number of load cycles increased toward two million, the shape of the load versus relative displacement plots changed, having increased curvature. The changing load versus relative displacement relationship is shown in Figure 4.38 by the plots of data at four times during the cyclic loading program of the Slab 2. Similar plots for Slabs 3 and 4, which were subjected to ten

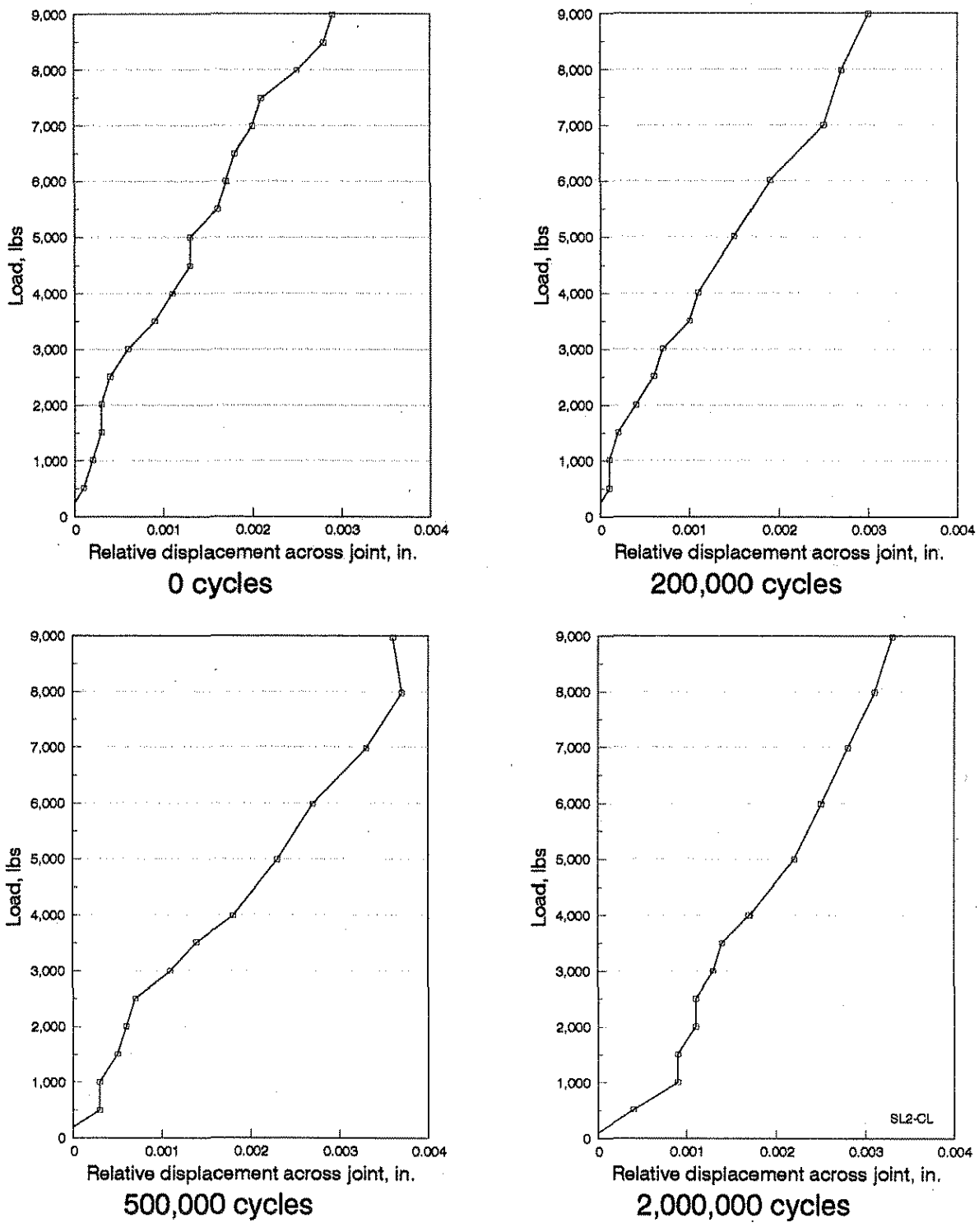

Figure 4.38 Load versus relative displacement diagrams at the joint of Slab 2

million cycles, are displayed in Figures 4.39 and 4.40, respectively.

The changes in the plots for Slab 3 were more significant than those for Slabs 2 and 4, which indicated a greater modification of the composite action of the steel dowel with concrete than for the FC dowel and concrete. An apparent increase in the slope of the data as the load increased indicated somewhat of a "seating" behavior of the specimen, meaning that any looseness of the dowel within the concrete was taken out as the load approached 9,000 pounds. From the results of the third slab, the seating behavior appeared to be more significant, which demonstrated greater looseness of the steel dowel compared to that of the FC dowel.

An additional observation made from Figures 4.38 thru 4.40, was that of significant change in the load versus relative displacement curves from 0 to 200,000 cycles, and less significant change beyond 200,000 cycles. The previous discussion of Figures 4.33 through 4.37, also noted this behavior.

A second method for evaluating the efficiency of pavement joints and dowels, besides relative displacements, is the load transferred across a joint by the dowels. For the full-scale test slabs, instrumentation was monitored during each static load test in order to determine the transfer across the joint. A method was developed to determine load transfer through individual dowels in the full-scale slabs by relating strain

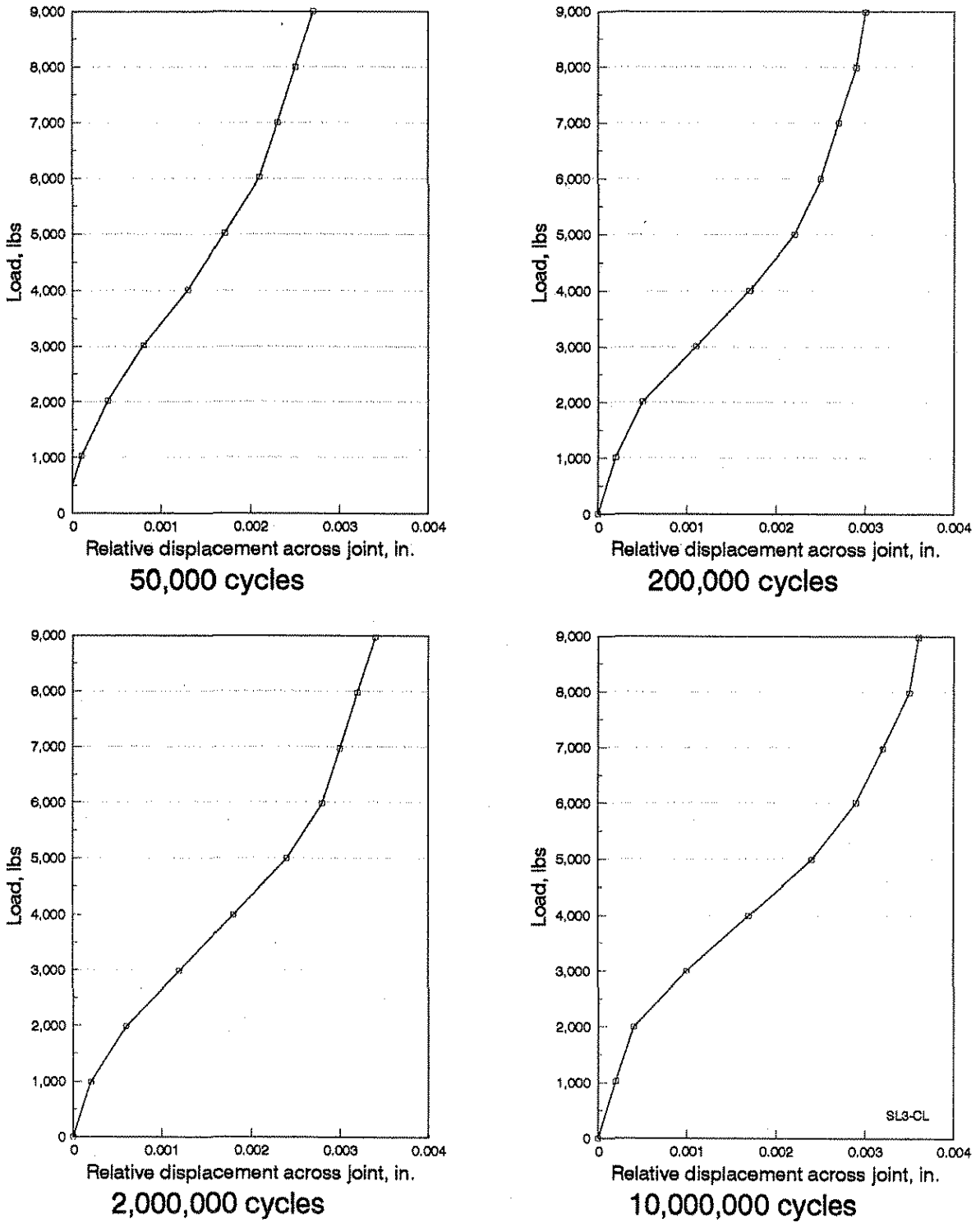

Figure 4.39 Load versus relative displacement diagrams at the joint of Slab 3

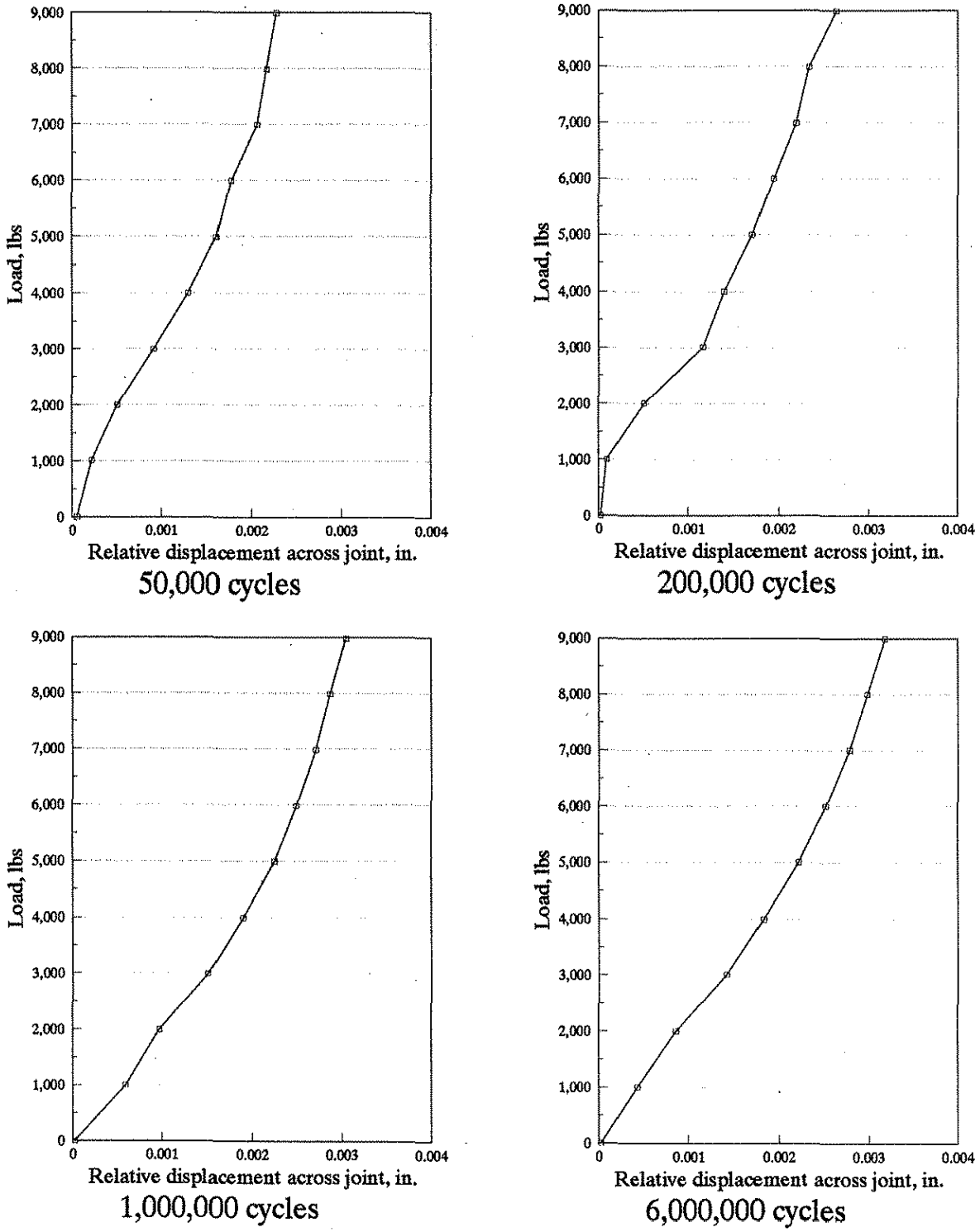

Figure 4.40 Load versus relative displacement diagrams at the joint of Slab 4

gage results from elemental and full-scale specimens. Strain gage data collected from the dowels placed in the slabs will be presented later in this section, while the relation of the elemental and full-scale dowel gage data will be discussed in Section 5.2. A discussion of the method for determining load transfer using the strain gage data from the supporting beams was included in Section 4.3.6.3, and the results from that data will be discussed here.

The amount of transfer, and thus the joint efficiency, was determined at each static load test using the supporting beam strain gage data. During this study, the joint efficiency was considered to be directly related to the percentage of the total load applied to one side of the joint that was transferred to the other side. The percentage of load transfer, then, is the quotient of the load carried by the beams on one side of the joint and the total load applied on the opposite side of the joint. Figure 4.41 includes diagrams of the load transfer efficiency plotted against the number of load cycles for Slabs 2, 3, and 4. As discussed earlier, the joint transfer efficiency was expected to decrease with increasing load cycles. Initially, the two dowel systems provided load transfer that differed only slightly from one another. From the plot of data for Slab 2, the percentage of load transfer appeared to stay rather constant over the two million applied load cycles, while Slab 3 results over the same number of cycles indicated a decrease

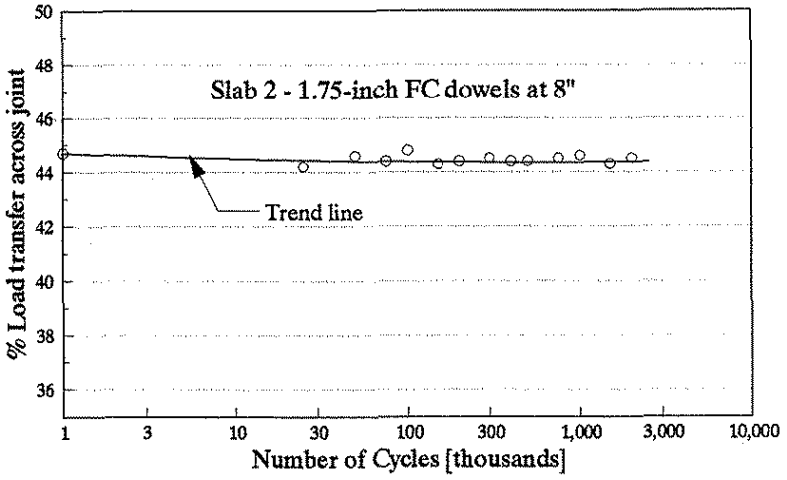

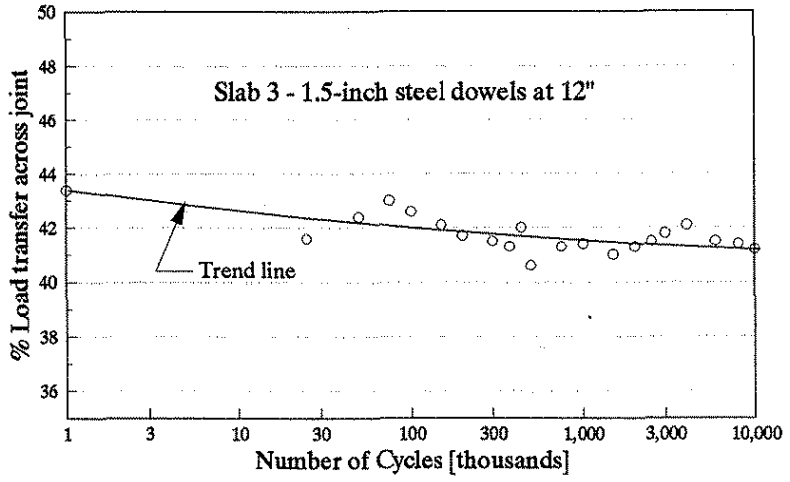

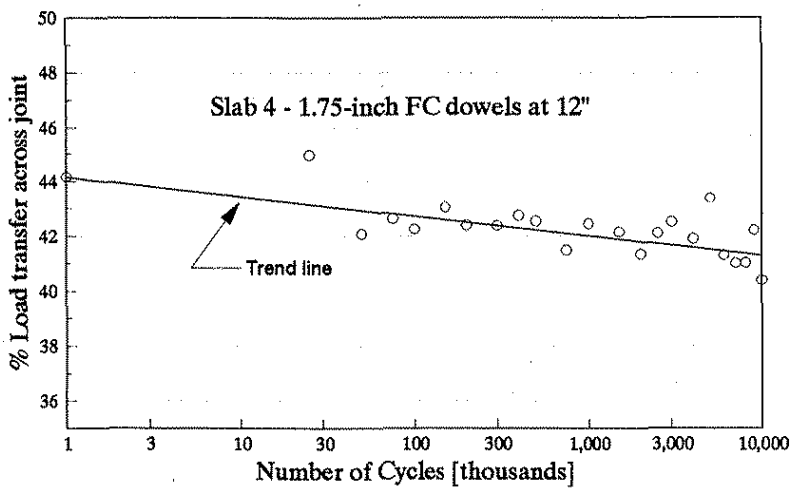

Figure 4.41 Percent of load transfer across the joint versus the number of applied load cycles for Slabs 2, 3 and 4.

in the percent transferred. These results indicated that the FC dowels spaced at eight inches provided a more efficient system initially, and a system that did not degrade as rapidly with repeated loads as did the steel dowels spaced at twelve inches, whereas the behavior of FC dowels spaced at twelve inches (Slab 4) is similar when compared to that of the steel dowels with the same spacing (Slab 3).

Strain gages mounted on some of the dowels placed in the two slabs allowed for the determination of the measured strains and bending moments at the gage locations. By observing the strains in the dowels, the distribution of the load transferred by each of these dowels could be determined. Also, as with the other types of instrumentation, the performance of the dowels as the number of load cycles increased could be monitored.

Details of the placement of strain gages on dowels of the slab specimens were included in Section 4.3.4.2. Placing the gages at identical locations on both types of dowels (FC and steel) allowed for a direct comparison of the actions experienced by the two while testing the Slabs 2 and 3. Results from both of the slabs indicated that the strains measured at 1.5 inches from the joint were significantly larger than those at 5.5 inches. For this reason, strains at 1.5 inches were assumed to provide more consistent results by avoiding readings near the resolution of the instruments and the data acquisition system. Providing further strength to

this assumption was the observation that the dowel strains for Slab 4 at 1.5-inch locations were considerably larger than those at 4.0 and 6.0 inches.

Three FC dowels in the center of Slab 2 were mounted with strain gages, and from these, moments at the gage locations caused by the static load testing were determined. Moments created by the maximum applied load of 9,000 pounds during each static test were then plotted along with the associated number of load cycles applied at the time of the test. Figure 4.42 includes moment versus number of cycles for all three dowels. The two dowels on each side of center performed much the same, though their moment values differed slightly. A trend of increasing moment at the 1.5-inch location with increased number of load cycles was observed. Results for the center dowel, though, were somewhat different, with a larger scatter of data and moment values that remained nearly the same, or decreased slightly.

A trend of increasing moment in the dowels agreed with the results of the relative displacement data collected, which indicated that cyclic loading increased the relative displacement caused by a static load of 9,000 pounds. An increase of the relative displacement might be considered to indicate a "looseness" which results in the dowels undergoing greater flexure when loaded. In other words, the transfer of load at the joint becomes less like a pure shear condition and was influenced by additional flexure of the dowels.

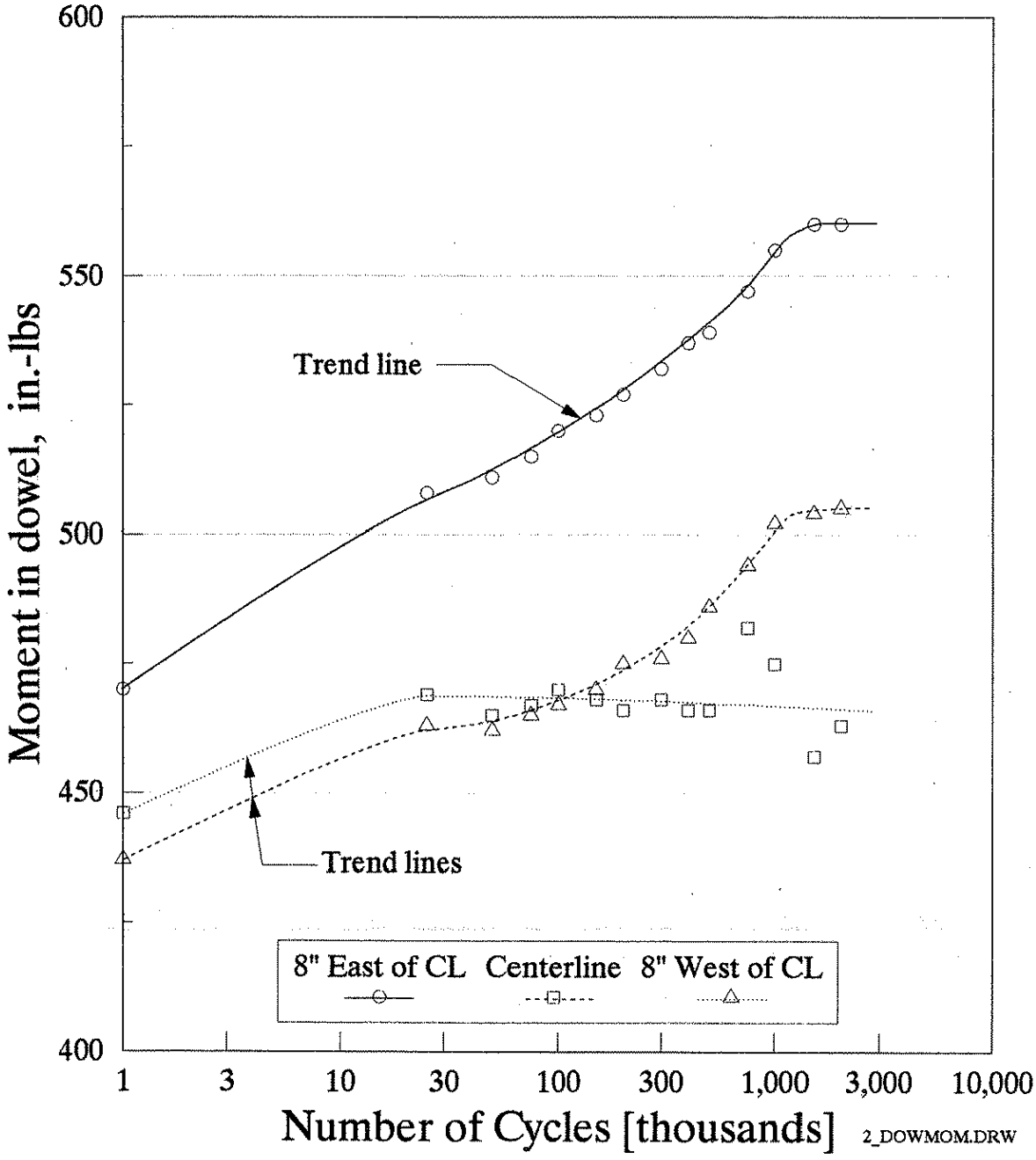

Figure 4.42 Dowel moment at 1.5 inches from the joint versus number of cycles for Slab 2

The performance of the dowel at the center, shown by the plot in Figure 4.42, appears not to agree with the results of the adjacent dowels. Such results do not necessarily indicate that the center dowel was behaving differently, but rather an influence of the applied load on the measured strains, or a shift of the moment curve in the dowel. Since the static and dynamic loads were applied directly above the center dowel, the distribution of moment may differ for the center dowel as compared to the adjacent two. The instrumentation provided on the center dowels, though, does not allow for a more detailed analysis of the moment along the length of the dowel.

As with Slab 2, the moments in two dowels in Slab 3 were determined for 9,000 pounds applied to one side during the static load tests. Again, these values were for the location at 1.5 inches from the joint, and were plotted versus the number of cycles for each static test. Figure 4.43 includes these diagrams, which indicate that the steel dowels of Slab 3 behaved somewhat differently from the FC dowels in Slab 2. First, before cyclic loading had begun, each of the two steel dowels adjacent to the load carried a moment of more than twice that of the FC dowels adjacent to the static load of 9,000 pounds. A difference existed in that the moments in the steel dowels changed quite differently than those of the FC dowels as cyclic loading was applied. One steel dowel showed a general increase in moment, while the other showed a decrease as the cycles increased. This behavior indicated

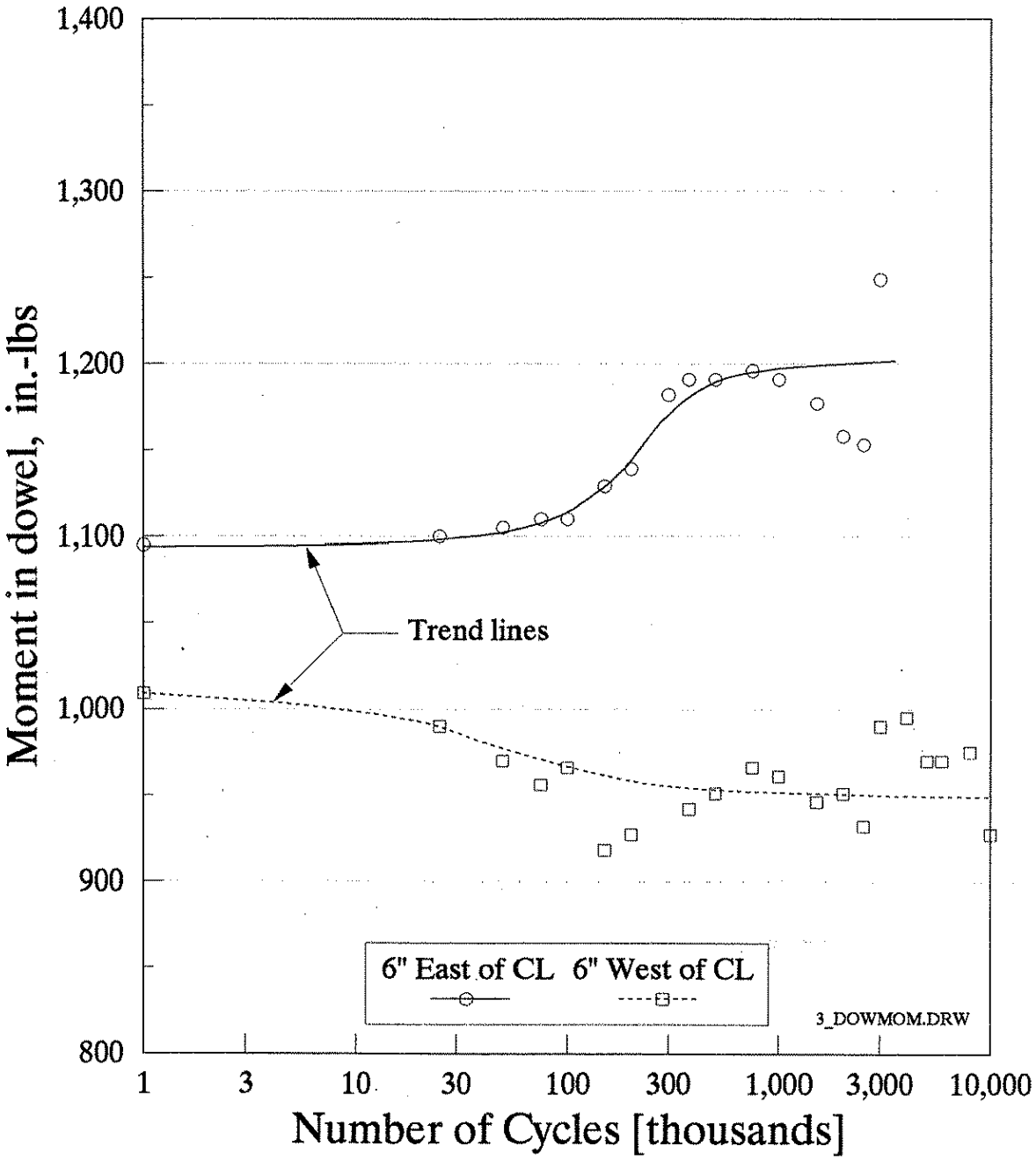

Figure 4.43 Dowel moment at 1.5 inches from the joint versus number of load cycles for Slab 3

that the two dowels nearest the load point were not performing the same in terms of flexure under the fatigue loading. A possible reason was the influence of the other steel dowels within the slab. Relative displacements of the steel dowels 18 inches from the load point were rather significant, which indicated that they were also involved in transferring significant load. Distribution of load transfer to the dowels 18 inches from the load acted to influence the moments in the center two dowels.

The dowel moments at 1.5-inch locations of the two middle dowels of Slab 4 were plotted to yield Figure 4.44. Results from the full-scale testing of the joints and dowels indicated that the long term behavior of pavement dowels could possibly be modeled in terms of relative displacements and load transfer efficiency at a joint. Results from testing of the Slabs 3 and 4, as discussed in this section, indicated a similar trend in performance of both 1.5-inch steel dowels spaced at 12 inches and 1.75-inch FC dowels spaced at 12 inches. Presented in Figures 4.35 through 4.37 and 4.41 along with the data points are lines indicating the general trends observed in the data. Note that the abscissa in each plot of relative displacement and load transfer data is the logarithm of the number of cycles. The relative displacement data followed a trend with a curved shape and with increasing values, which tended to approach a maximum value for the slab with FC dowels and tended to continue increasing for the slab

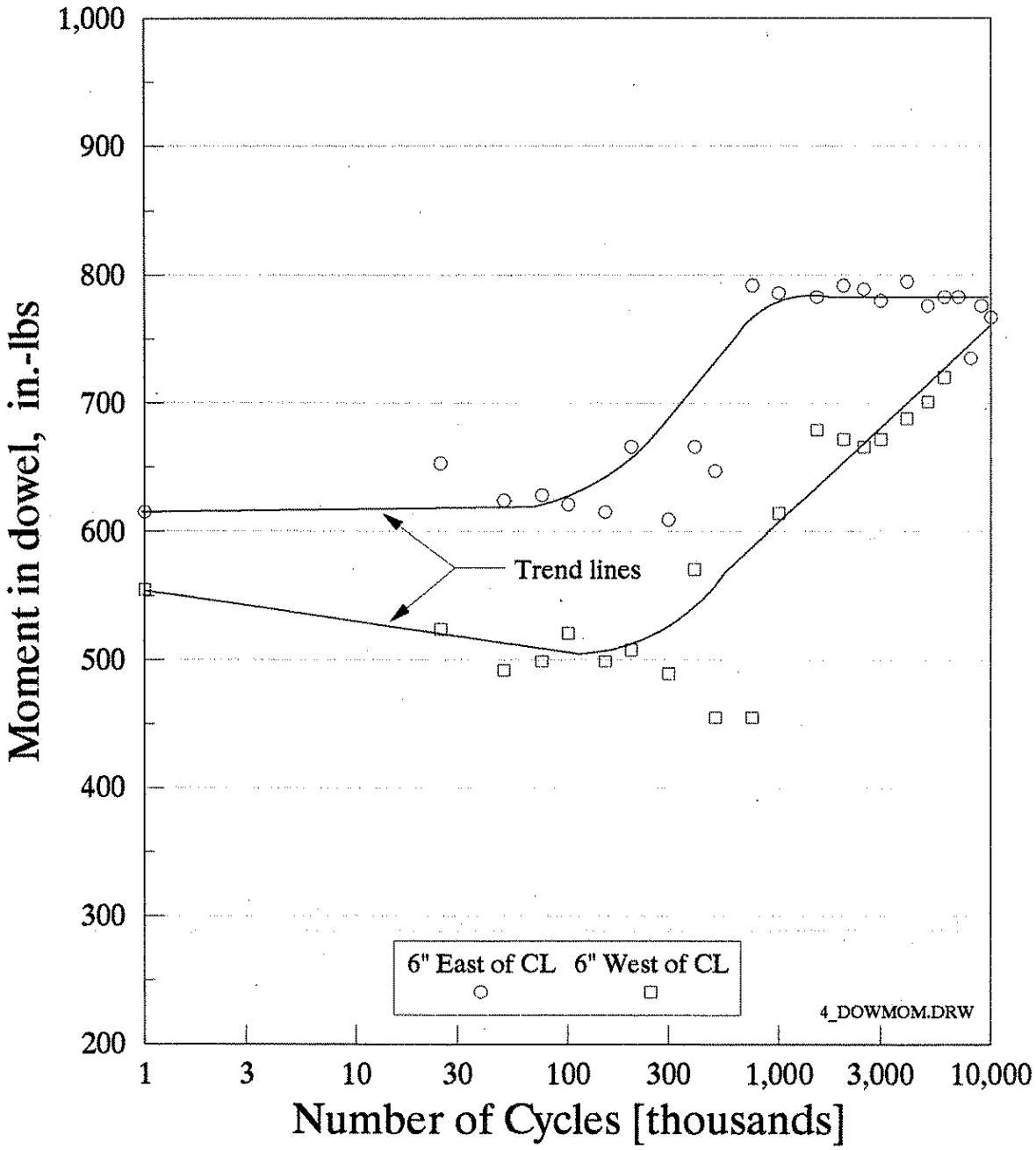

Figure 4.44 Dowel moment at 1.5 inches from the joint versus number of load cycles for Slab 4

with steel dowels. Load transfer data also followed a curved trend, which approached a minimum value for the slab with FC dowels and continued decreasing slightly for the slab with steel dowels.

Because the data indicated rather consistent behavior of the test slabs under fatigue testing, development of models relating the relative displacement and load transfer behaviors of pavement joints to the number of applied load cycles may be possible. Analytical models would be based on the trends noted in the data and would be similar in shape for both materials. Further studies may yield analytical models to estimate the proposed relationships, as well as relationships for other load transfer systems. Separate models would be required for each size and spacing of dowels, with each model specific to the particular parameters studied.

4.3.7.3 Dynamic load testing of full-scale slabs

Results of the dynamic testing were considered, first, by observing the graphical output for the applied load and displacements, and second, by analyzing measurements taken from the plotted output. A sample of the plotted output is shown in Figure 4.45. Included in the output plots are the load curves for the two actuators, labeled as Load 1 and Load 2, and the DCDT output curves for two locations on opposite sides of the joint, labeled DCDT 1 and DCDT 2. The plots in

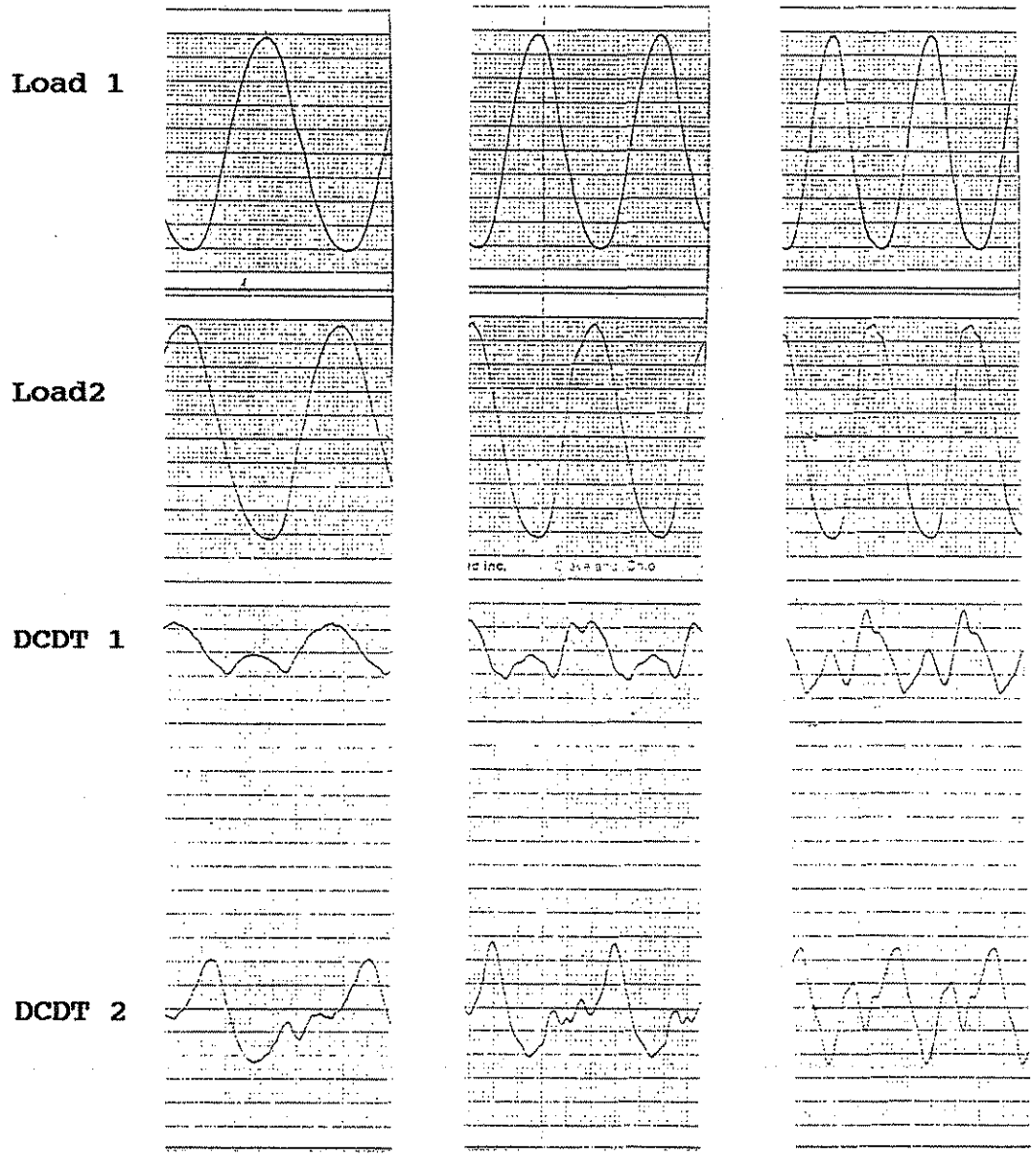

Figure 4.45 Plotted output from dynamic load testing of Slab 3

Figure 4.45 are representations of the output voltages from the load and displacement instrumentation. Therefore, appropriate conversion factors were applied to the values in order to determine actual load or displacement values. For ease of discussion, the behavior characteristics of the slab during dynamic loading will be considered by observing only the general trends exhibited by the output plots.

The general behavior of the slab, with respect to displacements measured at the joint, was considered by observing the output plots for DCDT 1 included in Figure 4.45. The slab displacement behavior during cyclic loading was understood by considering a DCDT curve to be a representation of the slab movement at the particular location of the DCDT. The DCDT 1 location was on top of the slab and directly adjacent to the joint.

Within one cycle, the DCDT 1 output curve included two peaks. The two peaks were due to the cyclic loading being applied by two actuators which were on opposite sides of the joint and were operating 180 degrees out of phase. The higher of the two peaks in the DCDT 1 curve was a result of the slab having been loaded with the maximum load of 9,000 pounds by the actuator on the same side of the joint as DCDT 1. The second, lower peak was the result of the maximum load applied by the actuator located on the opposite side of the joint as DCDT 1. At the exact times of both the higher and lower peaks, the actuator which is not applying the maximum load, is

then applying the minimum load set for the cyclic loading, which is 200 pounds.

Similar dispalcement behavior of the slab to that occuring during the cyclic loading, was noted during the static load tests. During the application of static loading, the displacements on the loaded side of the joint were noted to be greater than those on the unloaded side. The difference between the displacements was the relative displacement at the joint. Results of the dynamic testing indicate that the behavior of the slab during cyclic loading is quite similar to that measured during the static load tests. Because of the nature of the output, the magnitudes of the absolute displacements during cyclic loading could not be determined. By measuring the magnitudes of the amplitudes of the DCDT plots, the range of movement experienced by the slab at the joint, was determined.

Also of interest during the dynamic testing was the influence of the cyclic loading frequency on the load curves and on the displacement response of the slab at the joint. From the output plotted for each of the load cells mounted on the actuators while cycling, the load was observed to have been applied smoothly and consistently, for all of the frequencies tested.

By measuring the maximum amplitudes of the curves from the DCDT output plots, the influence of frequency on the displacement behavior of the slab, was observed. The

influence is shown graphically in Figure 4.46. In Figure 4.46 the values of the displacement range were determined by applying the appropriate calibration factors for the DCDTs to the measured amplitudes from the output. These values were determined for measurements taken from output plots recorded at frequencies of from one to five hertz.

4.3.7.4 Core samples of test slabs

At the conclusion of each of the fatigue testing cycles for the slabs, a core drill was used to remove core samples at the locations of several dowels and centered at the joint. The cores allowed for the evaluation of any fatigue of the concrete surrounding the dowel. Fatigue would be caused by the repeated transfer and reversal of loading applied during the cyclic loading of the slabs. Distress of the concrete surrounding a dowel had been observed in dowels placed in actual pavements after being subjected to many years of use. Concrete fatigue may manifest itself in an oval-shaped hole forming around the dowel (McWaters 1992). From the core samples taken from the three full-scale slabs described in this study, no fatigue of the concrete could be observed. The lack of clear evidence of fatigue is explained by considering the conditions experienced by the dowels in both the field and the laboratory.

As discussed earlier in Section 4.3.3.2, several

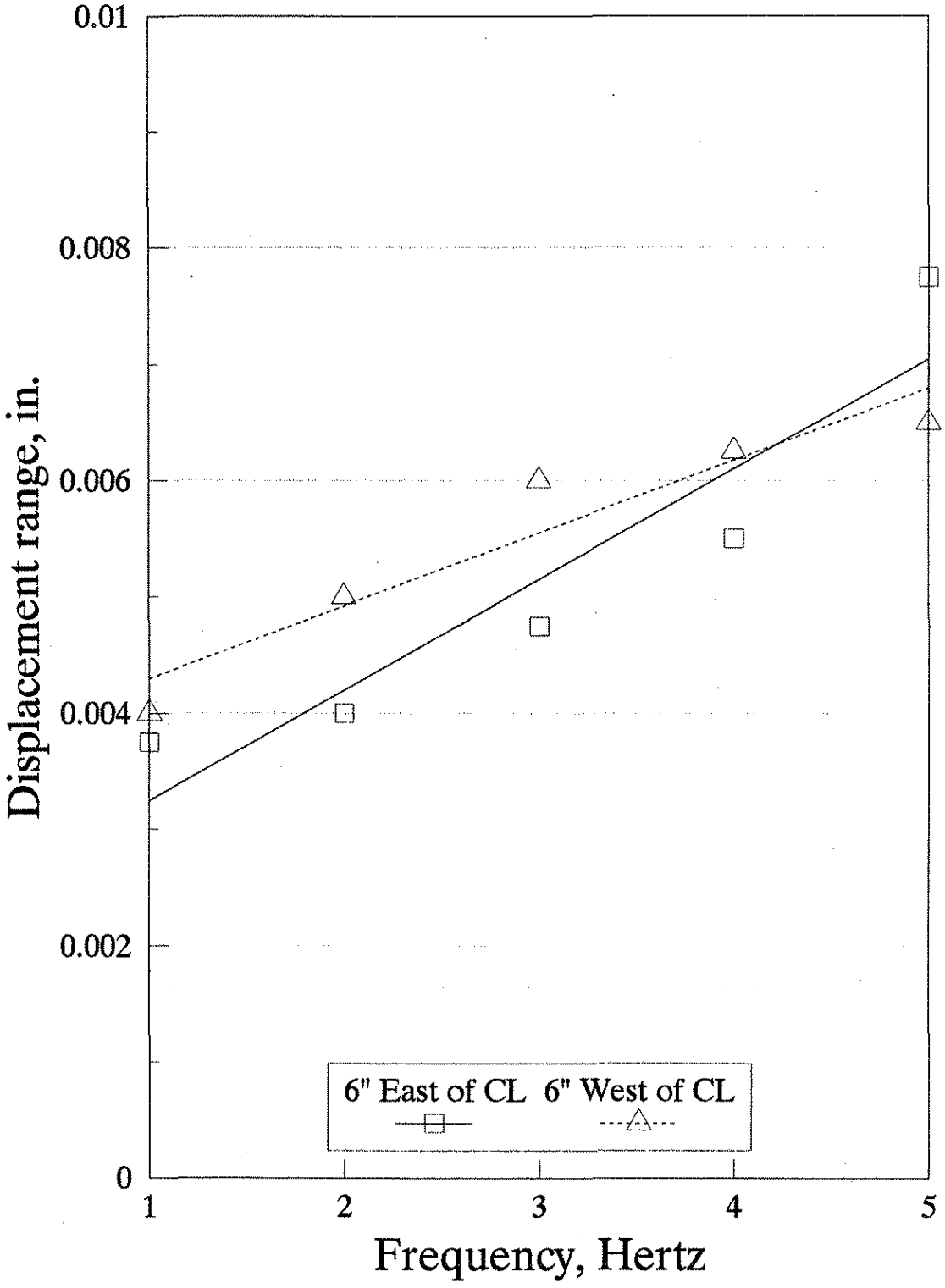

Figure 4.46 Range of movement at the joint during cycling versus the cycling frequency

differences existed between the laboratory setup conditions and those experienced by an actual pavement, one of which was the type of supporting system. An actual pavement is supported by a soil subgrade that changes over time to become non-uniform, resulting in conditions which influence the behavior of the joint and the dowels. One possible result of a changing subgrade would be that one side of the joint would become less fully supported than the other. Because of a lack of support on one side of the joint, the dowel becomes more highly stressed. Increased stress may lead to severe fatigue of the concrete surrounding the dowel, exhibited by an oval-shaped hole as discussed above. Conditions of the type described are referred to as "faulting" and are usually indicated when one side of the pavement joint drops slightly below the level of the opposite side (Heinrichs 1989). Because the steel supporting beams provided a constant support for the full-scale slab in the laboratory setup, situations such as are described above did not occur during the testing of the specimens.

4.3.7.5 Viewing FC dowels with scanning electron microscope

Of interest in this research was the performance of the FC dowel under fatigue loading applied during the testing. One means of evaluating the performance was to visually inspect the dowels after they had been tested. The portion of

the dowel removed along with the core samples taken from the second slab were inspected. No signs of distress were noted at the exterior of the dowel specimens, so a closer evaluation of the FC material was performed using a scanning electron microscope (SEM). If there was any distress within the material, such as at the fiber to matrix interface, an SEM inspection would allow the damage to be observed.

A small sample was cut from the dowel specimen removed from the second slab such that the center of the sample coincided with the location of the joint when the dowel was in place. The viewing surface was parallel to the direction of the fibers, and extended the full diameter of the dowel. The SEM evaluation, though, could find no locations on the viewing surface where the FC material appeared to be damaged or distressed. Such results indicated that the dowel did not experience sufficient fatigue to damage the fibers, the matrix, or the interface between the two materials.

4.4 FC Rod Bond Testing

4.4.1 Introduction

The use of FC rods in place of current steel products as tie rods between two adjacent lanes of concrete pavement requires that the rod be fully developed on both sides of the longitudinal joint between the two lanes. Previous testing

performed at Iowa State University resulted in the development of a test method for determination of the development length of FC rods (Porter 1992). Several advantages over other methods for determination of development length are present in the new method. The embedment length that is evaluated in each beam is in a section of changing shear and moment as well as curvature because of the load applied to the overhang. The same test method was applied in this project to analyze the development length of the FC rods studied.

4.4.2 Materials and specimens

The FC rod that was studied in this research was constructed with a helical wrap. This helical wrapping of the rod provided for a mechanical anchoring system when embedded in concrete.

Three groups of six ISU beams, as well as six pullout specimens were constructed and tested in order to study the bond development of the FC rod. The first group of beams were constructed in exactly the same manner as in the previous research. A beam depth of 12 inches and width of six inches were used, with outcroppings (dogbones) shown in Figure 4.47. Embedment lengths that were studied ranged from 15 inches to 25 inches at increments of two inches. A concrete compressive strength of approximately 5,100 psi was used in the construction of the first group.

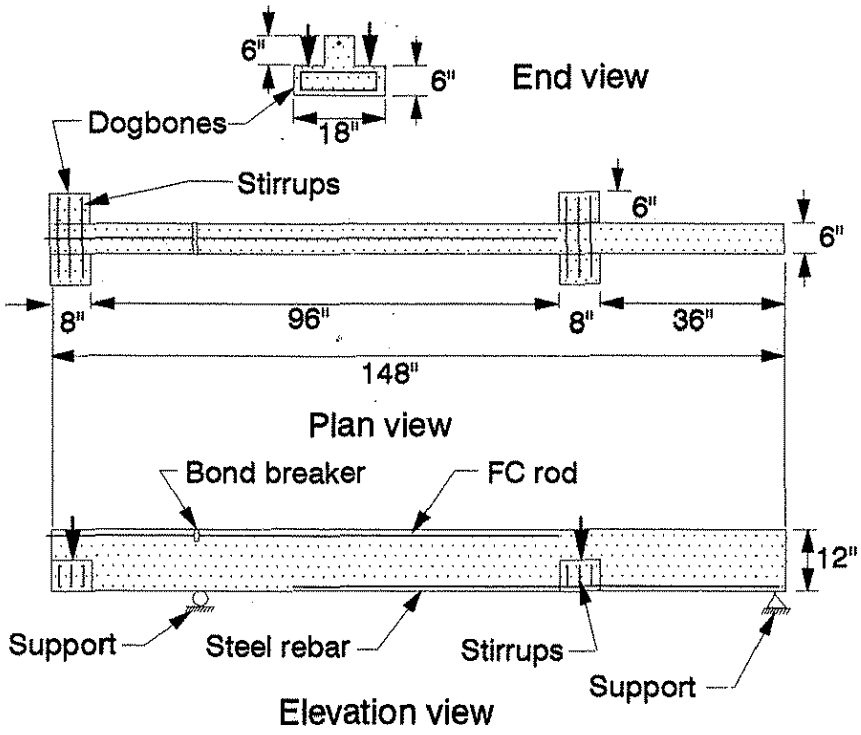

Figure 4.47 Beam specimen used for the development length tests of FC rod

Modifications were made to the beam configuration for the second group of test beams. In order to provide embedment lengths shorter than were used in the first group, while maintaining a sufficient lever arm for the cantilever load, the beams were notched at the top to expose the test rod as shown in Figure 4.48. The beams in the second group were setup to provide approximate embedment lengths ranging from 11 to 21 inches. Actual embedment lengths were measured at the time of testing. Another change made in the test setup from the first group involved changing the position of the FC rod. The rod was lowered in the section from 1.5 inches to 2.25 inches from the top of the beam. In effect, this resulted in a less efficient reinforcing system, so that smaller applied loads would be

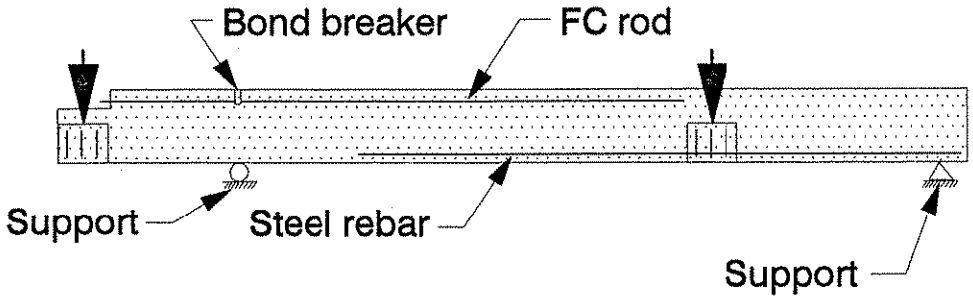

Figure 4.48 Modified beam specimens for development length tests used for groups 2 and 3

required to fully stress the rod. The concrete used was a C-4 mix, which is a typical highway pavement mix, with a compressive strength of approximately 6,500 psi.

The six test specimens of the final group were constructed to have approximately the same embedment lengths of the previous group, with the difference between the two groups being the concrete strengths. The concrete compressive strength for the third group was approximately 2,200 psi.

4.4.3 Test setup

Loads were applied to the beams at the dogbone locations using U-shaped steel load members that were constructed to slide

over the beams. Hydraulic rams were mounted to a heavy steel frame to apply loads to the U-shaped members. The frame was free-standing with the beams simply supported on steel members crossing under the beams. A roller supported the beam underneath the bondbreaker, while a "pin" provided support at the opposite end. The pin was actually a steel roller welded to a plate.

4.4.4 Instrumentation

Measurements of interest during the testing of the beams included vertical displacements at the cantilever end and near the load point between the supports. Also, the slip of the FC rod was measured at the end of the rod extending out of the embedment length. All of the displacements were measured using DCDT instruments. Vertical displacements were referenced to the load frame, while the DCDT for slip measurement was mounted to measure the slip between the concrete and the FC reinforcing bar at the exposed unloaded end.

Applied loads were measured using load cells placed between the two loading rams and the two loading members. Instrumentation was read using a data acquisition system interfaced with a personal computer using a controlling program.

4.4.5 Test procedure

Testing of the beams consisted of applying loads at the dogbone locations while reading the instrumentation at an interval entered into the computer controlling program. A load interval of 200 pounds was used for all tests, which provided sufficient data. Application of load continued until failure of the specimen.

4.4.6 Analytical investigation

The result of greatest interest from the testing was the ultimate load applied to the cantilever at bond failure. Throughout the test, the displacement data was collected, which provides for load versus displacement plots to indicate the behavior of the beam as the load increased. Slip of the FC rod within the concrete over the embedment length indicated the load at which the bond of the rod to the concrete was broken.

4.4.7 Results

The three groups of test specimens were tested at three different times, allowing for adjustments to be made to the next group of specimens after each group was tested. From the testing of the first group of beams, the results indicated that

the embedment lengths that were used were longer than the length required to develop the rod. No slipping of the rods was noted for any of the beams. Therefore, the range of embedment lengths for investigation was reduced in the second group of test beams. Also to reduce the load required to fully develop the rod, the position of the rod in the beam was lowered. However, no slipping of the rod could be observed in the second series of tests. Also there was little change in the load at failure. The reason for the similar loads can be attributed to the higher concrete strength of the second group of beam tests (6500 psi) compared to that of the first group (5100 psi). With the intention of developing slippage in the rod, the concrete strength for the third group of specimens was reduced to an experimental value of 2200 psi. In this group, slippage of the FC bar in the specimens could be observed at small development lengths of 11 to 19 inches. Figures 4.49, 4.50, and 4.51 present the load versus cantilever deflection curves for the beams tested in groups one, two, and three, respectively, for the designated embedment lengths shown in the legend boxes.

4.5 FC Rod Pullout Tests

4.5.1 Introduction

The pullout specimens used in this study were designed to minimize the effects of the loading apparatus. Reaction forces, a result of the pullout forces, can serve to confine a specimen

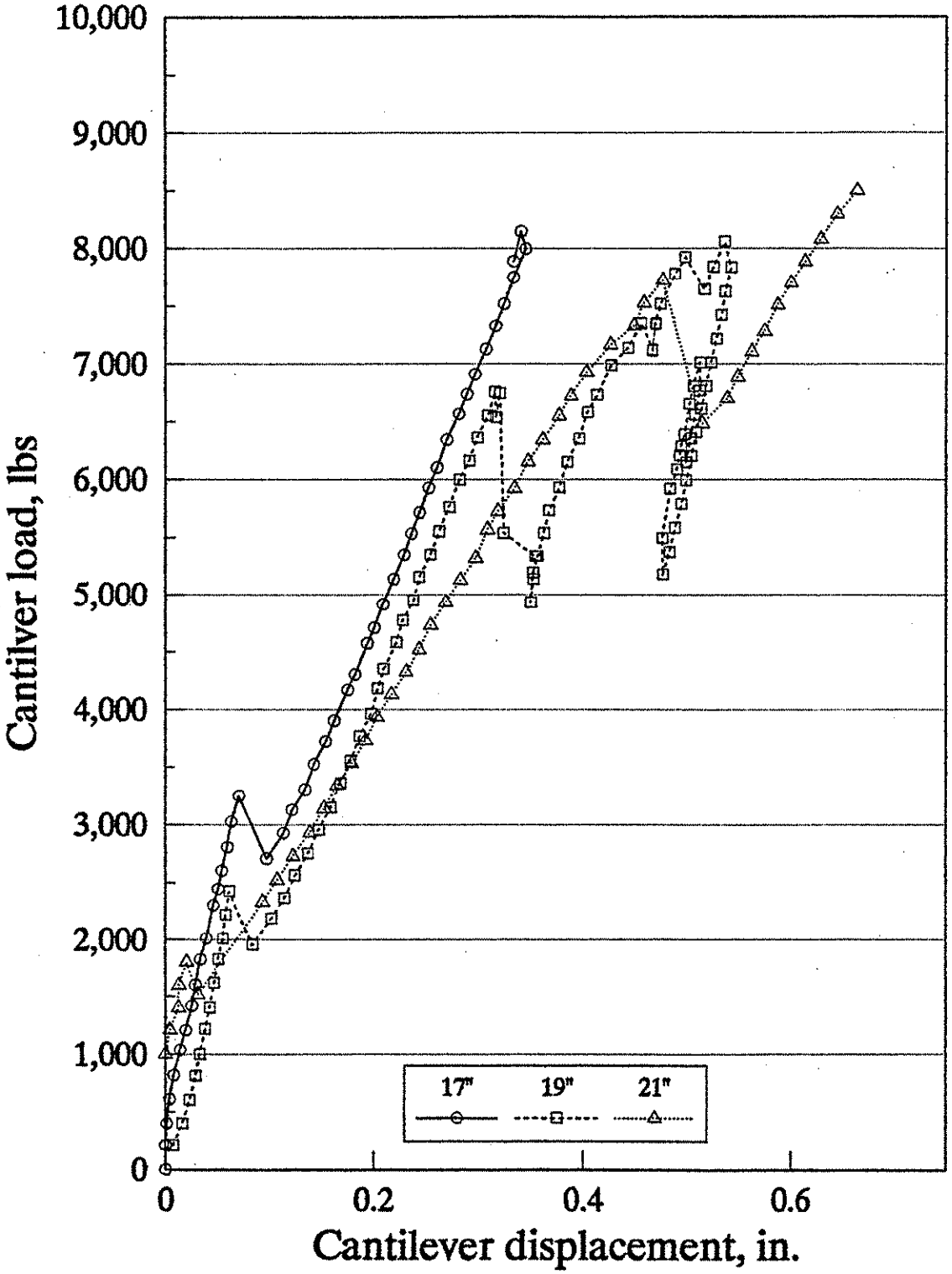

Figure 4.49 Load versus displacement for beam specimens tested in Group 1

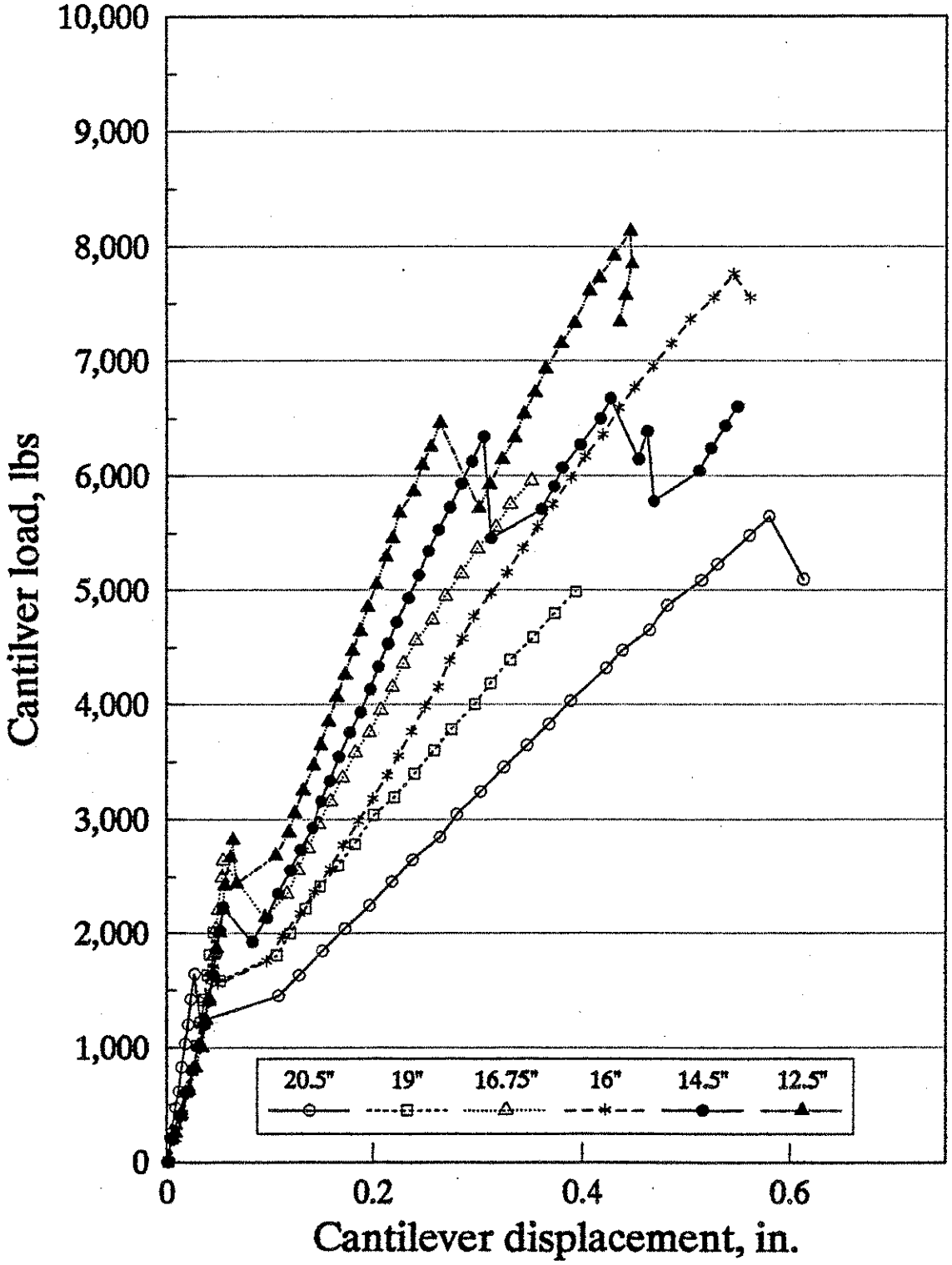

Figure 4.50 Load versus displacement for beam specimens tested in Group 2

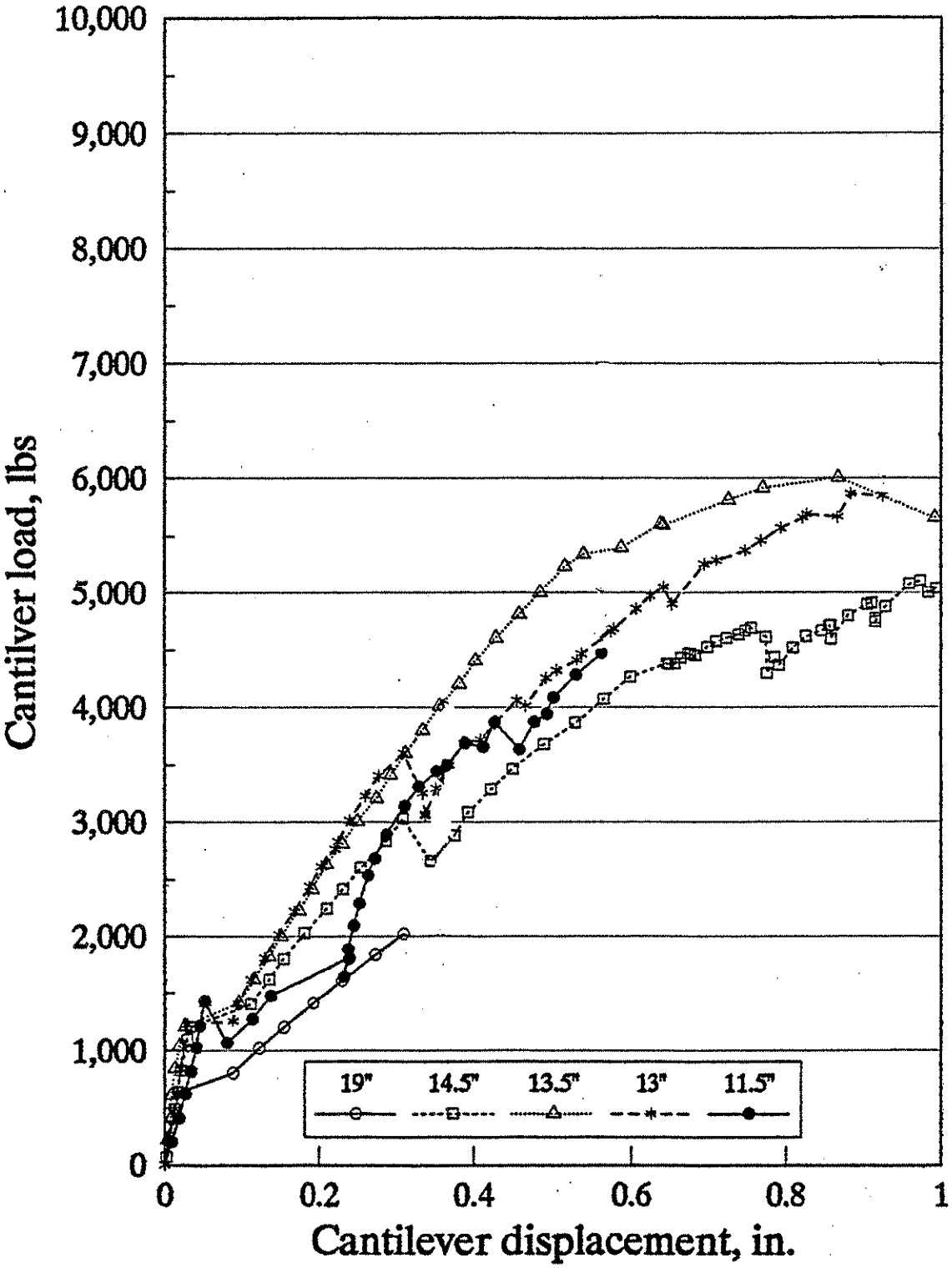

Figure 4.51 Load versus displacement for beam specimens tested in Group 3

and thus produce false strength characteristics by increasing forces normal to the pullout specimen. These normal forces will serve to confine the concrete surrounding the specimen and thereby possibly increasing the required pullout force. In order to avoid these reactions, the concrete surrounding the FC specimens was sized to minimize these effects. In addition to the physical dimensions of the concrete, the reaction forces were distributed at four locations and along the length of embedded threaded rods. The specimen configuration and force schematic are shown in Figures 4.52 and 4.53. The FC specimen was embedded in the center of the specimen. A two-inch slice of insulation was placed between the concrete blocks to provide for set embedment dimensions.

4.5.2 Pullout specimen construction

Construction of the pullout specimens addressed several important variables. These variables had a direct impact upon the pullout resistance of the specimen and concrete strength. The geometric shape of the specimens and rigidity during lifting operations could adversely affect the pullout resistance of the specimen by predamaging the specimen concrete interface. To avoid this pretest damage, the threaded rods were placed in the four corners of the concrete cubes. See Figure 4.52. In addition to this, these rods were continuous across the insulation gap. The continuous steel rods served to absorb any twisting or bending forces present during lifting, thereby removing them from the specimen. Furthermore, small recessed

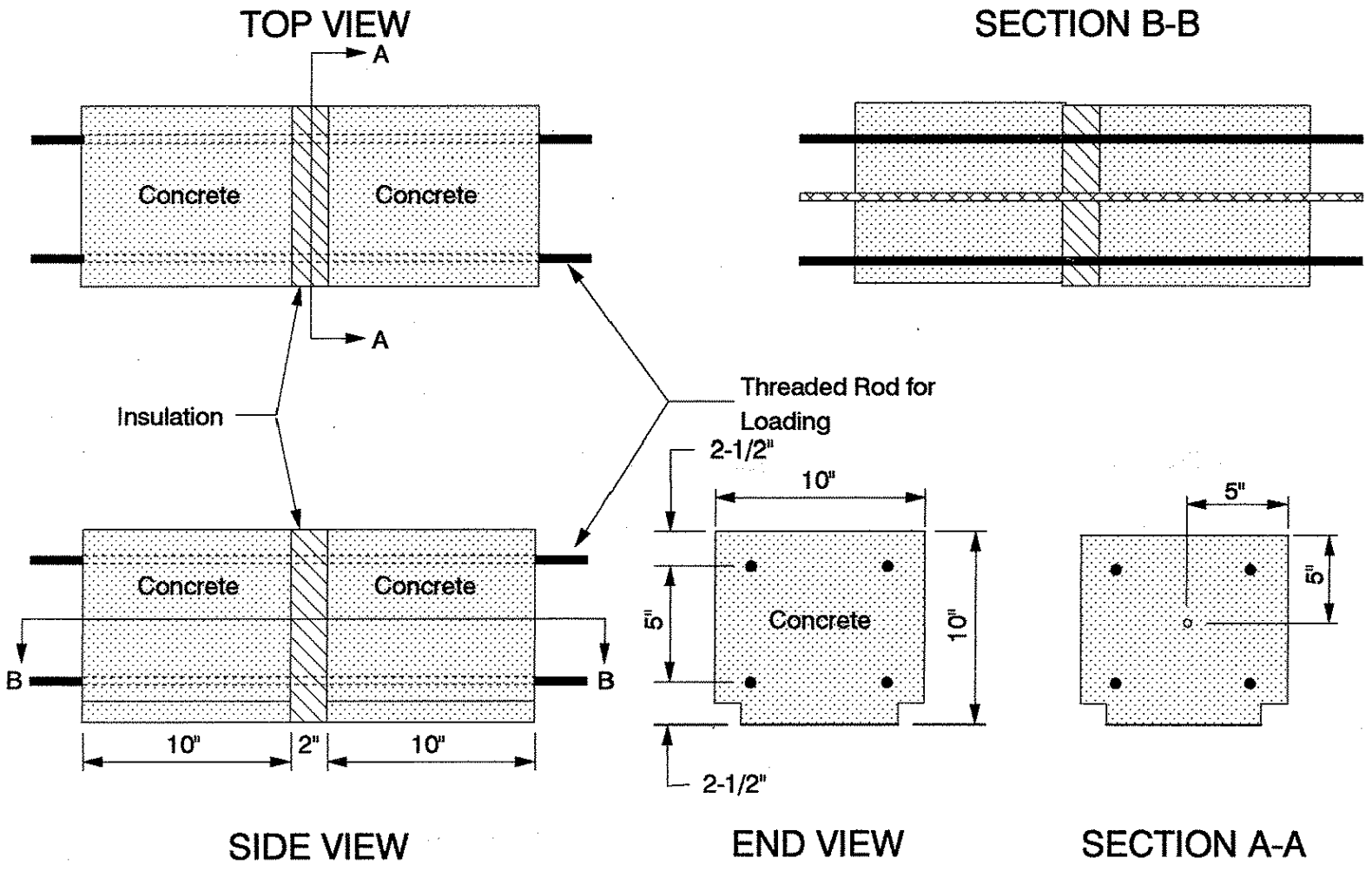

Figure 4.52 Pullout test specimen dimensions

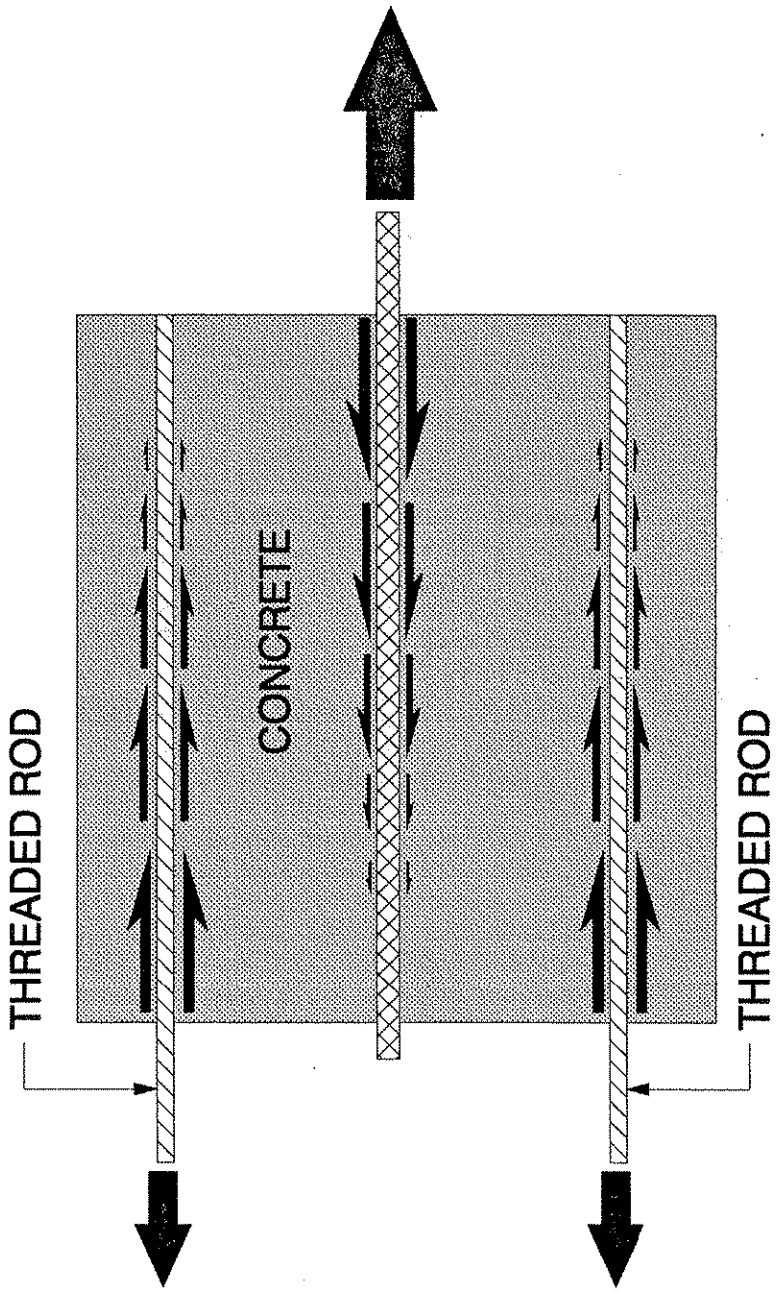

Figure 4.53 Pullout specimen force schematic

ledges were cast into the specimen as shown in Figure 4.52. These ledges allowed for lifting of the specimen without having to install lifting hooks into the concrete. The lifting apparatus was fabricated to provide support along the full length of the specimen. As a result of these precautions, any pretest damage to the specimen was minimized.

All pullout specimens were formed using steel formwork. The insulation and FC specimen were installed in the formwork and small pieces of Styrofoam™ were used to form the lifting ledges and also to secure the center insulation/specimen assembly in the formwork. The steel threaded rods were then installed in the four corners.

Concrete was delivered to the laboratory in a ready mix truck and the slump and air content were measured (standard C-4 mix). The concrete was transferred from the truck to a wheelbarrow and then to the individual specimens. Care was taken during the pour to ensure that both sides of the specimen were filled equally. This equal placement of the concrete prevented the insulation/specimen assembly from bowing or moving. All of the concrete was vibrated and finished. A specimen number was inscribed in the concrete, and all of the specimens were then covered with plastic and sprayed with water daily for the first week. At the end of the first week, the formwork was removed and the specimens were allowed to cure for 28 days in ambient laboratory conditions.

4.5.3 Pullout test procedure

The objective of the pullout test was to determine the required embedment length to attain zero end slip. This test was not designed to include shear and curvature effects since these effects are not a major component of the forces acting on the rods in the field. In order to reach this objective, a test procedure which minimized the confining effects of the loads and supports was designed.

In order to solve the aforementioned concerns, the pullout test frame was specially constructed. Load was applied to the specimens via threaded rods at the four corners of the specimens. These rods were located sufficiently far away from the specimen to remove the confining effects of the loads. The loading frame (see Figure 4.54) itself was constructed such that both ends of the framework were mounted on rollers. Rollers were located to guide the framework and keep the specimen aligned as shown in Figure 4.54. The roller assembly was then loaded through high strength threaded rods as shown in Figure 4.54. The East end of the frame served as a fixed support for all of the specimens, while the West end of the frame accommodated the hydraulic ram and the loading apparatus.

At the conclusion of the curing period, the specimens were lifted into the testing frame. The East end of the specimen (fixed support) was attached to the frame. Following the attachment of the East end, the West end was fitted into the

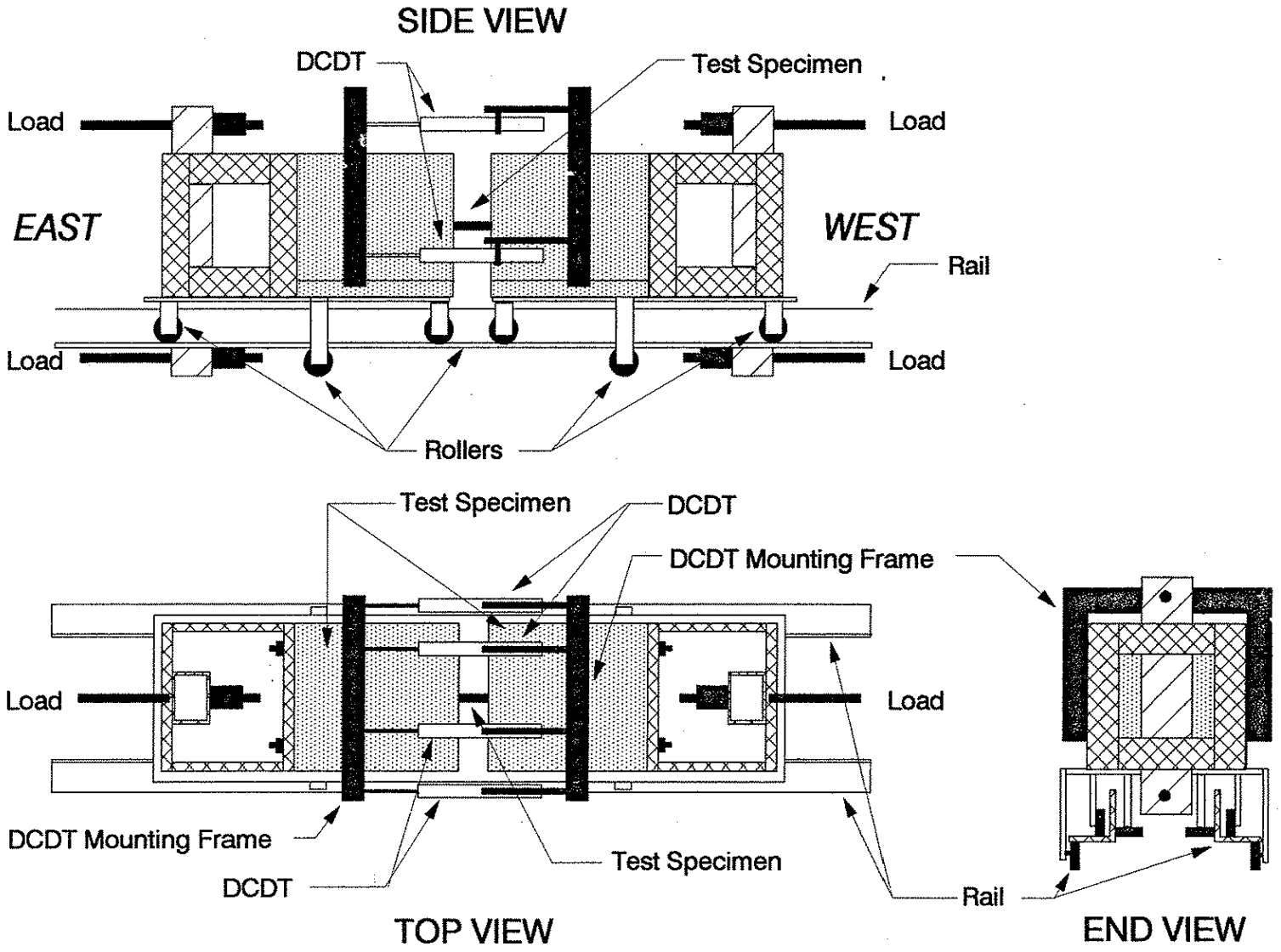

Figure 4.54 Pullout test frame

frame. The nuts which attached this end to the frame were only tightened to a snug condition. Any further tightening of these nuts could have led to eccentric forces induced into the specimen prior to the cutting of the threaded rod in the insulation gap.

Following the attachment to the frame, the threaded rod in the insulation gap were cut. During this cutting, the FC specimen was protected by leather. The tracks for the rollers were then cleaned of all debris and the instrumentation was mounted to the specimen. Load was applied by the hydraulic ram on the West end of the frame and the data was collected at approximately 100-lb intervals. This data was composed of load and deflection values collected from the instruments discussed in the following section.

4.5.4 Pullout test instrumentation

The instrumentation used in the pullout tests included load a cell and DCDTs. These instruments were connected to a Hewlett Packard (HP) Data Acquisition System (DAS) which was controlled by a MS DOS PC. Data was collected from the instruments, stored, and printed at specified intervals. All of the instruments were calibrated prior to testing and the calibration numbers used were input into the data acquisition program.

DCDTs were placed on the specimen in order to detect any possible rotation of the specimen. Four DCDTs were placed at

the corners of the insulation gap and one instrument monitored displacements inside the gap. The gap measurments were obtained by means of a scissors type device which transfered the specimen displacements from the inside of the gap to the outside of the specimen where an instrument could be installed. The data acquired from the four corner DCDTs were averaged to acccount for any rotational effects.

4.5.5 Results

The results from these tests are based upon the criteria of end slip. The pullout specimens tested had embedment lengths which varied from four to ten inches. Slip first ocurred in the six-inch embedment length specimen. The eight-inch embedment length specimen did not exhibit any end slip.

4.6 FC Rod Tensile Testing

4.6.1 Introduction

For a complete analysis of an FC rod as tie reinforcing, the tensile strength of the rod must be determined. The function of tie reinforcing is to link two adjacent lanes together, requiring that the rod resist tensile forces. Tensile testing was performed in conjunction with the bond development study for the FC rod material.

4.6.2 Materials and specimens

The FC rod consisted of E-glass fibers in a vinyl ester resin matrix as did the FC dowels tested. As a reinforcing rod, the resin and glass were formed into a helical wrapped rod, with a cross-section that was nearly oval-shaped. Because of the differing shape, no measurement could be used to determine the cross-sectional area. Therefore, a method of submerging sections of the rod in water while measuring the displaced water was applied. Measurements of the length of each section were made, and the quotient of the displaced volume and the length resulted in the average section area. Six sections of approximately 3 inches in length were analyzed for the purpose of determining cross-sectional area.

Specimens tested in tension were prepared in a manner to avoid damaging the FC rods during the tests. Because steel grips are used to pull the specimens in the testing machine, a copper tube and epoxy are used to protect the rod. The five-foot section of the rod had two 12-inch long pieces of the copper tube placed over each end of the rod, with epoxy filling around the FC. Each end of the specimen is then placed into the test machine with the grips in contact with the copper tubing. The dimensions and details of gripping are shown in Figure 4.55.

4.6.3 Test procedure

The procedure developed at Iowa State University (Porter 1991) was used to determine the tensile capacity of the FC rod. The rod with prepared ends was then placed in the wedge action grips of a hydraulic loading machine, and loaded in tension to failure at an approximate rate of 800 pounds per minute. The load frame control console recorded the peak load attained at failure.

4.6.4 Results

As mentioned before, the cross sectional area of the FC rod was found by determining the volume of the rod, and then dividing the volume by the length of the rod. The average area of the rod used in this research was found to be 0.115 in^2

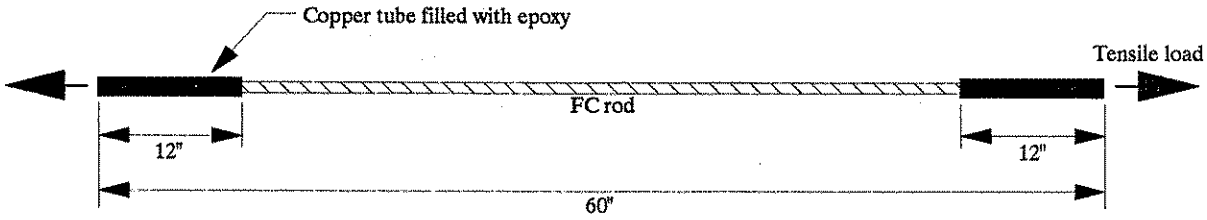

Figure 4.55 Dimensions and details of FC rod specimen used in tensile testing

of the rod used in this research was found to be 0.115 in^2 as calculated in Table 4.7. Results of tensile testing are presented in Table 4.8. The average tensile strength of the rod is reported to be 85.6 ksi.

Table 4.7 Determination of area of FC rod

Specimen No.	Length in.	Volume cm^3	Volume in^3	Area in^2
1	2.996	5.63	0.344	0.115
2	3.017	5.76	0.351	0.117
3	3.036	5.67	0.346	0.114
4	2.987	5.68	0.347	0.116
5	2.996	5.05	0.308	0.104
6	3.011	6.07	0.370	0.123

Table 4.8 Tensile Strength of FC rod

Specimen No.	Load at failure lbs	Tensile strength ksi
1	8260	72.0
2	11050	96.4
3	11380	99.2
4	8570	74.7

CHAPTER 5 COMPARISON AND RELATION OF RESULTS

5.1 Current and Previous Fatigue Testing of Pavement Dowels

Previous testing of steel pavement dowels in concrete pavement joints under repetitive loading was reported by Teller (1958). The test setup for the work by Teller and Cashell was the basis for the testing performed during the current research. The behavior of the dowel systems tested by Teller was very similar to the behavior of the dowels studied during this research.

During the previous research, relative deflections measured at the joint were shown to increase as the number of applied load cycles increased. A significant portion of the change in relative deflection occurred during the first 100,000 cycles. A similar trend was noted in the results from both the FC and steel dowel systems studied during this research.

Similarities in the results of the two studies were also observed related to the percentage of load transfer at the joint. In this research the 1.5-inch steel dowels showed a steady decrease in the portion of load transferred at the joint as the number of cycles increased. Such a reduction of the joint efficiency due to cyclic loading was also noted for steel dowels in the study by Teller. The load transfer efficiency of the FC dowels investigated in this research was atleast similar to that of the steel dowels throughout the fatigue testing, but

FC dowels were not included in the previous study.

Associated with the decreased load transfer by steel dowels under repeated loading in the previous research was the onset of a "looseness" of the dowels within the concrete. In the current study, increasing moments measured on the steel and FC dowels indicated a trend of loosening. In both studies, the apparent damage to the concrete related to the looseness of the dowel could not be visually observed.

The agreement of results from the two studies as discussed here is important in validating the results of both. Test procedures followed during the two projects were quite similar, though the work reported by Teller was performed only on steel dowels with diameters of from 0.75 to 1.25 inches. Despite the difference in dowel sizes during the two projects, general behaviors of the dowels were found to be similar. The noted similarities indicate general characteristics of round dowel bars in concrete pavements as load transfer devices.

5.2 Elemental and Full-Scale Testing

One objective of this study was to compare and relate the performance and behavior of dowels in elemental and full-scale testing. Sections 4.3.6.3 and 4.3.7.2 discuss the measured load transfer across the joint of the full-scale slabs during the static load tests. The analysis method for determining load transfer applied the strain gage data collected from the

supporting beams, and the result was the net load transfer provided by all of the dowels at the joint. Also of interest, though, was the portion of the total load that was transferred by each of the dowels. One method to calculate load transfer by individual dowels involved development of relationships between the strains measured in both FC and steel dowels and the associated load transfer. Relationships between strain and load transfer were generated by applying the results of the elemental tests.

Previous work related to steel dowels at a spacing of 12 inches had approximated that only two to four of the dowels nearest to the point of a load are affective in transferring load at the joint of a pavement (Heinrichs 1989). If a joint is idealized as perfectly rigid, 50 percent of the load, or 4,500 pounds for a 9,000 pound loading, is transferred across the joint by all of the dowels. Therefore, by distributing the transfer of 4,500 pounds among effective dowels, an approximate minimum of 1,125 and an approximate maximum of 2,250 pounds would be transferred by each of four or two dowels, respectively. Because the joints tested in this research were assumed to be less than perfectly rigid, which the results confirmed, the load transferred by a single dowel was expected to be less than 2,250 pounds.

Strain gage data from both elemental and full-scale slabs indicated a linear relationship between measured strains and loads. The data from elemental testing of 1.75-inch FC dowels,

as well as from elemental testing performed by Lorenz on 1.5-inch steel dowels (Lorenz 1993), exhibited such a relationship. Linear regression of the data from the FC dowel elemental testing was discussed in Section 4.2.7 and a linear expression was given in Equation 4.31, which is repeated here.

$$P_s = 6.697 S_{1.5} \qquad \text{Eqn. 4.31}$$

where,

P_s = dowel shear or load transferred by a dowel (lbs)
$S_{1.5}$ = measured strain in a dowel at 1.5 inches from the joint (μin./in.)

A similar analysis procedure was applied to strain and load data from elemental testing of 1.5-inch steel dowels performed by Lorenz. The combined load and strain data from the strain gages mounted on steel dowels in three elemental specimens are included in Figure 5.1. The data in Figure 5.1 is for the strain gage location at 1.5 inches from the joint and the resulting combined regression. Each of the data points in the figure includes a strain value that is the average of the strains measured by two gages on opposite sides of the dowel. The regression line equation for 1.5-inch steel dowels is expressed in Equation 5.1.

$$P_s = 9.442 S_{1.5} \qquad \text{Eqn. 5.1}$$

Because the FC dowels tested in the full-scale and

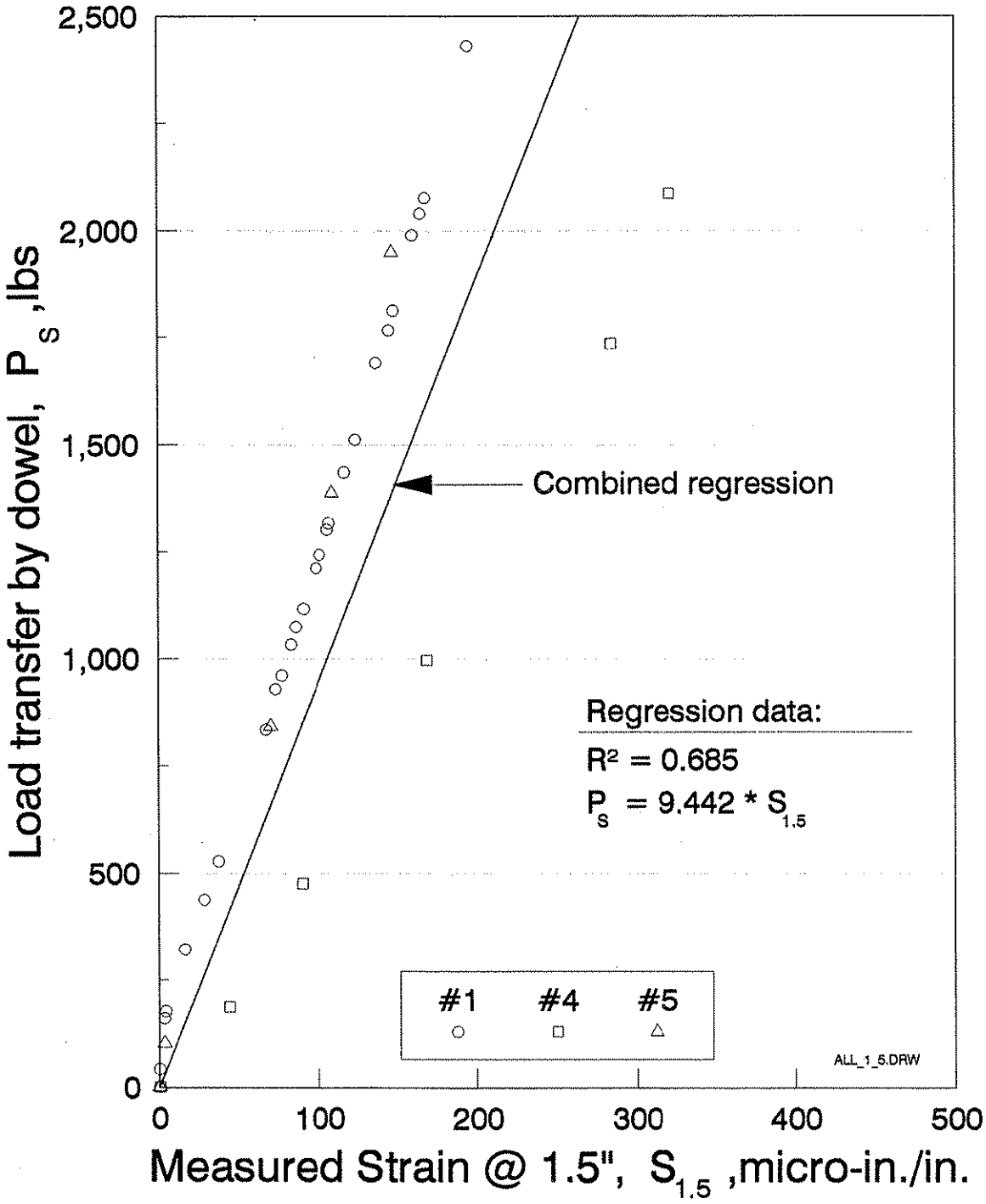

Figure 5.1 Load versus strain diagram at 1.5 inches from the joint of elemental tests with 1.5-inch steel dowels (Lorenz 1993)

elemental specimens were identical, calculation of moments from the dowel strains was not necessary in order to relate the results from the two tests. Therefore, measured strains from the elemental tests were used directly in the determination of the relationship with load transfer, as is shown in Equation 4.31. For the same reasons, the relationship developed for the steel dowels in Equation 5.1 directly relates strains to load transfer.

The scatter of the data shown in Figure 5.1 most likely resulted from experimental behavior similar to that discussed in Section 4.2.7. Regarding the load versus deflection data of the first group of elemental specimens with FC dowels, an initial slip of the dowel within the concrete possibly influenced the measured dowel behavior. Preloading of the elemental specimens with several cycles of a small load would eliminate the influence of initial conditions on strain as well as displacement results.

As discussed in Section 4.3.4.2, strain gages were placed on both the FC and steel dowels used in the second and third full-scale slabs, respectively. The locations of these gages, relative to the joint location, was the same as for the elemental specimens with FC dowels discussed in Section 4.2.4 and those with steel dowels tested by Lorenz (1993). Because of the similarity of the locations, the measured strains in the full-scale slabs were applied to Equations 4.31 and 5.1 to determine the load transferred by each dowel.

The dowel strain data from the second full-scale slab was considered in order to determine the load transfer by Equation 4.31. In Slab 2, the three center dowels were instrumented with strain gages, and data was collected during the static load tests. Measured strains at the maximum load applied to the slab, which was 9,000 pounds, were substituted into Equation 4.31, with the resulting load transfer values as given in Table 5.1. Because during the static load tests one side of the joint was loaded at one time, there are two sets of load transfer results. One set from when the North side of the joint is loaded, and the second when the South side is loaded.

The strain gage data shown in Table 5.1 indicates that quite consistent results were gathered from the instruments.

Table 5.1 Load transfer across the joint by 1.75-inch FC dowels in the second full-scale test slab

Dowel Name	Location	NORTH LOADED		SOUTH LOADED	
		Avg. Meas. Strain (μin./in.)	Load Transfer (lbs)	Avg. Meas. Strain (μin./in.)	Load Transfer (lbs)
1	8" East of CL	139	928	150	1,001
2	Centerline	139	928	135	904
3	8" West of CL	143	958	125	837
		Total = 2,814		Total = 2,742	

The authors believe that the variation of the strain values among the three dowels are within the experimental scatter of the instruments and the test setup. The totals of the three load transfer amounts are very similar for loading applied to both sides of the joint.

The same procedure as described above for FC dowels was followed for the strain data collected from the dowels in the third and fourth full-scale slabs. Only the center two dowels of these slabs were mounted with strain gages. The strain values for the dowels in Slab 3 due to 9,000 pounds applied to each side were substituted into Equation 5.1, which was developed from elemental testing of 1.5-inch steel dowels. Values for load transfer were then determined and are given in Table 5.2.

Table 5.2 Load transfer across the joint by 1.5-inch steel dowels in the third full-scale test slab

Dowel Name	Location	NORTH LOADED		SOUTH LOADED	
		Avg. Meas. Strain (μin./in.)	Load Transfer (lbs)	Avg. Meas. Strain (μin./in.)	Load Transfer (lbs)
1	6" East of CL	97	916	114	1,076
2	6" West of CL	98	925	105	991
		Total = 1,841		Total = 2,067	

Similar analysis was performed with the strains of the two center dowels of Slab 4, but now using Equation 4.31 for determinig the load transfer. The details calculation of the dowel load transfer are presented in Table 5.3.

Table 5.3 Load transfer across the joint by 1.75-inch FC dowels in the fourth full-scale test slab

Dowel Name	Location	NORTH LOADED Avg. Meas. Strain (μin./in.)	NORTH LOADED Load Transfer (lbs)	SOUTH LOADED Avg. Meas. Strain (μin./in.)	SOUTH LOADED Load Transfer (lbs)
1	6" East of CL	206	1,380	190	1,272
2	6" West of CL	188	1,259	179	1,199
		Total =	2,639	Total =	2,471

The relation of elemental and full-scale test data indicated that the individual FC and steel dowels acted similarly in transferring load across the joints in the full-scale specimens studied in this research. Load transfer values calculated for both types of dowels demonstrated the behavior of the dowels with instrumentation in the full-scale specimens before cyclic loading was applied.

In the full-scale specimen utilizing 1.75-inch FC dowels spaced at eight inches, the calculated values of load transfer exhibited a rather uniform distribution of load to the center three dowels. The remaining six dowels were assumed to

transfer the remaining load across the joint. Determination of the load transfer values for each of the dowels without strain gages would require speculation of their internal behavior, which was not attempted in this study. With regard to the previous work on the distribution of load transfer to the dowels nearest the load application (Heinrichs 1989), the FC dowels located 16 inches from the load point would most likely carry a large portion of the remaining amount of transferred load.

Results of the calculated load transfer amounts by the individual 1.5-inch steel dowels at 12 inches were similar to those for the FC dowels. The load transfer was determined for only two of the steel dowels in the third slab. Because only four additional dowels were available to transfer load, significant loads were most likely transferred by all of the steel dowels in the full-scale specimen. As a result, the load transfer was distributed further away from the load point than for the specimen with FC dowels. Results from the static load testing of the two slab specimens indicated that the relative displacements at the steel dowels 18 inches from the load point were more significant than those at the FC dowels 16 inches from the load point.

The results from the fourth slab with 1.75 inch diameter FC dowels spaced at 12 inches indicate that the load transferred through the individual dowels located nearest the load point was higher than in previous slabs. However, since

the total number of dowels near the load in Slab 4 was less than in Slab 2, the total load transfered across the joint by the dowels was less. The difference between Slab 3 and Slab 4 load transfer could be attributed to the difference in dowel diameter.

The total load transfered by the dowels closest to the load point in Slabs 2, 3, and 4 is tabulated in Tables 5.1, 5.2, and 5.3. Slab 2 (1.75-inch diameter FC dowels spaced at 8 inches)transfered the largest amount of load due to the close spacing of the dowels and the diameter of the dowels. Slab 4 dowels (1.75-inch diameter FC dowels spaced at 12 inches) had the next highest loading. This loading follows the rational of Slab 2 since the dowels were the same diameter as Slab 2 but spaced further apart. The dowels in Slab 3 (1.5-inch diameter steel dowels spaced at 12 inches) exhibited the smallest dowel loading due to the smaller dowel diameter and large spacing.

An additional consideration was made regarding the full-scale slab data. Because the elemental tests were run on a dowel specimen which had not been previously loaded, the relationships in Equations 4.31 and 5.1 should only be considered for the results of the initial static load tests. These tests were performed before fatigue loading of the slab had begun, and the same relationship will not apply after cyclic loading of the full-scale pavement slabs begins.

5.3 Experimental and Computer Modeling

The use of a computer model in the analysis of a full-size highway pavement was required because of a lack of sufficient data on the performance of an actual pavement under service loads. In addition, computer modeling was used in the design of the laboratory experimental setup for testing of full-scale pavement joints. Because of the idealizations required in order to model such a complex system by finite element methods, differences were found between the experimental and modeling results.

Pavement displacements, both relative at a joint and absolute, were of most interest from the results. Relative displacements were the primary means of monitoring load transfer efficiency of a doweled joint. From the computer model of both the laboratory setup and the full-size pavement, the maximum displacement of the pavement at the joint under a load of 9,000 pounds was approximately 0.016 inches. The results of testing of the full-scale pavement slabs indicated a maximum displacement of approximately 0.025 inches at the joint. The difference is rather significant when comparing the two values, though the magnitude of the difference is very small.

The discrepancy between the two results may come from the idealizations made in the computer model of the system. As discussed in Section 3.1, and shown in Figure 3.3, the dowels

at the joint were modeled as beams which were rigidly connected to the slab at each end. An actual dowel, though, would most likely have end restraints with less stiffness than a rigid connection. The theoretical idealization discussed in Section 4.2.6 included some displacement and rotation of the dowel within the concrete, while a rigid connection does not permit displacements or rotations to occur. The computer analysis results indicated that the relative displacement at the joint was very near to zero. Modeling of the dowel to allow some rotation at the dowel to slab interface would reduce the stiffness of the system, and thus the efficiency of the joint. Such a model may result in displacements in the computer model which approach those from the laboratory experimentation.

5.4 Potential Design Applications

Current highway pavement dowel design practices are based upon previous studies of highway pavement test sites, as well as experience gained during many years of the use of dowel bars in pavements. The objective in the design of the FC dowel system in Slab 2 was to provide a dowel system equivalent to the current standard steel system. Equivalence was based upon displacements, which were related to the stiffness of the dowel system, determined during the computer analysis. Results from the fatigue study indicated that the

performance of the two systems was similar under fatigue loading conditions, demonstrating that design based upon stiffness may be appropriate. Continued research similar to that included in this study will be required in order to include the influence of fatigue in the design of pavement dowels.

CHAPTER 6 SUMMARY AND CONCLUSIONS

6.1 Summary

6.1.1 General

Included in this study of non-metallic highway pavement dowels were several types of experimental and analytical investigations. Laboratory testing was conducted on full-scale concrete pavement and elemental dowel specimens, as well as full-size and reduced-size FC dowel flexure specimens. In addition, FC dowels were placed in transverse joints in an actual highway construction project, and the performance of the dowels was monitored and evaluated. The following sections include summaries of the work related to each of the primary portions of the research.

6.1.2 Full-scale slab fatigue testing

Laboratory testing was performed on full-scale highway pavement slabs using both steel and FC dowels placed at test joints. Static and fatigue evaluations of pavement dowel performance were accomplished under conditions simulating that of an actual highway pavement. A simulated subgrade was built to support the test slabs and to allow displacements approximating those of an actual pavement under service loads.

Fatigue loading was applied to both sides of the test joints to simulate truck traffic passing over a joint.

Testing of four full-scale pavement specimens was completed, two with 1.5-inch diameter steel dowels spaced at 12 inches along the joint, one with 1.75-inch diameter FC dowels placed at an 8-inch spacing along the joint, and one with 1.75-inch diameter FC dowels spaced at 12 inches along the joint. The first specimen, Slab 1, using steel dowels, was subjected to a total of two million fatigue cycles. The second specimen, with FC dowels, was referred to as Slab 2 and was again subjected to two million load applications. Ten million fatigue cycles were applied to Slabs 3 and 4, which had the same configuration of steel dowels at the joint as the first slab. Relative displacements and load transfer at the pavement joints during static load testing were the primary means of evaluation and comparison in the study of full-scale pavement slabs.

By simulating the in-service performance of an actual highway pavement, the applicability of FC dowels as pavement load transfer devices was evaluated relative to that of steel dowels. A comparison of the two types of dowels was valuable because any consideration of replacing steel dowels with a FC equivalent requires that the FC perform as well as the current standard.

Because the performance of the FC dowels spaced at eight inches in Slab 2 was very encouraging, a fourth slab

wasincluded in the project which was constructed with the same FC dowels, but with a spacing of 12 inches. By placing the dowels at the same spacing as that of the 1.5-inch steel, a more direct comparison of performance was possible. Again, as in previous specimens, strain gages were mounted on the dowels to monitor the flexure experienced by the dowels.

6.1.3 Elemental dowel specimen testing

Static shear testing was performed on 1.75-inch FC dowels cast in concrete elemental specimens. A total of nine specimens were tested, three of which had strain gages mounted on them to monitor flexure during the tests. The results of the elemental study were applied to determine values for the modulus of dowel support, k_o, for the FC dowel in concrete of two strengths.

Elemental testing of the 1.75-inch FC dowels resulted in several observations regarding the test specimens and test procedure. Because the magnitude of load that is transferred by an actual pavement dowel is significantly less than the load at failure of an elemental specimen, the behavior of greatest interest during elemental testing was in the service level load transfer range for pavement dowels. The need for steel shear reinforcing in the elemental specimens was evaluated to determine whether the reinforcement was necessary for all applications.

From the elemental testing, experimental values for k_o were determined for the 1.75-inch FC dowels in concrete of two strengths. Results from elemental testing from testing of FC dowels were compared to those of steel dowels.

6.1.4 Field testing of FC dowels

Placement of the FC dowel test specimens in two pavement joints in Highway 30 east of Ames provided a means of direct comparison of the performance of FC dowels to steel dowels under field conditions. Two transverse contraction joints in the construction of a new highway pavement had the standard 1.5-inch steel dowels at a 12-inch spacing replaced with 1.75-inch FC dowels spaced at eight inches. A program was developed for monitoring and evaluating the performance of the test joints, including visual inspections and experimental evaluations of the joints. The two FC test joints and four adjacent steel joints were evaluated by IDOT personnel and equipment, which included the Road Rater™. Load testing was performed on the two FC test joints and two adjacent steel joints using a loaded truck. Discussions of the visual inspections and initial results of Road Rater™ tests were included in this report.

6.1.5 FC material property testing

Both experimental testing and analytical methods were utilized to determine values for flexural and shear properties of the FC materials evaluated in this research. Flexural tests were performed on four full-size FC dowels and four reduced-size FC specimens cut from dowels in order to determine the flexural modulus of elasticity.

Properties of the individual components of the FC material were applied to determine theoretical composite properties. Using the rule of mixtures and the modified rule of mixtures as discussed by Tsai (1980), theoretical flexural modulus values were determined and compared to those determined experimentally.

6.2 Conclusions

6.2.1 Overall

The following conclusions were made regarding the overall scope of work included in this report:

1. The joints utilizing FC dowels studied in this research performed as well as joints utilizing standard steel dowels when both were subjected to conditions which simulated actual highway pavement use, including cyclic loading.

2. The laboratory test methods for evaluation of highway pavement dowel bars, which were developed during this research, provided good behavioral results for highway pavement joint conditions.

3. The full-scale pavement testing procedures applied in this research provided a good method for monitoring and evaluating the behavior of dowels bars when placed in a concrete pavement joint and subjected to cyclic loading.

Specific conclusions related to full-scale, elemental, and field testing of pavement dowels are included in the following sections.

6.2.2 Full-scale slab fatigue testing

Several conclusions specifically related to the full-scale testing are included in the following:

1. The 1.75-inch FC dowels spaced at eight inches performed at least as well as 1.5-inch steel dowels at 12 inches in transferring static loads across the joint in the full-scale pavement test specimens. The performance of the 1.75-inch FC dowels spaced at 12 inches was similar to that of the 1.5-inch steel

dowels spaced at 12 inches with any difference being attributed to dowel diameter.

2. The load transfer efficiency of 1.75-inch FC dowels spaced at eight inches in a full-scale pavement slab was nearly constant (approximately 44.5% load transfer) through two million applied load cycles with a maximum of 9,000 pounds.

3. The load transfer efficiency of 1.5-inch steel dowels spaced at 12 inches in a full-scale pavement slab decreased (approximately from 43.5% to 41.0% load transfer) over the first two million load cycles.

4. The load transfer efficiency of 1.75-inch FC dowels spaced at 12 inches in a full-scale pavement slab decreased from and initial value of approximately 44% to a final value of approximately 41% after 10 million cycles.

5. Load transfer by 1.5-inch steel dowels spaced at 12 inches in a full-scale pavement slab remained rather constant (approximately 41.0%) beyond two million cycles through ten million load cycles.

6. The behavior of increasing relative displacements at a pavement joint, due to a 9,000 pound load, as the number of load cycles increased occurred for both the FC and steel dowels studied in this research.

7. Relative displacements measured at pavement joints with 1.75-inch FC dowels spaced at eight inches were slightly smaller than at joints with 1.5-inch steel dowels spaced at 12 inches. Both were subjected to similar load and support conditions during the testing. The relative displacements for Slabs 3 and 4 were similar.

8. Load transfer by individual FC and steel dowels in a full-scale pavement joint can be determined by relating the measured dowel strains to the strains measured during elemental testing of the same types of dowels.

9. The use of steel beams as a simulated subgrade in place of a soil subgrade was effective for the study of pavement dowel performance under fatigue and static loading.

10. The test procedure developed and applied in the full-scale pavement slab testing provided results

which were valuable in performing an analysis of dowel behavior.

11. Using hydraulic actuators to simulate truck traffic in laboratory testing of full-scale pavement joints was effective for the evaluation of dowel behavior at the joints.

6.2.3 Elemental dowel specimen testing

Conclusions related specifically to elemental specimen testing include the following:

1. Elemental specimen testing, by examining the performance of a single dowel in shear, was valuable in support of full-scale pavement testing.

2. The behavior under static loading of FC dowels during elemental shear testing was similar to their behavior during full-scale slab specimen testing.

3. Results from previous testing of steel dowels in elemental specimens (Lorenz 1993) and results from full-scale testing in this study indicated that steel

dowels behaved similarly during full-scale and elemental static testing.

4. The modified Iosipescu shear test procedure for elemental dowel testing provided an adequate method for evaluating the shear properties of a pavement dowel/concrete system.

5. Values of the modulus of dowel support, k_o, for dowels tested in elemental shear specimens with equal concrete strengths were directly related to the flexural rigidity of the dowels.

6. Values of k_o for 1.75-inch FC dowels were determined to be 358,300 and 247,000 pci for elemental specimens with concrete compressive strengths, f_c', of 7,090 and 5,092 psi, respectively. These values compare to those determined by Lorenz (1993) of k_o = 650,000 pci for 1.5-inch steel dowels in concrete with f_c' = 7,090 psi.

7. Steel shear reinforcing was not required in elemental specimens for the evaluation of the performance of highway pavement dowels under service level loads.

6.2.4 Field testing of FC dowels

Specific conclusions related to the field testing of FC dowels in actual highway pavement joints are included in the following:

1. Evaluation using the Road Rater™ testing machine indicated that the performance of FC dowels in two test joints was equivalent to that of steel dowels in four adjacent joints. Average relative displacements were measured at the outside wheel track to be 0.035 and 0.03 mils for the joints with FC and steel dowels, respectively, and 0.05 mils at the inside wheel track for both types of joints.

2. No difference in joint performance was observed during visual inspections of pavement joints with FC dowels and adjacent joints with steel dowels.

3. The FC dowels placed in two test joints allowed the pavement to crack at the joint locations.

4. During very cold weather, the FC dowels in the test joints functioned properly by allowing the pavement to contract and the joint opening to increase.

CHAPTER 7 RECOMMENDATIONS

Upon consideration of all of the results included in this study, several recommendations are made regarding: testing related to highway pavement dowels, future investigations related to highway pavement dowels, use of FC dowels in highway pavements, and testing of FC materials. These recommendations are listed in the following:

1. Additional full-scale test slabs with FC and steel dowels should be tested to a number of load cycles which approaches the number experienced by an actual pavement over its service life, which may range from 50 to 100 million ESAL.

2. Additional field testing at other highway locations would be beneficial in order to subject the dowels to a variety of conditions, such as traffic and soil subgrade. Subjecting FC dowels to more severe loading and subgrade conditions than were experience in the field test in this research would facilitate the study of FC dowels as load transfer devices.

3. Further Road Rater™ evaluations of the two field test joints with FC dowels and the adjacent joints with steel dowels are recommended. Testing should be performed over the service life of the pavement in order to completely

evaluate the performance of the joints and dowels over time.

4. In addition to fatigue testing of full-scale slab specimens, consideration should be given to testing of elemental dowel specimens under cyclic or fatigue loading. By considering a single dowel element in such a test, the performance of the dowel, as well as the structural interaction of the dowel with concrete, can be more closely and easily studied.

5. By combining the principles studied in previous work regarding accelerated aging (Lorenz 1993) with fatigue testing of elemental specimens as discussed above in Recommendation 4, the performance of FC dowels under environmental and loading conditions representative of actual pavement conditions could be studied.

6. As a means of further studying the dynamic performance of the concrete slab and dowel system, dynamic testing of full-scale pavement slabs is recommended. Use of a dynamic data acquisition system capable of monitoring the instrumentation applied in this research would provide information as to the behavior of the individual components of the test setup under conditions similar to actual dynamic conditions.

7. Consideration should be given to the development of support "baskets" for the field placement of FC dowels similar to those now used for steel dowels. Problems experienced during the field placement of FC dowels indicated that such a system is necessary for future use.

8. The use of the elemental shear test method is valuable in the study of dowels embedded in concrete, but the results must be considered in the context of actual applications. This research was aimed at studying the behavior of pavement dowels as they act while in service, and the results were analyzed to provide information that relates to performance under service conditions.

9. Shear properties should be considered when studying the structural behavior of FC materials. The determination of these properties, including shear modulus and shear strength, should include using the most advanced experimental method, which appears to be the Iosipescu shear test for composite materials.

10. Additional work is necessary to improve the computer modeling used for the study of full-size pavement joints. Inclusion of a more precise pavement dowel model, is recommended for future studies.

REFERENCES

AASHTO Guide for Design of Pavement Structures. (1986). American Association of State Highway and Transportation Officials, Washington, D.C.

Adams, D.F. and Walrath, D.E. (1987, June). "Further Development of the Iosipescu Shear Test Method." Experimental Mechanics, Volume 27, pages 113-119.

Annual Book of ASTM Standards, Volume 8.02, Plastics (II). (1991). American Society for Testing and Materials, Philadelphia, PA, pages 328-329.

Auborg, P.F. and Wolf, W.W. (1986). "Glass Fibers." Advances in Ceramics, Vol. 18. Eds. D.C. Boyd and J.F. MacDowell. American Ceramic Society, Columbus, OH, pages 51-78.

Beer, F.P., Johnston, Jr., E.R. (1981). Mechanics of Materials. McGraw-Hill Book Company, New York, NY.

Bradbury, R.D. (1933). "Design of Joints in Concrete Pavements." Proceedings of the 12th Annual Meeting of the Highway Research Board, Washington D.C., December 1-2, 1932, pages 105-136.

Bryden, J.E. and Phillips, R.G. (1975). "New York's Experience with Plastic Coated Dowels." Transportation Research Record #535, TRB National Research Council, Washington D.C.

DERAKANE Resins, Chemical Resistance and Engineering Guide. (1990). The Dow Chemical Company.

EXTREN Fiberglass Structural Shapes, Design Manual. (1989). Morrison Molded Fiber Glass Company, Bristol, VA.

Friberg, B.F. (1938). "Design of Dowels in Transverse Joints in Concrete Pavements." Proceedings, American Society of Civil Engineers, Vol. 64, Part 2, pages 1809-1828.

Fiber Reinforced Concrete. (1991). Portland Cement Association, Skokie, IL.

Heinrichs, K.W., Liu, M.J., Darter, M.I., et al. (1989, June). "Rigid Pavement Analysis and Design." Turner-Fairbank Highway Research Center, McLean, VA, Report No. FHWA-RD-88-068.

Load and Resistance Factor Design Manual of Steel Construction. (1986). American Institute of Steel Construction, Chicago, IL, pages 3-132 to 3-133.

Lorenz, E.A. (1993). Accelerated aging of fiber composite bars and dowels. M.S. thesis, Iowa State University, Ames, IA.

McWaters, B. (1992-1993). Personal Interviews. Iowa Department of Transportation, Ames, IA.

Munjal, Ashok K. (1989). "Test Methods for Determining Design Allowables for Fiber Reinforced Composites." Test Methods for Design Allowables for Fiber Composites. ASTM STP 1003, C.C. Chamis and K.L. Reifsnider, eds., ASTM, Philadelphia, pages 93-110.

Pavement Design for Federal, State, and Local Engineers: a Training Course. Participant Notebook. Federal Highway Administration, National Highway Institute, Washington, D.C.

Porter, M.L., Barnes, B. A. (1991, Feb). "Tensile Testing of Glass Fiber Composite Rod." Advanced Composites Materials in Civil Engineering Structures" New York, NY.

Porter, M.L., Lorenz, E.A., Viswanath, K.P., Barnes, B.A., Albertson, M. D. (1990). "Thermoset Composite Concrete Reinforcement: Final Report, Part 1." Iowa State University, Ames, IA.

Potter, C.J., Dirks, K.L. (1989, May). "Pavement Evaluation Using the Road Rater™ Deflection Dish." Final Report for MLR-89-2, Highway Division, Iowa Department of Transportation, Ames, IA.

Talreja, Ramesh. (1987). Fatigue of Composite Materials. Technomic Publishing Co., Lancaster, PA.

Teller, L.W., Cashell, H.D. (1958). "Performance of Doweled Joints Under Repetitive Loading." Highway Research Board, Bulletin No. 217, pages 8-49.

Timoshenko, S., Lessels, J.M. (1925). Applied Elasti

Tsai, S.W., Hahn, H.T. (1980). Introduction to Composite Materials. Technomic Publishing Company, Inc., Lancaster, Pennsylvania.

Walrath, D.E., Adams, D.F. (1983, March). "The Iosipescu Shear Test as Applied to Composite Materials." Experimental Mechanics, pages 105-110.

Westergaard, H.M. (1928). "Spacing of Dowels." Proceedings, 8th Annual Meeting of the Highway Research Board, Washington, D. C., pages 154-158.

Westergaard, H.M. (1926). "Computation of Stresses in Concrete Roads." Proceedings of the 5th Annual Meeting of the Highway Research Board, Washington, D.C., December 3-4, 1925, pages 90-112.

Young, W.C. (1989). Roark's Formulas for Stress and Strain, 6th edition. McGraw-Hill Book Company, New York, NY.

ACKNOWLEDGEMENTS

The research described herein was conducted at the Iowa State University Structural Engineering Laboratories in the Department of Civil and Construction Engineering through the auspices of the Engineering Research Institute and sponsored by the Highway Division of the Iowa Department of Transportation (IDOT) and the Iowa Highway Research Board. The authors would like to thank the personnel at the IDOT who provided support through their experience and knowledge toward the project, namely Mr. Brian McWaters and Mr. Vernon Marks. Additional consultation and input from several individuals, including: Mr. Phil Catsman of Corrosion Proof Products, and Mr. Jerry Mass of W.G. Block, is also acknowledged by the authors. The authors wish to recognize and thank several firms for providing materials and advice, including: Economy Forms of Des Moines, Iowa; W. G. Block of Des Moines, Iowa; Steel Warehousing of Des Moines, Iowa; and Corrosion Proof Products of Bellevue, Nebraska.

The authors would like to acknowledge the support provided by Mr. Douglas L. Wood, Structural Engineering Laboratory Supervisor, for his expertise and assistance.

Appreciation is also extended to the many laboratory assistants, without whom this work could not have been completed. All of those involved are acknowledged for their efforts, but, special thanks are given to: Mr. David Grant,

Mr. Brent Brubaker, Mr. Brian Rath, Mr. Trevor Brown and Mr. David Neuberger.

The "burn-down" testing of the FC dowel material as discussed in Section 4.1.2 was performed by the Materials Analysis and Research Laboratory at Iowa State University. Their knowledge and advice was greatly appreciated.

APPENDIX

The principles of internal and external work were applied in the analysis of the effect of shear deformation on the flexural testing of full-size FC dowels. Figure A1 includes a diagram of the loading condition as well as the shear and moment diagrams for the flexural tests performed on FC dowels discussed in Section 4.1.4.2.

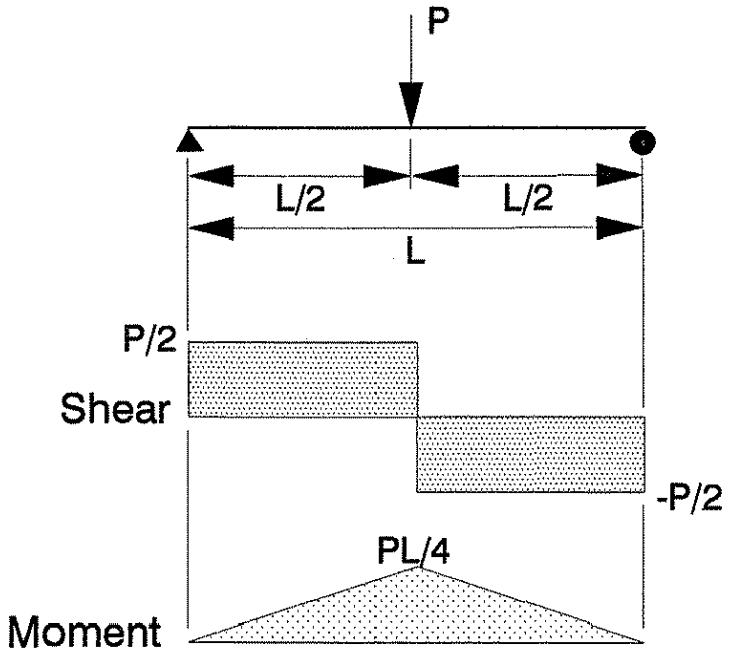

Figure A1 **Load, shear and moment diagrams from flexural testing of FC dowels**

The following includes the procedures followed to develop an expression for displacement which includes deflection due to flexure and shear deformation.

Internal work = External work

$$w_i = w_e \qquad \text{Eqn. A1}$$

Internal work:

$$w_i = \frac{1}{2} F \int \frac{V^2}{GA_d} dx + \frac{1}{2} \int \frac{M^2}{EI} dx \qquad \text{Eqn. A2}$$

$$w_i = \frac{1}{2} F \int^{L} \frac{(\frac{P_1}{2})^2}{GA_d} dx + 2 \left[\frac{1}{2} \int^{(\frac{L}{2})} \frac{(\frac{P_1 x}{2})^2}{EI} dx \right] \qquad \text{Eqn. A3}$$

$$w_i = \frac{P_1^2 LF}{8GA_d} + \frac{P_1^2 L^3}{96EI} \qquad \text{Eqn. A4}$$

External work:

$$w_e = \frac{1}{2} P_1 \Delta \qquad \text{Eqn. A5}$$

Equating internal and external work,

$$\frac{1}{2} P_1 \Delta = \frac{P_1^2 LF}{8GA_d} + \frac{P_1^2 L^3}{96EI} \qquad \text{Eqn. A6}$$

Resulting total deflection:

$$\Delta = \frac{P_1 LF}{4GA_d} + \frac{P_1 L^3}{48EI} \qquad \text{Eqn. A7}$$